THE GRAVITY FIELD AND PLATE BOUNDARIES IN VENEZUELA

by

Robert Allin Folinsbee

B.Sc., University of Alberta
(1964)

S.M., Massachusetts Institute of Technology
(1969)

SUBMITTED IN PARTIAL FULFILLMENT OF THE
REQUIREMENTS FOR THE DEGREE OF
DOCTOR OF PHILOSOPHY

at the

MASSACHUSETTS INSTITUTE OF TECHNOLOGY

and the

WOODS HOLE OCEANOGRAPHIC INSTITUTION

January, 1972

Signature of Author___ _____

Joint Program in Oceanography, Massachusetts Institute of Technology - Woods Hole Oceanographic Institution, and Department of Earth and Planetary Sciences, and Department of Meteorology, Massachusetts Institute of Technology, January 1972

Certified by_____ _____
Thesis Supervisor

Accepted by_____ _____
Chairman, Joint Oceanography Committee in the Earth Sciences, Massachusetts Institute of Technology - Woods Hole Oceanographic Institution

ABSTRACT

THE GRAVITY FIELD AND PLATE BOUNDARIES IN VENEZUELA

by

R. Allin Folinsbee

Submitted to the Joint Oceanography Committee in the Earth Sciences on January 14, 1972, in partial fulfillment of the requirements for the degree of Doctor of Philosophy.

Free-air and simple Bouguer anomaly maps of the Venezuelan continental margin (from 60°W to 72°W and from 7°N to 13°N) are presented. The major features of the free-air map are: the large lows associated with the deep sedimentary basins, -200 mgal in the Eastern Venezuela basin and -164 mgal in the Maracaibo basin; the high of greater than 300 mgal over the Venezuelan Andes; and a belt of highs associated with the offshore islands extending from Blanquilla to Curacao and then over the Guajira peninsula, where they terminate. The Bouguer anomaly map shows a large low (-196 mgal) over the Eastern Venezuela basin and relative minimums over the coastal mountains. A minimum associated with the Venezuelan Andes is shifted to the northwest of the topographic axis and lies over the flank of the Andes and part of the Maracaibo basin.

Using the gravity data, structural sections were constructed for a series of profiles across the Venezuelan Andes and Caribbean mountains. They show that there is no light crustal root under the Andes, the relative mass excess is as much as 600 kg/cm^2, and that there is an excess of low density material under the Maracaibo basin. This appears to be caused by a combination of a southeastward dipping shear zone in the lithosphere under the basin-mountain boundary and a component of compressive stress perpendicular to this zone, both of which have resulted in the uplift of the crust under the Andes, and downwarp under the basin. The apparent flexural rigidity of the lithosphere under the Maracaibo basin is 0.6×10^{23} newton-m, a normal value for lithosphere deformations of Miocene age.

The Caribbean mountains have a light crustal root which has been formed by the sliding of blocks of crustal material from the north over the rocks to the south, and perhaps by the underthrusting of oceanic crust under the continental crust. This underthrusting may have been a result of the formation of a downgoing slab of lithosphere along the Venezuelan continental margin during the late Cretaceous. The downgoing slab may have existed until mid-Eocene time. The gravity minimum over the Eastern Venezuela basin is due to the downwarping of lighter crustal material into the higher density mantle. This may be a result of compression from the north along a north-south direction causing plastic downbuckling of the lithosphere. The present deformation along the northern boundary appears to be due to differences in relative motion between the North and South American plates.

Because the Caribbean mountains are partially isostatically compensated, while the Venezuelan Andes are above isostatic equilibrium, this suggests that the relative motion of the Caribbean plate with respect to the South American plate is eastward. The compressive stress across the boundary in the region of the Venezuelan Andes is probably greater than the compressive stress across the Caribbean mountains.

Thesis Supervisor: Dr. C. O. Bowin
Title: Associate Scientist

ACKNOWLEDGEMENTS:

I wish to thank my thesis advisor Dr. C. O. Bowin for his constant encouragement, valuable advice, and many helpful discussions, during the course of this study. The initiation of this project was in part a result of suggestions by Dr. Bowin and Dr. S. Biehler. Thanks are due the other two members of my thesis committee: Dr. B. Luyendyk, who critically reviewed the manuscript and made suggestions, and Dr. N. Toksoz who aided in the interpretation of the first motion studies. Dr. R. Stainforth and Mr. A. Peirson provided much helpful information about Venezuelan geology.

The following oil companies graciously made available the unpublished results of their gravity measurements: American International Oil Co., Chevron Oil Co. de Venezuela, Compania Shell de Venezuela, Continental Oil Co. of Venezuela, Creole Petroleum Corp., Mene Grande Oil Co., Mobil Oil Co., Pan American Venezuela Oil Co., Signal Oil and Gas Co., Texas Petroleum Co., Venezuelan Atlantic Refining Co. and Venezuelan Sun Oil Co.

The following people and organizations were particularly helpful during my trip to Venezuela. The members of the Venezuelan Project of the Inter American Geodetic Survey provided office facilities, transportation, and introduced me to people in the Venezuelan government mapping agency, Direccion

de Cartografia Nacional. Dr. J. Romero and Sr. M. Fermin of Direccion de Cartografia Nacional provided a vehicle and driver, bench mark descriptions, and unpublished gravity data from their files. Without their help the tieing of all the land data to a common datum, and the gravity survey across the Venezuelan Andes could not have been accomplished. Mr. J. Van Bertsburgh of Cia Shell de Venezuela provided gravity and topographic maps, as well as information about the coordinate systems in use in Venezuela.

Thanks are due my wife, Carol, who spend endless hours drafting the figures, and providing encouragement, and Mrs. G. Mosier who typed the manuscript.

This investigation was supported by a grant from the National Science Foundation GA-12204, and by contract N00014-66-C-0241 with the Office of Naval Research. Part of the cost of the computer time was paid for by a grant from the National Science Foundation GJ133. During part of this investigation the author was supported by a Woods Hole Oceanographic Institution fellowship. A contract from the Aeronautical Chart and Information Center and a grant from an oil company to C. O. Bowin provided partial support for travel costs.

CONTENTS

LIST OF FIGURES

Figure 1: A geographical map of Venezuela, Colombia, and Trinidad. The area for which gravity data are presented is outlined by dashed line.

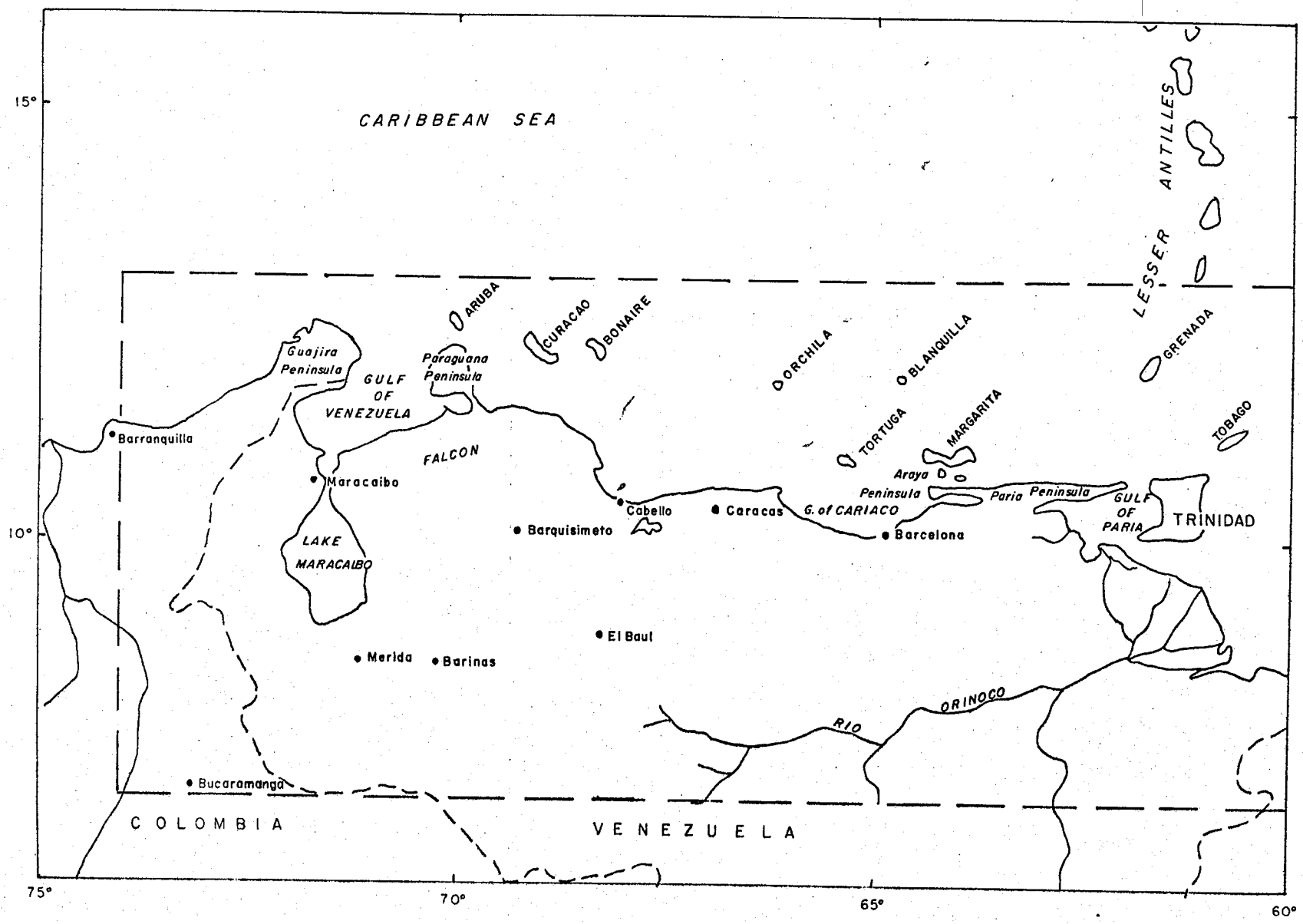
CARIBBEAN SEA
LESSER ANTILLES
ARUBA
CURACAO
BONAIRE
ORCHILA
BLANQUILLA
GRENADA
TOBAGO
TORTUGA
MARGARITA
Araya Peninsula
Paria Peninsula
GULF OF PARIA
TRINIDAD
Guajira Peninsula
Paraguana Peninsula
GULF OF VENEZUELA
FALCON
LAKE MARACAIBO
Barranquilla
Maracaibo
Cabello
Caracas
G. of CARIACO
Barcelona
Barquisimeto
El Baul
Merida
Barinas
Bucaramanga
RIO ORINOCO
COLOMBIA
VENEZUELA
15°
10°
75°
70°
65°
60°

INTRODUCTION

Purpose of Study

The concept that the Earth's surface is divided into a number of areas that appear to move as rigid plates has provided a new basis on which to interpret the large scale features of the Earth's crust. The region of the Caribbean and the north coast of South America is such a feature, and includes a boundary between an oceanic plate (the Caribbean) and a continental plate (the South American plate). This study examines geologic and geophysical data from the region in an attempt to interpret the tectonic history of the area, including the development and present dynamics of the plate boundary.

Land and sea gravity data are compiled for the region from 60°W to 72°W, and 7°N to 13°N. This area includes all of northern Venezuela, Trinidad, parts of Eastern Colombia, and the Caribbean north of Venezuela and Trinidad (Fig. 1). Principal facts for 2500 stations are used to produce free-air and Bouguer gravity anomaly maps. The gravity data, the results from marine surveys, and land geologic data are used to determine the crustal structure in Venezuela. An analysis is made of the different modes of crustal deformation that

Figure 2: Topography and bathymetry of the study area (modified from the London Times Atlas, 1957).

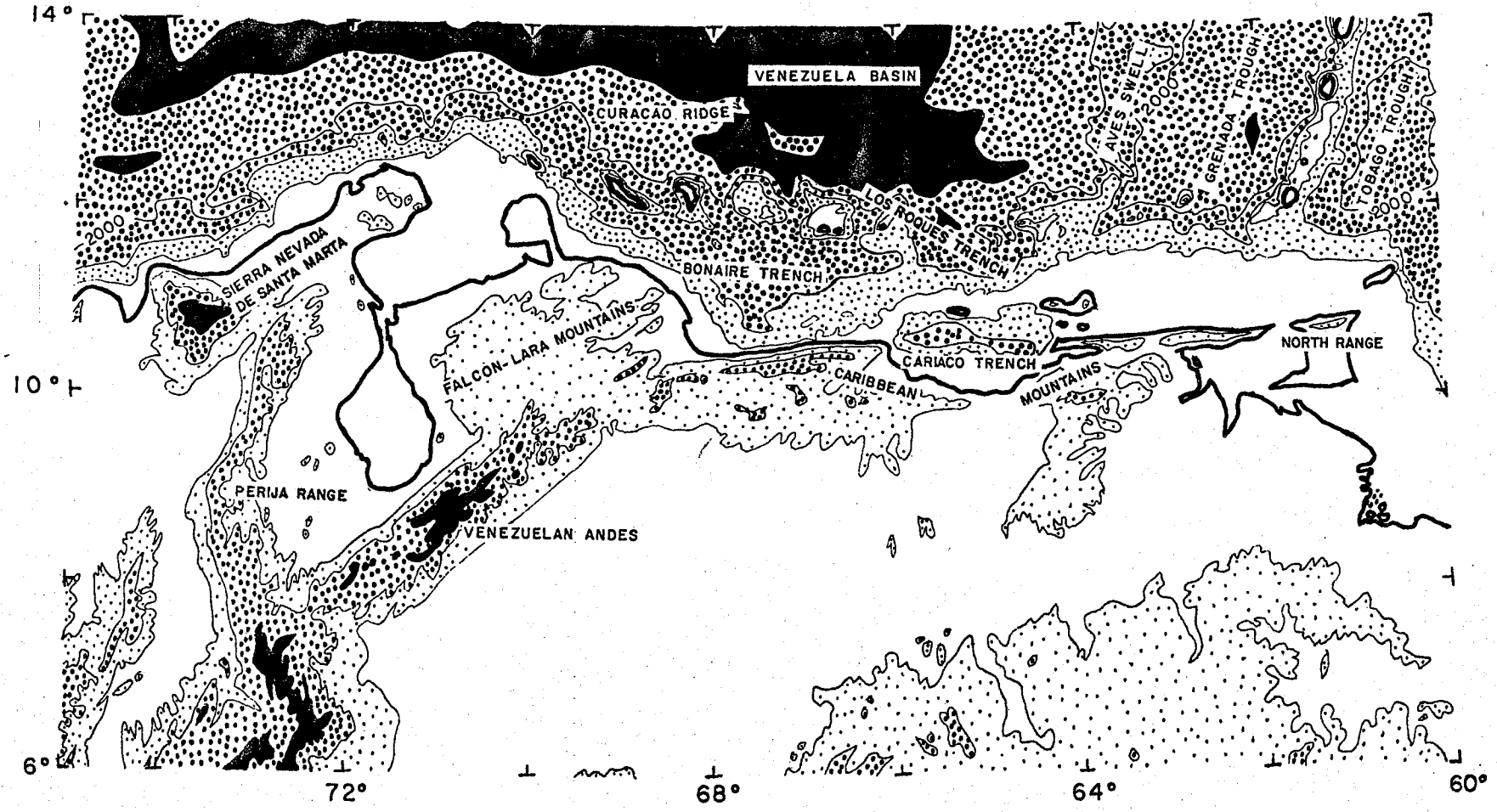
14°
10°
6°
72°
68°
64°
60°
VENEZUELA BASIN
CURACAO RIDGE
AVES SWELL
GRENADA TROUGH
TOBAGO TROUGH
2000
SIERRA NEVADA DE SANTA MARTA
LOS ROQUES TRENCH
BONAIRE TRENCH
FALCON-LARA MOUNTAINS
CARIACO TRENCH
CARIBBEAN
MOUNTAINS
NORTH RANGE
PERIJA RANGE
VENEZUELAN ANDES
ELEVATION, meters
0 - 200
200 - 1000
1000-3000
>3000
DEPTH, meters
0 - 200
200-1000
1000-4000
>4000

would give rise to the observed crustal structure. The relationship between the different modes of deformation that are observed and the tectonic history of the area is also discussed.

Physiography

The bathymetry and topography of the study area are shown in Figure 2. The Venezuelan basin is a major depression in the Caribbean with an average depth of 4500 meters (Edgar, 1968). It is bounded on the west by the Beata ridge, and on the east by the Aves Swell. The Grenada trough extends north-south and separates the Aves Swell from the Lesser Antilles. A series of east-west trending ridges, trenches and islands extends along the southern boundary of the Caribbean. These include the Curacao ridge separated from the islands of Curacao, Aruba, and Bonaire by the Los Roques trench. The Cariaco trench lies between the islands of Blanquilla and Margarita, and the Venezuelan mainland.

On land the Caribbean mountains extend along the northern coast of Venezuela and into Trinidad. This mountain system is divided into two east-west striking ranges, which are separated by a central valley. The mountains on the north are known in Venezuela as the Coast range, and in Trinidad as the North range, while the mountains to the south are known as the Interior

range. The Venezuelan Andes are separated from the Caribbean mountains by the Barquisimeto-Acarigua depression. The Venezuelan Andes are a northeastward trending spur of the Eastern Colombia Cordillera. The Perija range is a northward trending spur of the Eastern Colombia Cordillera. Between the two ranges of mountains is the Maracaibo basin, a flat low lying area partially covered by Lake Maracaibo. Southeast of the Venezuelan Andes is the Barinas-Apure basin (Fig. 3). The Eastern Venezuela basin lies to the south of the Caribbean mountains. These two basins are partially separated from each other by the El Baul swell.

Review of Geology

In the following section the geologic history of Venezuela and adjacent areas from pre-Mesozoic to the Holocene is summarized.

Much of what is known of the geologic history of Venezuela prior to the late Mesozoic, is due to the geologic mapping done as part of the Caribbean research project by members of the Department of Geology, Princeton University (Hess and Maxwell, 1953). Most of the other geologic mapping done in Venezuela was oriented towards petroleum exploration, and since almost all oil production in Venezuela

Figure 3: A geologic map of Venezuela, (modified from tectonic map of Venezuela, 1963).

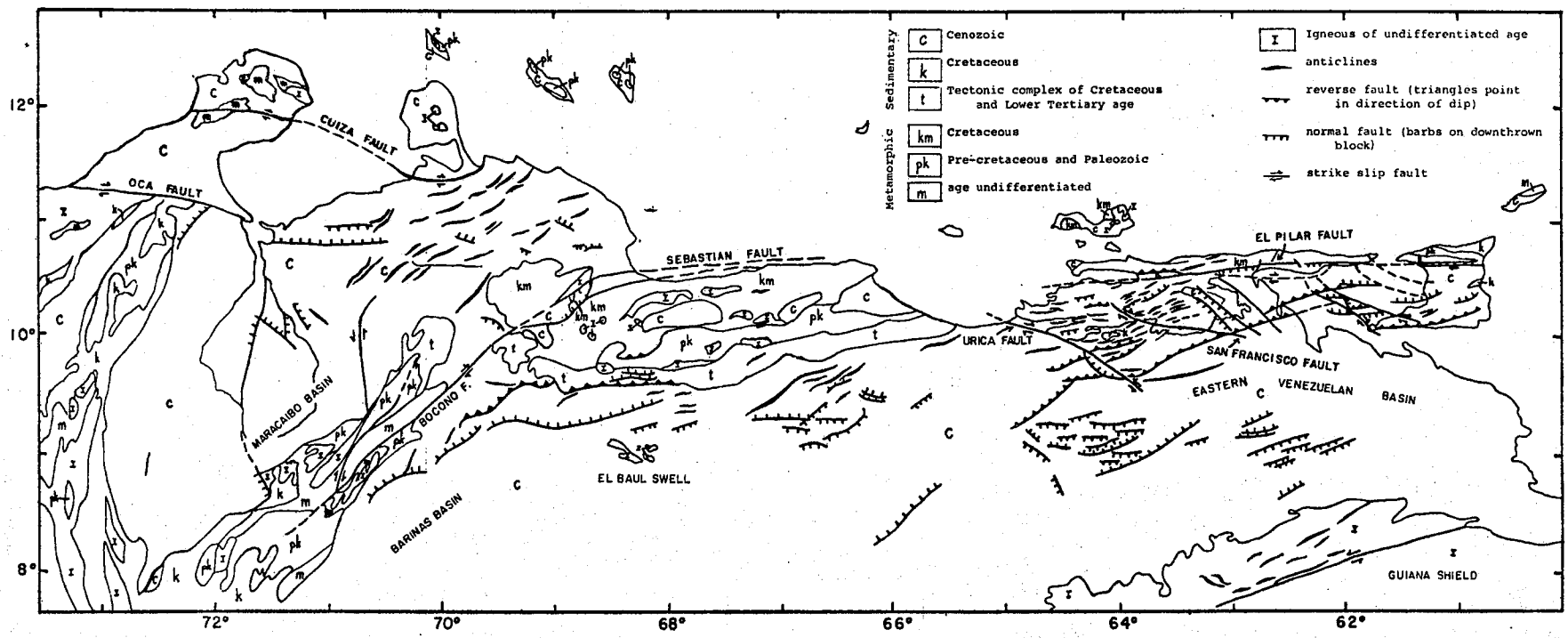
Sedimentary
C Cenozoic
k Cretaceous
t Tectonic complex of Cretaceous and Lower Tertiary age
Metamorphic
km Cretaceous
pk Pre-cretaceous and Paleozoic
m age undifferentiated
I Igneous of undifferentiated age
anticlines
reverse fault (triangles point in direction of dip)
normal fault (barbs on downthrown block)
strike slip fault
CUIZA FAULT
OCA FAULT
SEBASTIAN FAULT
URICA FAULT
EL PILAR FAULT
SAN FRANCISCO FAULT
MARACAIBO BASIN
BOCONO F.
BARINAS BASIN
EL BAUL SWELL
EASTERN VENEZUELAN BASIN
GUIANA SHIELD
12°
10°
8°
72°
70°
68°
66°
64°
62°

is from late Cretaceous or younger rocks, this has resulted in less knowledge about older rocks.

The Guiana shield extends across Venezuela on the southeast. It consists primarily of gneisses and gneissoid granites of Precambrian age (Mencher et al., 1953). Like other central cratons, it has been a relatively stable area since the Precambrian time.

North of the Orinoco river in the Eastern Venezuela basin, several wells penetrated granite below Cretaceous, but no ages are available for these rocks.

The Sierra Nevada formation which is a series of mica schists, gneisses, and other crystalline metamorphic rocks, makes up the central portion of the Andes. These rocks are probably equivalent to the rocks of the Perija range and to the Sierra Nevada de Santa Marta (Kovisars, 1971), which have been dated as 1,400 m.y. (MacDonald and Hurley, 1969).

During much of the Paleozoic, seas covered western Venezuela depositing the Palmarito series (observed in the Sierra de Perija and the Andes) and possibly the sediments that were later metamorphosed to form the El Baul phyllites. In late Paleozoic time a geosyncline developed with the center of deformation east of the Andes, as evidenced by the fact that

El Baul phyllites are more highly metamorphosed than the equivalent rocks in the Andes, while the Palezoic rocks in the Perija mountains are unmetamorphosed (Mencher et al., 1953).

During the early Mesozoic the La Quinta redbeds were deposited in western Venezuela with the greatest thickness aligned along the axis of the Venezuelan Andes and the Perija mountains (Stainforth, 1969). The deposits were intruded by basaltic magmas during and shortly after their deposition (Mencher et al., 1953).

In Trinidad more than 2000 m of sericitic sandstones and sericitic phyllites (the Maracus formation) are found along the axis of the North range, and extend into the Paria peninsula (Fig. 1) in Venezuela (Potter, 1968). The Maracus formation appears to have originally consisted of siltstones and mudstones. The age of the formation is uncertain, but it is pre-upper Jurassic, and may actually be as old as Triassic. During the mid-Jurassic there was continued deposition of sediments along the northern border of Venezuela: in Trinidad, the Rio Seco and Maraval formations consisting of calcerous phyllites with interbedded recrystallized limestone (Barr, 1963); on the Araya peninsula (Fig. 1) the Gaumache formation (Salvador and Stainforth, 1968); on Margarita, the Juan Griego group

(Taylor, 1960); and of the Coast ranges, Las Brisas and Las Mercedes formations (Bell, 1967). According to Bell it is probable that most of these formations were deposited to the north of their present locations, but have since been moved south by gravity sliding and/or thrust faulting.

In western Venezuela there was uplift and disturbance, but no metamorphism after the deposition of the La Quinta formation. The uplifted region was then eroded to a peneplain at the beginning of the Cretaceous. During the early Cretaceous the extensive sedimentation along the northern border continued. The Villa de Cura group of west-central Venezuela was deposited sometime during the late Jurassic or early Cretaceous (Bell, 1967). At the beginning of the Cretaceous a shallow sea began to invade Venezuela from the north depositing a series of sandstones and sandy shales known in the east as the Barranquin, El Cantil and Chimana formations and in the west as the Cogollo group. By the end of the early Cretaceous (Albian) the seas had extended to a point midway between the present coast and the Orinoco river (Mencher et al ., 1953).

In the southern part of Venezuela the deposition of miogeosynclinal deposits continued through the late Cretaceous. The change in character of the sediments from the glauconitic

clastic sediment of Albian time to the deep water limestones of Cenomanian time is evidence that the sea in this region may have deepened at the beginning of the Cenomanian (Hedberg, 1950). In northern Venezuela this period was marked by the formation of an orogenic belt located in the region of the present Venezuela coastline. The belt extended from east of the present location of the Andes, to the North range of Trinidad. The islands of Curacao, Aruba, and Bonaire were apparently included in this unstable zone. The geology of these islands is reviewed by Lagaay (1969). On Aruba the basement complex consists of an intensely folded series of submarine lavas and tuffs, which has been intruded by quartz diorite. The intrusion was apparently contemporaneous with the deformation. The basement formation of Curacao is a thick sequence of submarine basic lavas. The formation is overlain by a complex unit of Campanian-Maestrictian age, composed primarily of chert-rich sediments. The basement complex of Bonaire is known as the Washikemba formation. The formation consists primarily of basic lavas interlayered with tuffs in the lower part and cherts in the upper part. The formation is unconformably overlain by shallow water deposits of Upper Campanian-Lower Maestrictian age. Isotopic age determinations of biotite from the quartz-diorite of Aruba by the K-Ar and Rb-Sr method yield ages of 73±3 m.y. Quartz-diorite that

intrude the basement complex of Curacao show whole rock K-Ar ages of 72±7 m.y. (Priem et al., 1966). No age measurements have been made of the rocks of the Bonaire basic complex, but the similarity of the rocks of the Washikemba to those of the basement complex of Curacao indicates that these two units were probably formed contemporaneously (Lagaay, 1969).

During the late Cretaceous the Villa de Cura group of central Venezuela began to move southward by submarine gravity sliding as a result of uplift in the north, and downwarping in the south (Bell, 1967). The movement terminated in Paleocene time. The formation of the metamorphics of the North range of Trinidad and of the Coast range of Venezuela probably took place in the late Cretaceous. The degree of metamorphism decreases from north to south. In the Caracas group (Oxburgh, 1966) the northern part is in the epidote-amphibolite facies, while the southern part is in the greenschist facies.

At the same time as the orogenic belt was being formed along northern Venezuela, the sea that had extended as far south as the present location of the Orinoco river began to retreat to the north and west (Mencher, et al., 1953). Some volcanic activity and deformation continued into the Paleocene, but in general the rocks are less deformed than those of the Cretaceous. Paleocene deposition was restricted to a narrow

trough which ran from the state of Falcon (Fig. 1) in the northwest, to Trinidad in the east. The uplifted area on the north provided a source for the flysch and wildflysch deposits of the Guarico formation that filled the trough in the east (Stainforth, 1966). During the early Eocene much of Venezuela was apparently emergent. Deposition in the Eastern Venezuela geosyncline was confined to a zone south of the present location of the Araya and Paria peninsulas and south of the North range of Trinidad (Dallmus, 1965). Lower Eocene limestones are present on the southern portion of the island of Margarita (Taylor, 1960).

In western Venezuela there was more extensive sedimentation. To the northwest of the present location of the Andes the Trujillo formation, a series of possibly as much as 6000 meters of dark carbonaceous and micaceous sandy shales and micaceous sandstones, was deposited. The sediments are undeformed, and there is a lack of igneous materials, indicating that this was not a eugeosynclinal area. In the remainder of western Venezuela the sediments are thinner, but of a similar lithology.

The mid-Eocene orogeny was an event that affected most of the Caribbean. Eocene volcanic rocks are present in the Greater Antilles (Mattson and Pessango, 1971) and in the

Guajira and possibly the Paraguana peninsulas (Fig. 1). Layer A" which is continuous over most of the Caribbean is a chert layer of Eocene age. According to Mattson and Pessango, Layer A" may have been formed by the input of large amounts of siliceous material from the nearby volcanic centers.

The Paleocene-Lower Eocene trough south of the Coast range was uplifted during this orogeny and the shelf to the south was downwarped creating a new trough which swung to the southwest and formed the Barinas basin (Fig. 3). The Maracaibo platform was deformed by tilting and block faulting. In western Venezuela the Misoa formation was deposited conformably on the Truijillo formation, and unconformably on Cretaceous and lower Eocene sediments. Deposition continued at the present location of the Andes through the late Eocene.

From Oligocene to Recent time the east-west trending axis of deposition in the Eastern Venezuela geosyncline moved progressively southward from its location in the Eocene on a line running through Barcelona (Fig. 1), to its location in the Pliocene midway between the present north coast and the Orinoco River (Hedberg, 1950). A series of northward dipping thrust faults developed on the southern boundary of the Coast range and the Interior range during the Oligocene and Miocene (Peirson, 1965; Hedberg, 1950). The faulting and uplift on

the northern boundary continued until the Pliocene.

During Oligocene and early Miocene time a narrow east-west trending trough covered most of the state of Falcon, and also parts of the adjoining states. The total thickness of sediments is about 4000 meters (Wheeler, 1963).

Uplift began in the Venezuelan Andes and the Perija range during the early Oligocene and reached its climax in Miocene-Pliocene time. The formation of terraces in some valleys of the Venezuelan Andes indicate that uplift may still be occurring (Kovisars, 1971). At the same time as the Andes were being uplifted the Maracaibo basin was subsiding. As much as 6000 meters of post-Eocene sediments were deposited (Miller, et al., 1958).

The El Pilar fault zone (Fig. 2) extends from the Gulf of Cariaco, south of the Araya peninsula to the Gulf of Paria, and may extend into Trinidad. Molnar and Sykes (1969) proposed that there have been large amounts of right lateral strike-slip motion along the fault and that the Caribbean plate is moving eastward with respect to the South American plate at approximately 1 cm/yr. Rod (1956) estimated that there was more than 100 km of right lateral displacement along the fault. Metz (1968) believes that the motions along the El Pilar fault are vertical, and that the horizontal movement along this fault

since the end of the Cretaceous is less than 15 km. The evidence for this is: 1) the lower Cretaceous Cutacual formation outcrops on either side of the fault and since this facies does not occur elsewhere it limits the horizontal movement along the fault; 2) the upper Cretaceous San Antonio rocks on both sides of the fault are of the same light colored facies; 3) the east-northeast trending belt of lower Cretaceous El Cantil limestones appears to continue across the fault into the metamorphic belt of the Araya-Paria peninsula.

Potter (1968), from mapping of the North range of Trinidad, estimated that the northern block has been uplifted by as much as 1800 meters, and feels that there is no evidence for lateral movement.

Seismic profiles (Bassinger et al., 1971) from the Dragons Mouth (between Trinidad and Venezuela) east to 59°W indicate a high angle vertical break between the El Pilar block and the sediments to the south. No gouge zone can be seen on the seismic profiles as would be expected in a wrench fault.

The Sebastian fault (Fig. 3) extends along the north coast of Venezuela and appears to join the northeast end of the Bocono fault, which runs in a northeast-southwest direction along the central valley of the Venezuelan Andes. A study of the postglacial movement of the Bocono fault was made by

Schubert and Sifontes (1970). Based on an examination of the Victoria and Zerpa lateral moraines they concluded that the two sets of moraines had been offset by an average distance of 66 m since the time of the deposition of the moraine, about 10,000 years ago. The sense of movement was right lateral, with no evidence of recent vertical displacement.

Acquisition and Reduction of Gravity Data

The gravity data used in this study were obtained from many different sources. Land data were obtained from oil companies operating in Venezuela and Trinidad, Cartografia Nacional (the Venezuelan government mapping agency), and from surveys made by the author and others using LaCoste and Romberg geodetic gravity meters. Previously published sources of data included measurements over the Venezuelan Andes (Hospers and Van Wijnen, 1959), across the Coast range near Caracas (Smith, 1957), on the islands of Aruba, Curacao, and Bonaire (Lagaay, 1969), and a few widely spaced measurements in Venezuela (Woollard and Rose, 1963).

Sea data were obtained from oil companies, the Atlantis II-54 cruise of the Woods Hole Oceanographic Institution, and from ESSA (now part of the National Oceanic and Atmospheric Administration).

The primary gravity base station to which the gravity data are referenced is the Cartografia Nacional gravity base station, St. Innes #1, in Caracas. A description of this station is shown in Figure 4. A gravity value of g = 978065.87 mgal was assumed for this station. Secondary base stations were established at several other cities in Venezuela; descriptions and measured gravity values for these stations are given in Appendix I.

Since the oil company data comprised numerically the largest portion of the land data, the reduction of these data will be described in detail.

The gravity measurements were made by or for the exploration departments of companies operating in Venezuela. Most of the measurements were made in the time period between 1946 and 1957. Several different types of gravity meters were used in obtaining land data, but those most frequently used were the LaCoste and Romberg exploration meter and the North American exploration meter. These instruments had high drift rates and a limited range of gravity over which the meter could be used without having to be reset. (For LaCoste and Romberg meter #72, drift was of the order of 0.1 mgal/hr. and the range was 150 mgal.) The high drift rate necessitated making reoccupations of base stations several times a day. The drift

Figure 4: A description of the main base station used for the gravity survey in Venezuela.

COUNTRY	NEAREST CITY	GRAVITY STATION DESCRIPTION		
Venezuela	Caracas			
STATE / PROVINCE		STATION NAME		
Dto Federal		Sta. Ines.		
LATITUDE	LONGITUDE	ELEVATION	W.H.O.L STATION NO.	GRAVITY VALUE (g)
10°30.7'N	66°55.2'W	914.16	643	

DESCRIPTION

In the Sta Ines Building opposite the office of "Ferrocarril Nacional" the building is now occupied by the National Guard. The building is in Cano Amarillo at the west end of Avienda Oeste 2. The station is a bronze disk set in concrete ledge. 1 disk inscribed "MOP Cartografia Gravidad Sta. Ines.

DESCRIBED BY A. Folinsbee — DATE May 19, '70

POSITION CONTROL DESCRIPTION

M.O.P.Cartigrafia

ELEVATION CONTROL DESCRIPTION

Same as above.

DIAGRAM

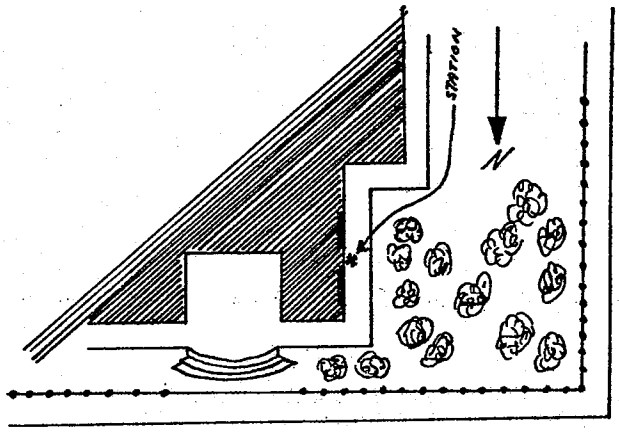

DIAGRAM BY Jose Campero — DATE Feb 70

Assumed Gravity Value of 978065.87

This station is known as St. Innes#1

determined from these reoccupations was applied linearly (with respect to time) to the measurements made between reoccupations. For a more detailed account of methods used in exploration gravity surveys, see Dobrin (1960).

It was necessary to make new gravity measurements at one or more of the stations in each oil company survey, in order to determine the correction required to convert the relative gravity values of the survey to values based on the St. Innes base station. These new measurements were made by the author during a trip to Venezuela in February 1970. The most serious problem encountered in making these new measurements was ensuring that the new measurements were made as close as possible to the same location and elevation as the measurements made by the oil companies. Some surveys contained one or more stations for which a description of the location was available. For surveys with described stations the elevation differences between the measurements was probably no greater than .3 meters, even though in some cases, for example, it was not clear whether the measurements had been made on the sidewalk or the road. The difference corresponds to errors in gravity of ±.07 mgal. Some surveys, however, had no descriptions of locations available at all. In these cases undescribed stations were used, but were chosen from areas having low relief and constant gravity in order to minimize the difference between the old

measurement and the reoccupation, and were then located on the ground with the aid of Cia. Shell de Venezuela Gr series maps. The horizontal positions of these stations could be determined to ±50 meters, and vertical errors could be held below ±1 meter by occupying only stations in flat terrain, causing errors in g of ±0.3 mgal for these stations. (See Appendix IV for a discussion of how the errors were estimated.) A series of four stations approximately 5 km apart was located on the Shell map and reoccupied. A plot (Fig. 5) of the correction which was required to reduce these stations to the St. Innes datum, versus observed gravity shows that the maximum deviation of these four stations from their mean is 0.2 mgal, which agrees with the estimated error.

All surveys made by the Cia. Shell de Venezuela were tied to one base station in Maracaibo. The scale factor for the Shell gravity meters was determined over a 32 mgal calibration range south of Maracaibo. An attempt was made to reoccupy this range but because of construction in the last ten years none of the stations could be located. In order to determine the accuracy of the Shell calibration range, measurements were made at a series of Shell gravity stations extending from north of Maracaibo to Merida in the

Figure 5: The correction to convert the Shell gravity value to a datum level based on the St. Innes #1 gravity station: plotted versus observed gravity. The circles are stations which were described and the triangles are stations which were located from maps.

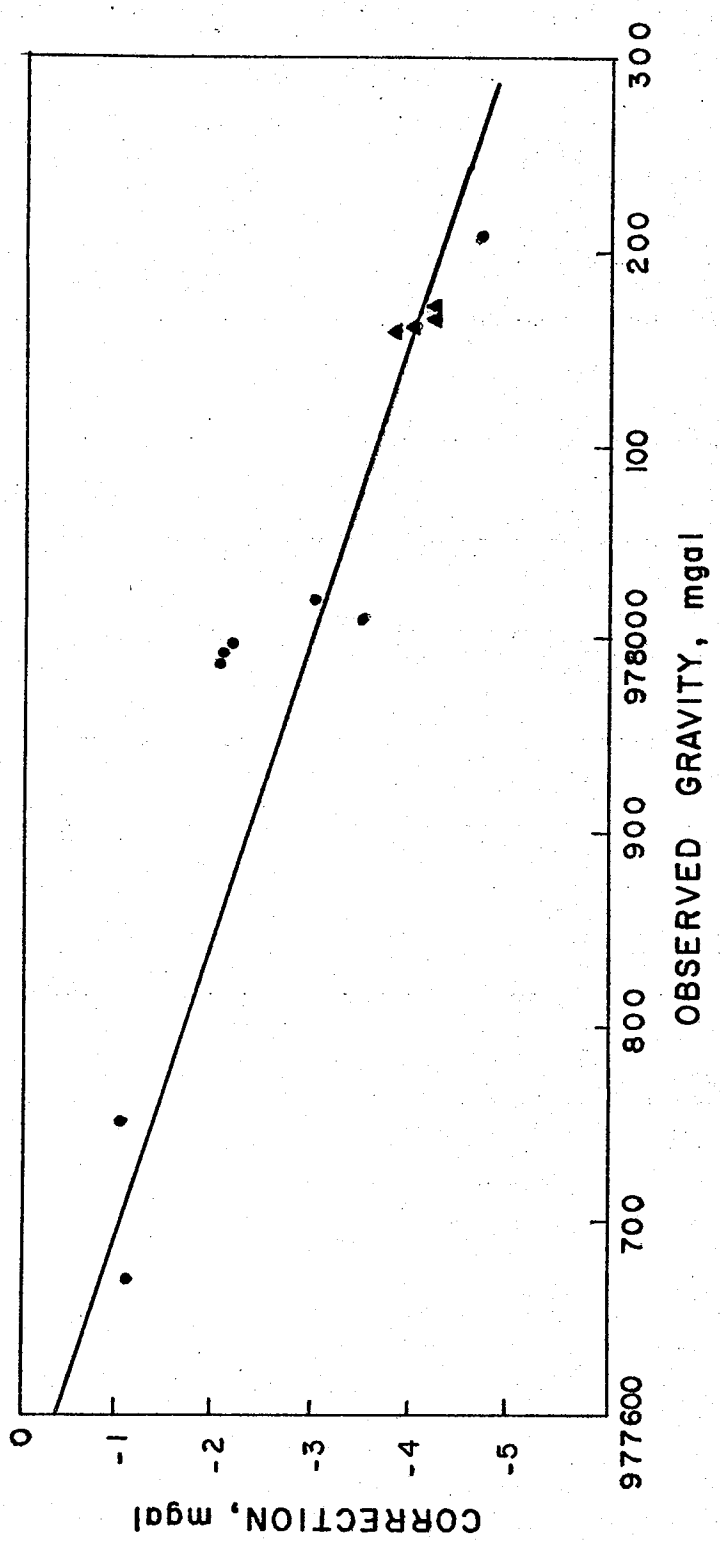
CORRECTION, mgal
0
-1
-2
-3
-4
-5
977600
700
800
900
978000
100
200
300
OBSERVED GRAVITY, mgal

Venezuelan Andes. The corrections versus observed gravity were then plotted (Fig. 5). Since the corrections vary systematically with observed gravity the Shell calibration range appears to have been in error by 0.6%; i.e., the nominal value of g for the calibration range was 0.6% higher than the actual value of g for the range. The error was taken into account in the reduction of the Shell data.

For the land data obtained from the other oil companies, it was not possible to determine a scale factor correction because of the limited amount of data. However, since these surveys were tied to local bases for each prospect area and the range of observed g in each survey area was usually less than 150 mgal, the errors caused by an incorrect scale factor are probably less than 1 mgal.

In the land data obtained from the various oil companies, the quality of the elevation control for the stations varied from survey to survey. For the reconnaissance surveys, the elevation control was provided by precision micro-barometers (altimeters), while for other surveys a transit and stadia rod were used. The internal precision of a survey was probably better than ±4 meters for transit and stadia rod, and ±8 meters for the microaltimeter. In the case of a Mene Grande survey in the Barinas basin the measured elevations were consistantly

shifted by +20 meters with respect to a Cartografia Nacional level line running through the area. This was probably a result of an estimated elevation being used as the take-off point for the survey. After the 20 meter bias was removed the elevations agreed to ±2 meters. Where possible the other surveys were checked against elevation on the topographic maps, but no other significant biases were found. In summary, the elevations are probably good to ±10 meters, and in most cases are as good as ±5 meters.

The station locations were given in coordinates North and East with respect to various coordinate systems. The origins and basic coordinates of each system were obtained from Coordinate Systems of Venezuela, (Venezuelan Oil Scouting Agency, 1957). A program originally designed to convert universal transverse Mercator coordinates to latitude and longitude was modified to convert the positions to latitude and longitude. (See program COORD, Appendix II.) The coordinates were given to the nearest 10 meters. An estimate of the accuracy of the coordinate was obtained by converting to latitude and longitude the coordinates of stations whose actual location relative to a topographic feature (i.e., a road, intersection, or stream junction) was known. The location of the station was then plotted on a 1:100,000 scale topographic map. The indicated and actual locations of the station were compared and from this comparison

an estimate of ±0.2 km error in the coordinates was obtained. The above errors in principal facts give rise to an estimated maximum error of ±4 mgal in the free-air anomalies and ±3 mgal in the Bouguer anomaly for the land data collected from the oil companies.

Cartografia Nacional (C. N.) was another source of land measurements. Twenty percent of the measurements from this source were actually made by C. N. along level lines, and the remainder were originally made by oil companies in eastern Venezuela. C. N. made gravity and elevation ties to the oil company surveys, and recalculated the scale factors for the gravity meters used in the surveys. The estimated accuracy of these measurements is ±1 mgal. The C. N. measurements along level lines are of high accuracy with elevation errors of .5 meters and closing errors on the gravity loops of .1 mgal.

In order to fill in the gaps left in the data from oil company and C. N. surveys, a survey was made by the author across the Venezuelan Andes using the LaCoste and Romberg geodetic meter (G-18). The stations were located at bench marks put in by C. N. Additional data were obtained from a survey made by Dr. S. Biehler and the author in 1968 across the North range in Trinidad using the LaCoste and Romberg meter, G-153. The stations were located at bench marks. Ties were

made to a Texaco of Trinidad gravity survey which covered the southern part of the island. This resulted in almost complete coverage of the island.

A source of gravity data over water was offshore oil company surveys. The regions surveyed were Lake Maracaibo, the Gulf of Venezuela, the Gulf of Paria, and the Gulf of Cariaco. For these surveys, depth was measured to a tenth of a meter, and position was measured by various electronic methods with a relative accuracy better than .2 km. For the surveys of Lake Maracaibo, Gulf of Venezuela, and Gulf of Paria ties were made to the base stations used for these three surveys. For the Gulf of Cariaco survey no direct tie could be made since the location of the base station could not be determined. A tie was made by comparing the contoured sea data with contoured land data, and determining what adjustment had to be made to the sea values so that the contour lines would match. The tie is believed to be better than 1 mgal.

Another source of sea data was the Atlantis II-54 cruise survey. The data were collected with a gyrostabilized vibrating string accelerometer in December of 1969 on a cruise going from Panama to the Virgin Islands. For a review of the data collection and reduction procedures see Bowin, et al (in preparation).

Chain cruise 55 was an additional source of sea data.

The tieing together of the land and the oil company offshore surveys was done with a LaCoste and Romberg geodetic gravity meter, G-18. The meter readings were corrected for earth tides and for an instrument drift of .001 mgal/day. There was a total of 15 repeated measurements at 8 different stations. The standard deviation between measurements was 0.02 mgal, with the largest difference being 0.1 mgal.

The combined data points from all sources gave a total of 6000 stations with principal facts, but in some areas the stations were separated by less than 1 km. In order to remove some of the closely spaced points, the data were sorted and abstracted to a grid spacing of 10 x 10 per degree square. If there were more than one point in a grid square, then the point closest to the center of the square was chosen. A total of 2500 abstracted points was obtained. Free-air and Bouguer anomaly maps of the region between 75°W to 60°W and 8°N to 14°N were made at a contour interval of 20 mgal. A map of the distribution of the points is shown in Figure 6.

The gravity data were reduced in the following way. The 1930 International Gravity Formula was used to compute the theoretical gravity.

Figure 6: A map of the gravity data used for producing contour maps and profiles. Each dot represents one gravity measurement.

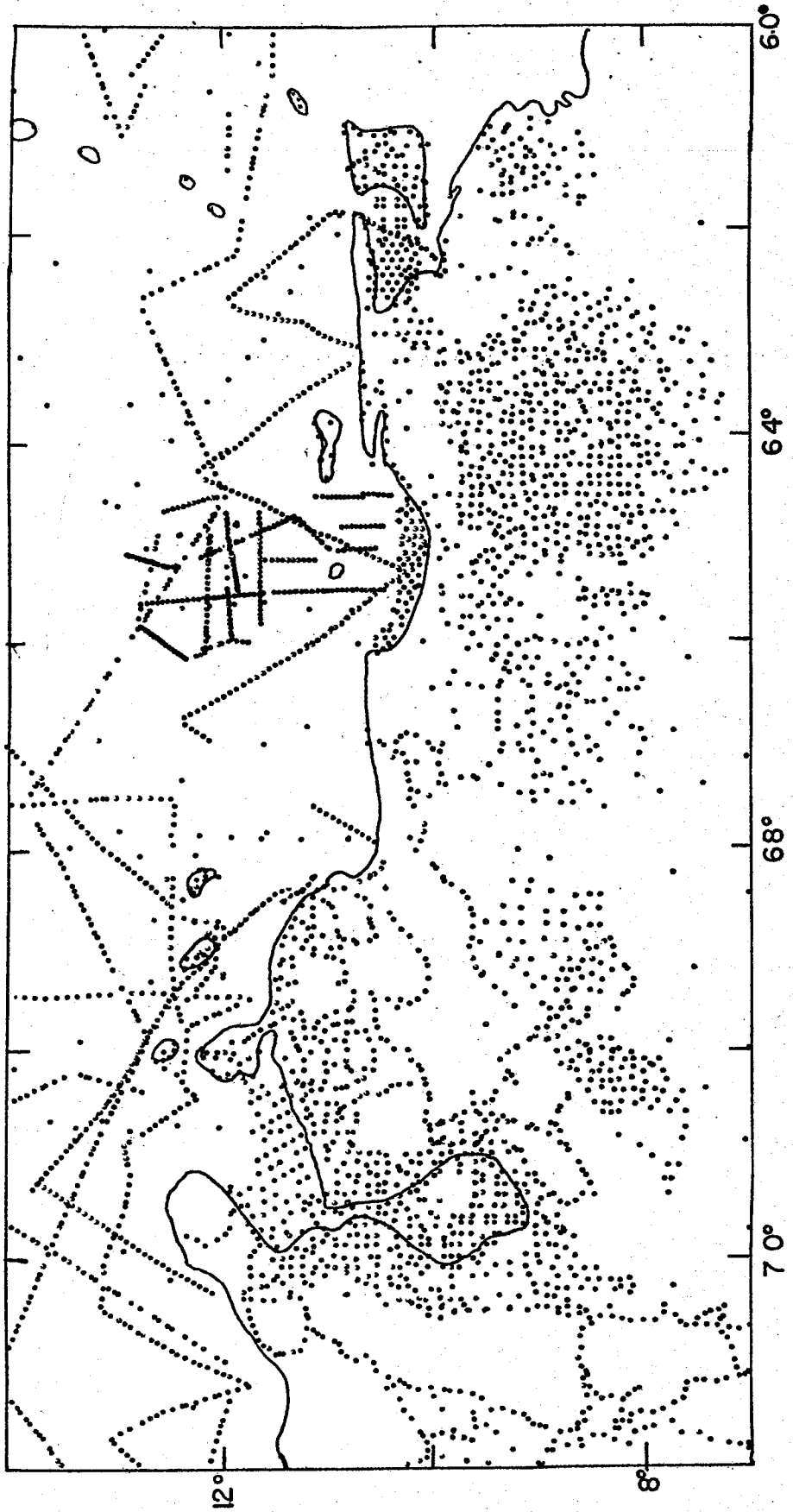
60°
64°
68°
70°
12°
8°

$$\text{Theoretical gravity} = 978{,}049.0(1 + 0.0052884 \sin^2\phi - 0.0000059 \sin^2 2\phi) \text{ mgal} \qquad \phi = \text{latitude}$$

The following formula was used to compute the free-air correction:

$$\text{free-air correction} = 0.30855 + .00022 \cos(2\phi)\, h - (.001h)^2 \times .072$$

h = elevation in meters

For the calculation of Bouguer anomalies a density of 2.67 grams/cm^3 was used. Complete Bouguer anomalies were not calculated except in the case of the two profiles that cross the Venezuelan Andes. Hospers and Van Wijnen (1959) calculated the terrain correction for the profiles they made across the Andes. It was not possible to directly calculate terrain corrections, for the profile made by the author with the G-18 meter across the Andes, because the only topographic map of the region that was available was a scale of 1:1,000,000. This scale did not provide enough detail to make it possible to calculate the contribution to the terrain correction from Hayford zones B through F (Dobrin, 1960). However, where possible the stations were located in areas of minimum relief, and terrain corrections were estimated from the topography shown on the 1:1,000,000 sheet. The terrain corrections are as large as 25 mgal, and are probably accurate to 5 mgal.

RESULTS

The trends of the free-air anomaly map (Fig. 7) are similar to the structural trends on the geologic map. In eastern Venezuela the anomalies trend east-west. At the junction of the Caribbean mountains and the Venezuelan Andes, the trend is to the southwest. There is a trend of high anomalies over the Venezuelan Andes which joins the highs over the Perija range, and a trend of low anomalies over the Maracaibo basin which terminates at the junction of the Perija range and the Andes. There is a series of positive and negative gravity anomaly belts running north-south parallel to the Lesser Antilles. From east to west these belts are: the negative gravity belt running west of Tobago and north along the Lesser Antilles to north of Cuba, the belt of highs over the Lesser Antilles, and the belt of lows over the Aves swell. The southern ends of this last feature can be seen on the free-air anomaly map.

The belt of highs over the Aves swell swings to a westerly direction and runs along the chain of offshore islands from Blanquilla to Curacao, and then moves shoreward over the Guajira peninsula where it terminates. The magnitude decreases

Figure 7: Free-air anomalies of the study area at a contour interval of 20 mgals. The heavy lines labeled A-E show the location of profiles used to compute structural models.

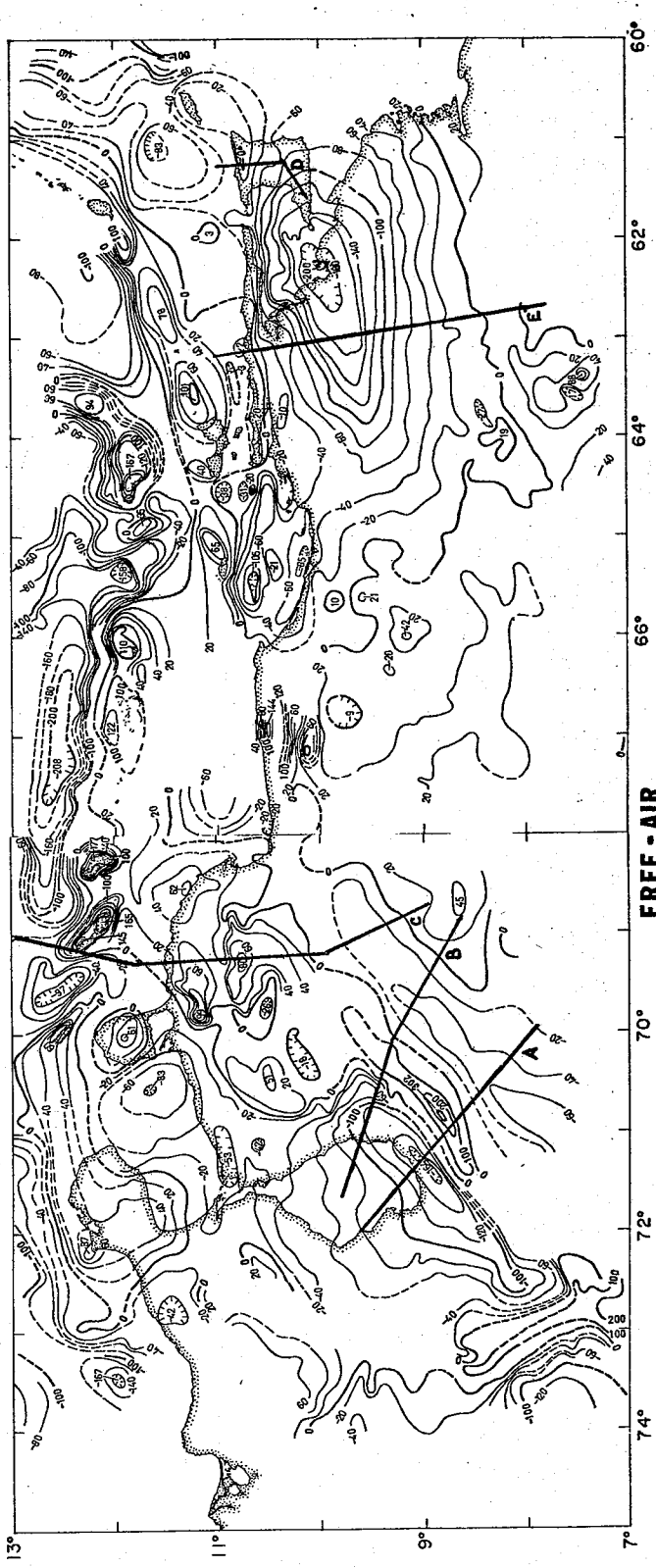
60°
62°
64°
66°
70°
72°
74°
13°
11°
9°
7°
A
B
C
D
E
FREE-AIR
ANOMALIES

at the western end. The free-air anomaly over Bonaire is 177 mgal, over Curacao 165 mgal, and over Aruba 60 mgal.

The belt of highs over the Antilles swings to the southwest and the axis of the high passes over the northern edge of the islands of Margarita and Tortuga. Along the southern edge of the Venezuelan basin there is a region of negative free-air anomalies. There are two lows over the Gulf of Cariaco, both of which run east-west. The inner low (-85mgal) is centered over a deep sedimentary feature, the Cariaco basin, and the outer low (-105 mgal) is centered over the Cariaco trench. Over the sedimentary basin in the Gulf of Venezuela there is a low of -83 mgal. Located over the Eastern Venezuela basin is a prominent low, 400 km long and 180 km wide. A low of -164 mgal is located over the southeastern edge of the Maracaibo basin, and there is a high of more than 300 mgal to the southeast over the Venezuelan Andes.

The regional free-air anomaly map shown in Figure 8 is calculated from a spherical harmonic expansion of the Earth's gravity field and is referenced to the international gravity formula. The coefficients used in the expansion were determined from measurements of satellite orbits by Gaposchkin and Lambeck (1969), and contained coeficients up to the twenty-second order. This means the the regional free-air value at

Figure 8: Regional free-air map. Values are computed from a satellite derived spherical harmonic expansion of the potential field of the Earth using the 1969 SAO coefficients (Gaposchkin and Lambeck, 1969), and are referenced to the International Gravity formula of 1930.

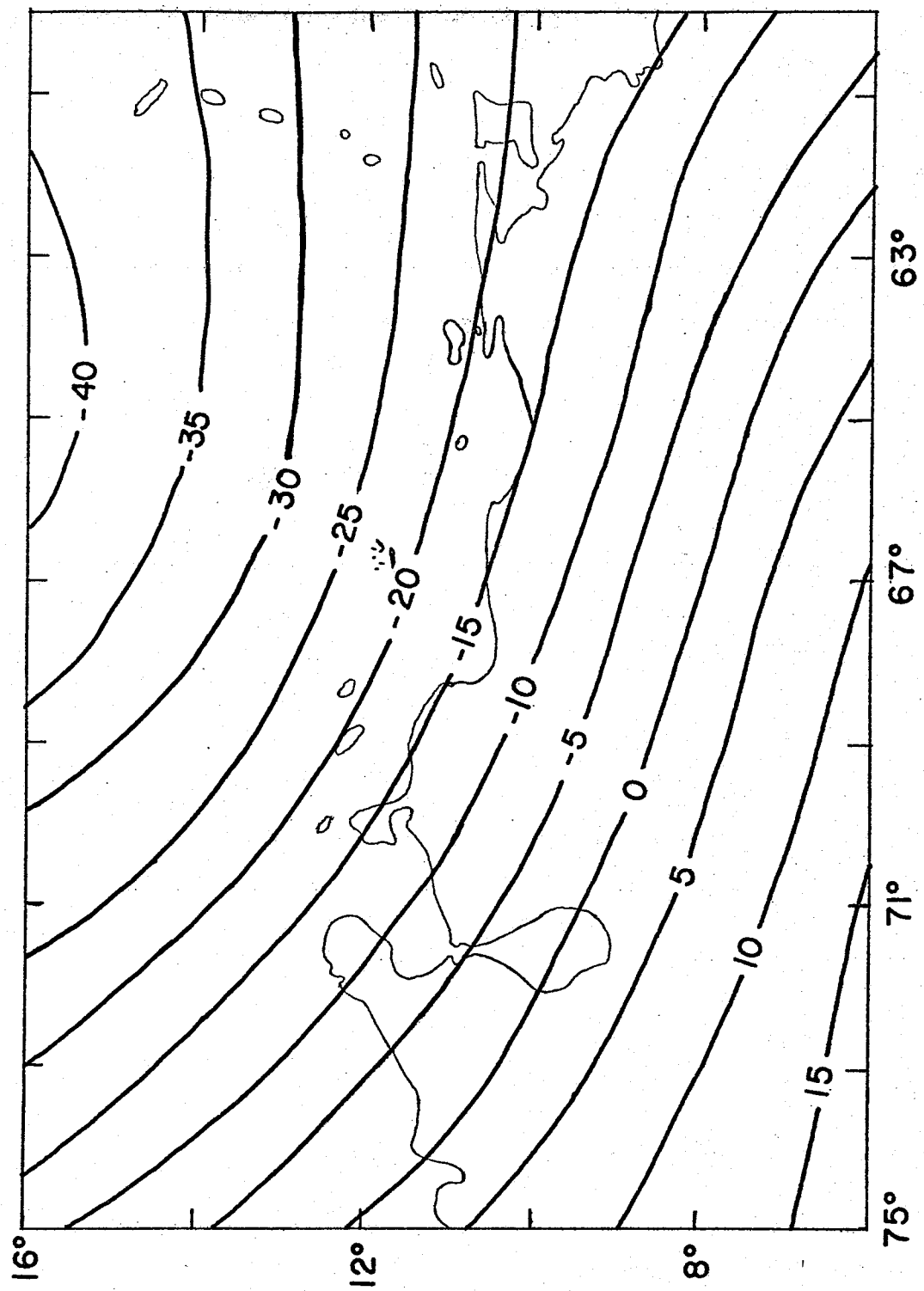
-40
-35
-30
-25
-20
-15
-10
-5
0
5
10
15
16°
12°
8°
75°
71°
67°
63°

a point approximately represents the average free-air anomaly in a circle of 500 km radius about the point. From Figure 8 it can be seen that southern Venezuela has a regional free-air value of about 0 mgal, while the value over the offshore islands to the north is about -20 mgal. If the difference between the free-air anomalies and the regional free-air anomalies were contoured, the map would be similar to that shown in Figure 7, except that the level of the highs over the offshore islands would be increased by about 20 mgal.

Bouguer Anomaly Map

The most prominent feature on this map is the large negative anomaly centered over the Eastern Venezuela basin. The anomaly is elongated with the major axis bearing 60° east of north. The minimum anomaly is -199 mgal. The low is a-symmetrical: the -20 mgal contour is located 80 km north of the axis, and 130 km south of the axis.

Along the North range in Trinidad there is a minimum Bouguer anomaly of -45 mgal, compared to values of -35 mgal on the north and south sides. Because of the sparseness of the data over the Paria peninsula, it is not possible to determine if the low continues to the west. Further to the west (67°W) the Bouguer anomaly across the Coast range does, however, show

Figure 9: Bouguer anomalies of the study area at a contour interval of 20 mgals.

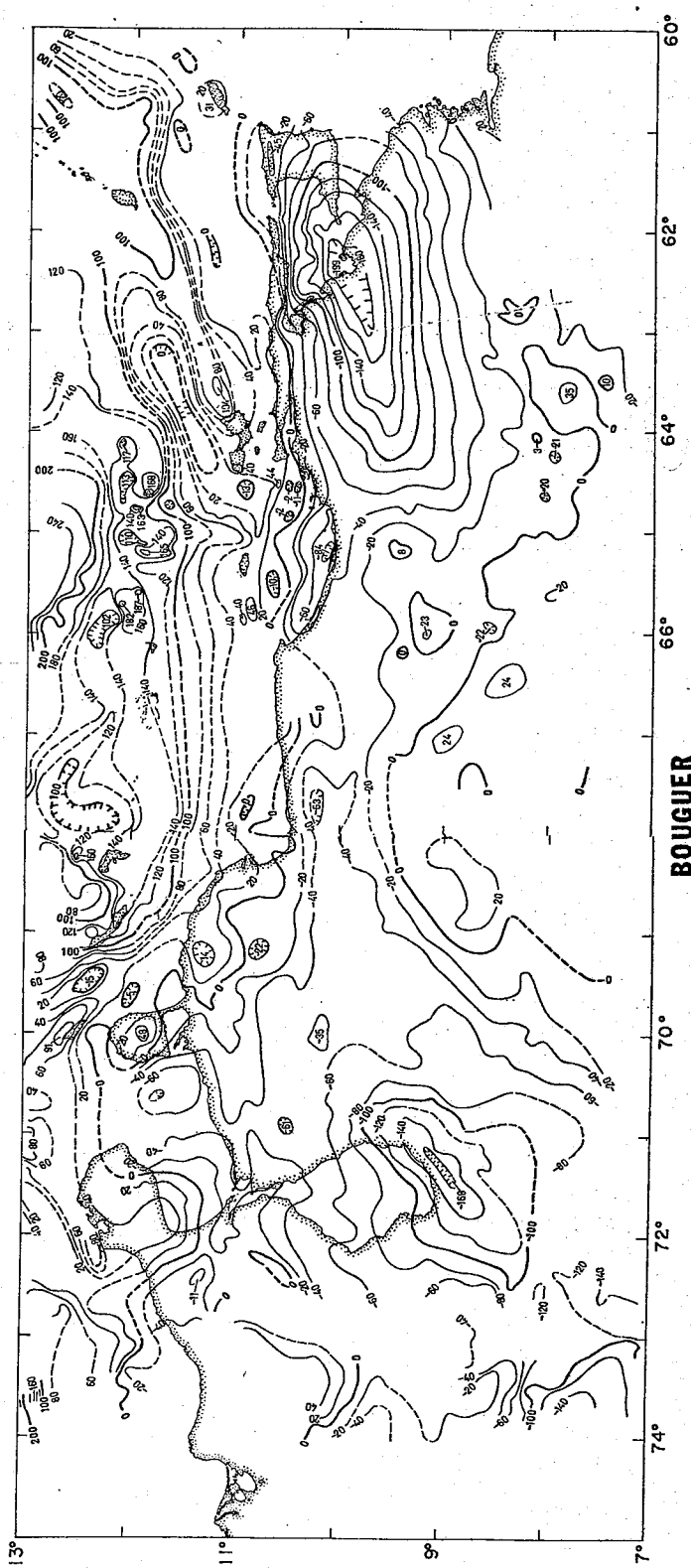

BOUGUER ANOMALIES

a minimum of -60 mgal centered over the highest topography.

Another low is centered over the Gulf of Cariaco. The feature runs east-west, and has a minimum value of -80 mgal. The axis of the low is landward of the Cariaco trench. A large low is associated with the Maracaibo basin. The Bouguer anomaly decreases slowly from -10 mgal at the northwest edge of the basin to -160 mgal at the center of the basin. Then it rises sharply to -40 mgal over the Venezuelan Andes. There is no minimum in the Bouguer anomaly over the Venezuelan Andes. Over the Barinas basin to the southeast of the Andes, the Bouguer anomaly decreases to -50 mgal.

There is a gravity high centered over the El Baul swell with a Bouguer anomaly of 20 mgal. A high of 48 mgal occurs over the Pariguana peninsula. To the west of this high there is a low of -80 mgal in the eastern part of the Gulf of Venezuela. Over the Guiana shield the Bouguer anomaly is close to zero. There is a north-east to south-west trending high of greater than 80 mgal offshore of the Guajira peninsula, and further to the north over the continental slope is a low of +20 mgal. A high is centered over the Dutch island of Aruba and an east-west trending high runs from the island of Curacao in the west to the island of Blanquilla in the east.

EARTHQUAKE FOCAL MECHANISMS

Numerous earthquake epicenters are found in a zone about 20 km wide centered on the Bocono fault (Figs. 3 and 10). An effort was made to determine focal mechanisms for some of these earthquakes, using data from WWSN stations. Only one of the events was large enough to provide good records at WWSN stations. This event occurred on July 19, 1965 at 0413 GMT with a magnitude of 5.3. The epicenter was located at 9.1°N, 70.5°W, at a depth of 41 km. This locates the event within 10 km of the surface trace of the Bocono fault. The short and long period vertical seismometer records for all available WWSN stations were examined to determine if the movement at the station was compressional or dilational. When possible the data from the long period seismometers were used, but for half the stations this could not be done due to the low amplitude of the signal. The results were plotted on a Schmidt stereographic net (Fig. 10) and a focal mechanism was determined. As can be seen from Figure 10 there are almost no data in the southwestern quadrant. The results appear to indicate an almost vertical fault plane with strike-slip movement along the plane. The two possible solutions are: 1) a fault plane striking N30°E, with right lateral strike-slip movement, or

2) a fault plane striking N60°W with left lateral strike-slip movement. Because the first solution shows a fault plane approximately aligned with the Bocono fault which strikes N40°E, it is the most probable solution.

Figure 10: Earthquake epicenters in the Caribbean for the period 1/1/61 through 17/9/68, as compiled by U.S. Coast and Geodetic Survey.

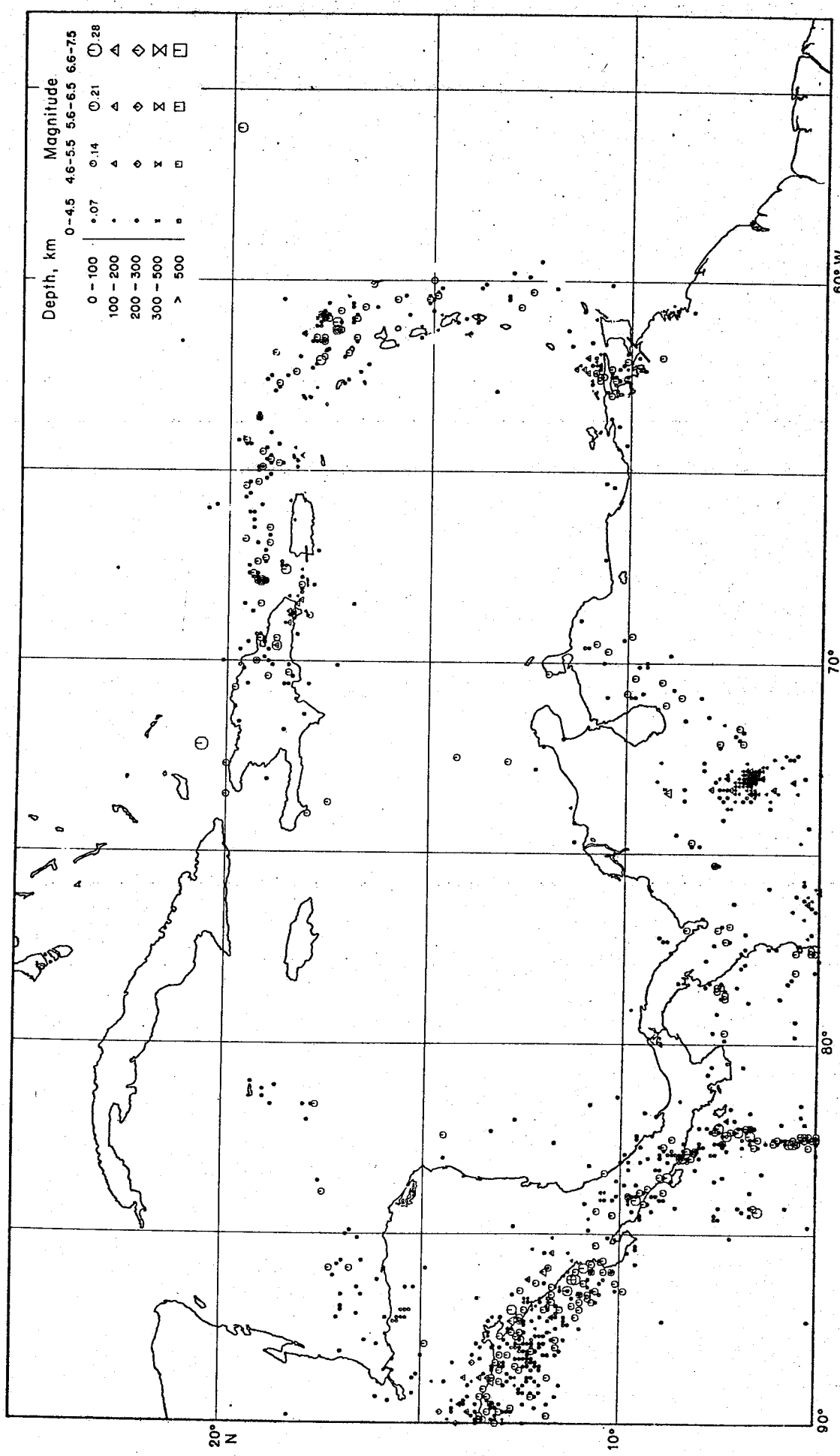
Depth, km
Magnitude
0-4.5
4.6-5.5
5.6-6.5
6.6-7.5
0 - 100
100 - 200
200 - 300
300 - 500
> 500
.07
.14
.21
.28
60° W
70°
80°
90°
20° N
10°

Figure 11: A plot of the first motions for an earthquake occurring in the region of the Bocono Fault in the Venezuelan Andes. Open circles indicate dilation and solid circles indicate compression.

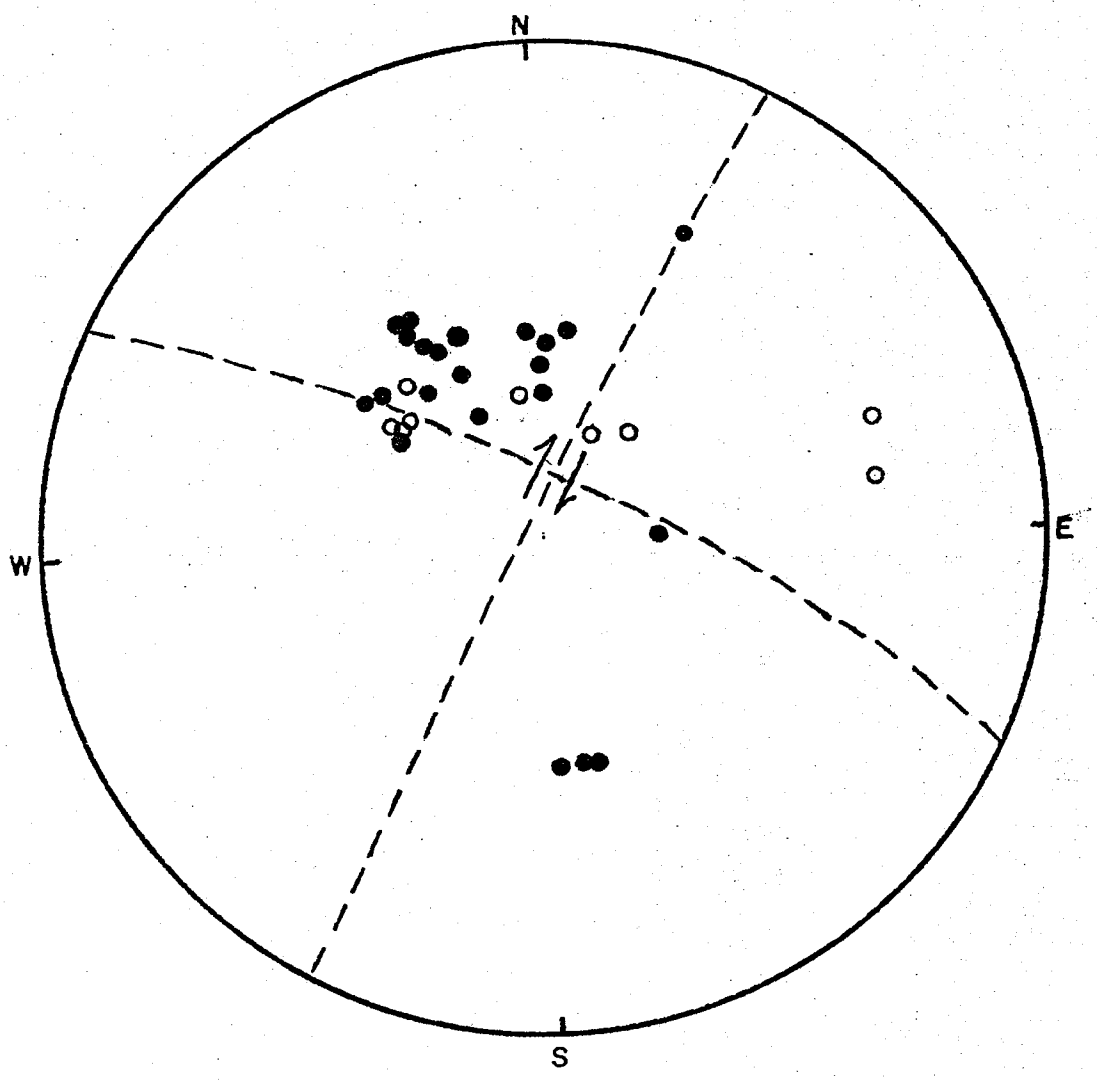

ORIGIN TIME: 9-07-65 0413GNT
LOCATION: 9.1°N 70.5°W
DEPTH: 41km
MAGNITUDE: 5.3

INTERPRETATION

A polygon method (Talwani and Ewing, 1960) for the calculation of gravity due to a two dimensional structure was used in the interpretation of the gravity data. The structure along a profile is represented in two dimensions by a set of polygons each of constant density. (The structure in the third dimension is assumed to be uniform.) The program then calculates the gravity anomaly produced by the set of polygons. The shape of the crust mantle boundary was determined by an iterative procedure such that the RMS difference between the theoretical and the observed gravity is a minimum. (See Appendix II for a more complete discussion of the iterative procedure used.) Since the inverse gravity problem is non-unique (i.e. there are an infinite number of mass distributions that will give rise to a given observed gravity anomaly), this computation procedure provides a quick method of determining what range of models will give an acceptable fit to the observed gravity.

The following approximations and assumptions will cause the theoretical structure to differ from the actual structure. All the models used make the assumption that there are no lateral density variations in the upper mantle. The actual structure may diverge considerably from two dimensionality, and the density value used for the rock layers may be incorrect, but the models will still give an estimate of the structure.

In addition to calculating the theoretical gravity associated with a particular model, the mass in a column of material of 1 cm^2 area to a depth of 40 km, was also calculated. The mass/cm^2 of a normal column of crustal material is 11840 kg/cm^2 (Emery, et al., 1970). Although there may be a bias of the calculated mass/cm^2 away from the normal value due to an incorrect choice of densities, changes in the calculated value indicate the amount by which a region is out of isostatic equilibrium. A mass variation of 10 kg/cm^2 corresponds to a change in gravity of 4.2 mgal for an infinite slab.

A total of 5 profiles were constructed for the purpose of making model studies. (See Figure 7 for location of profiles.) These profiles were constructed in the following way. Each profile was defined by a straight line or several

straight lines that run perpendicular to the structure and gravity anomalies. All gravity data within a distance of 20-40 km, depending on the profile, were then projected at right angles onto this line. A smoothed curve was then drawn through the data points.

The densities assumed for the sediments in the basins were from Hospers and Van Wijnen (1959) and were based on measurements of core samples and density logs run in wells in the Maracaibo basin. The sediments were divided into two groups, Eocene and post-Eocene. Within each of these two groups, densities were assigned on the basis of depth of burial of the sediment. The densities varied from 2.2 gm/cm^3 for shallow post-Eocene sediments to 2.65 gm/cm^3 for deeply buried Eocene sediments. A plot of density versus depth is shown in Figure 12. A basement density of 2.7 gm/cm^3 and a mantle density of 3.3 gm/cm^3 were used.

Profile A

The first profile (profile A, Fig. 13) under consideration runs from the northwest side of Lake Maracaibo, southeast across the Venezuelan Andes and the Barinas basin to the El Baul swell. The Bouguer anomaly at the northwestern end of the profile is -40 mgal. It decreases to a minimum of

Figure 12: A plot of the density vs depth for various ages of sedimentary rocks. The heavy lines represent an average of data from the Maricaibo Basin (Hospers and Van Winjen, 1956), while the light lines are taken from well logs made in Trinidad (Higgins, 1959).

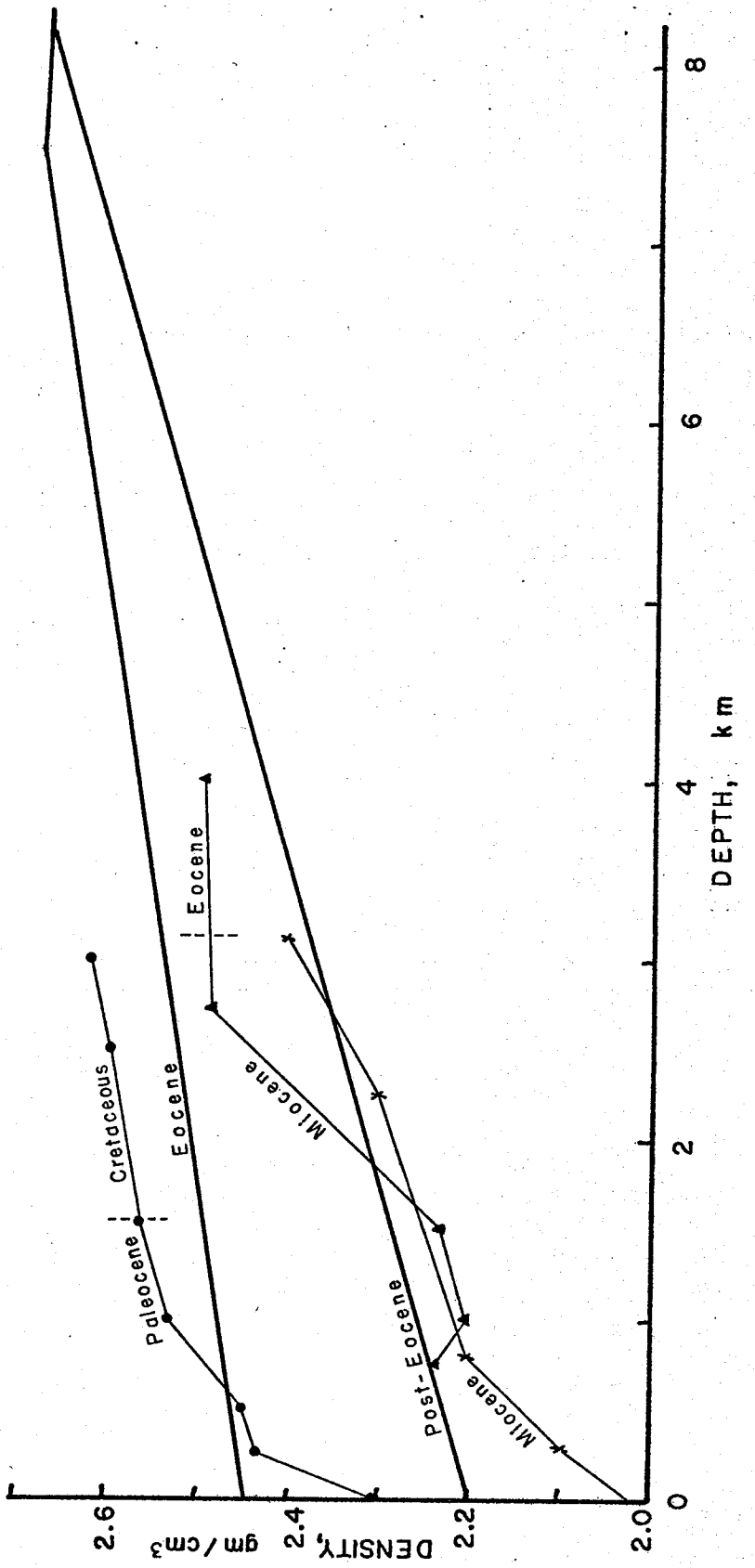
DENSITY, gm/cm³
2.0
2.2
2.4
2.6
DEPTH, km
0
2
4
6
8
Cretaceous
Paleocene
Eocene
Eocene
Miocene
Post-Eocene
Miocene

Figure 13: Profile A

Figures 13-17 include Profiles A-E, to which the following explanation applies. These profiles contain gravity anomalies and theoretical structure sections. The structure section which is derived from available geologic data has been modified so that the observed and calculated gravity anomalies are similar. For the purpose of computation of the theoretical gravity anomalies the structure is assumed to be two dimensional. The numbers of the polygons are at the bottom of each caption and give the general rock type and the density of each polygon. The rocks making up a single polygon are of approximately the same density, but they are not continuous stratigraphic units, and in some cases are not even the same age or lithology. This is particularly applicable to the polygons that extend across the ocean-continental boundary. The crustal mass in kg/cm^2 is calculated to a depth of 40 km.

1. Post-Eocene Sediments, 2.3 gm/cm^3
2. Post-Eocene Sediments, 2.36 gm/cm^3
3. Post-Eocene Sediments, 2.48 gm/cm^3
4. Eocene Sediments, 2.5 gm/cm^3
5. Eocene Sediments, 2.56 gm/cm^3
6. Eocene Sediments, 2.64 gm/cm^3
7. Basement, 2.67 gm/cm^3
8. Sediments, 2.53 gm/cm^3
9. Mantle, 3.3 gm/cm^3

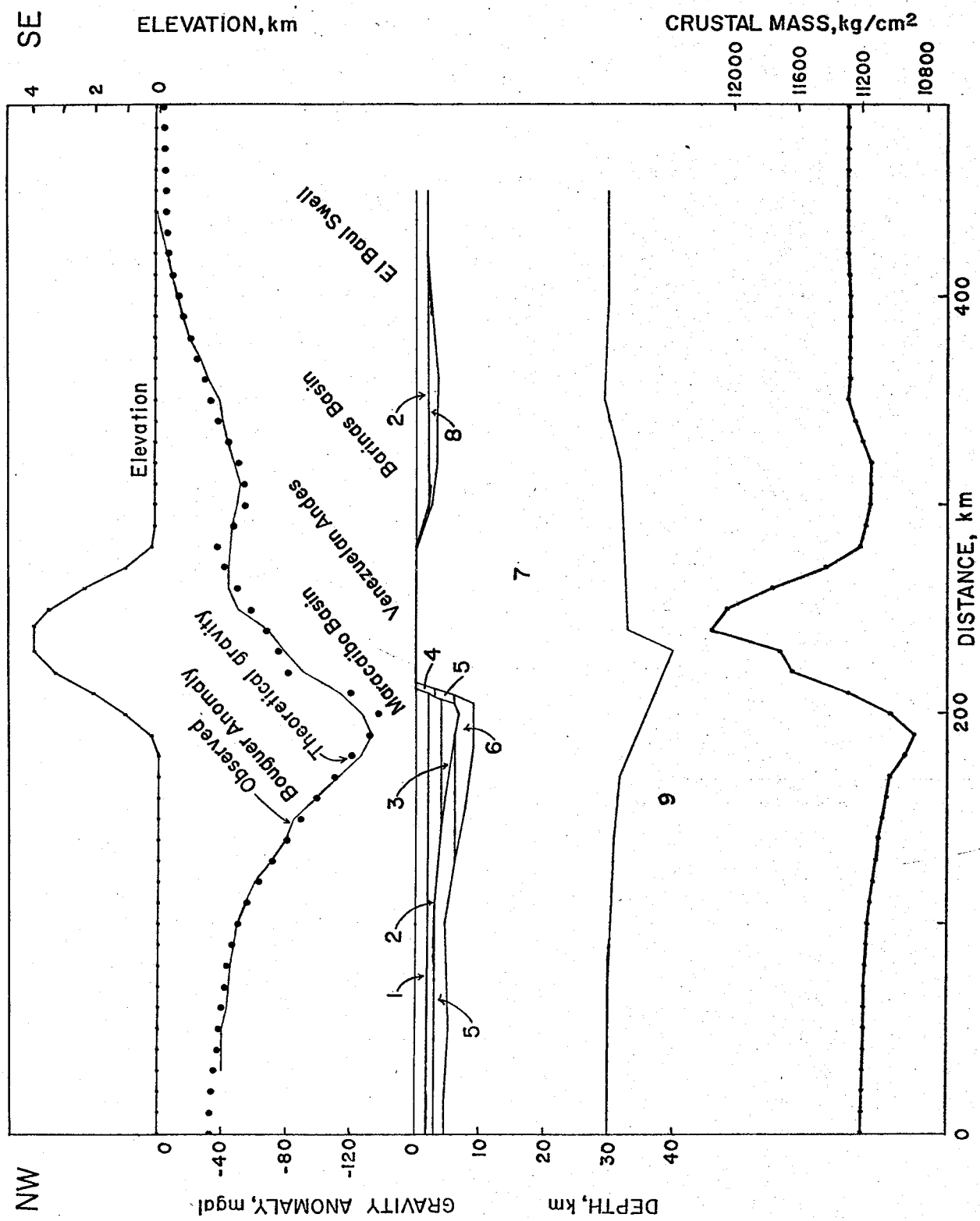
SE
NW
ELEVATION, km
CRUSTAL MASS, kg/cm²
12000
11600
11200
10800
4
2
0
Elevation
El Baul Swell
Barinas Basin
Venezuelan Andes
Maracaibo Basin
Observed Bouguer Anomaly
Theoretical gravity
GRAVITY ANOMALY, mgal
0
-40
-80
-120
DEPTH, km
0
10
20
30
40
DISTANCE, km
0
200
400
1
2
3
4
5
6
7
8
9

-130 mgal over the Maracaibo bason. Over the Venezuelan Andes the anomaly increases sharply on the western flank to a value of -44 mgal, 20 km east of the center of the Andes. It decreases slowly over the east flank of the Andes and the Barinas basin to a value of -50 mgal in the center of the basin. It then increases to 0 mgal approaching the El Baul swell.

The most interesting feature of this profile is that the minimum Bouguer anomaly does not occur over the center of the Venezuelan Andes, which indicates that the crust does not thicken under the Andes, and that the Andes are not isostatically compensated. The minimum is shifted 50 km to the northwest of the center of the Andes, and is approximately coincident with the axis of the greatest thickness of sediments in the Maracaibo basin. The free-air anomaly follows the Bouguer anomaly over the Maracaibo and Barinas basins. However, over the Andes the free-air anomaly increases to +280 mgal indicating a large mass excess in this region.

The structure calculated for Profile A is seen in Figure 13. The structure to the top of the basement in the Maracaibo basin was obtained from geologic sections of the area (Miller, et al., 1958) and from depth-to-basement information presented on a tectonic map of North America (King, 1969).

There were no measurements in this region of the depth to the mantle. The depth to the mantle at the southeastern end of the profile was assumed to be that of a normal continental region, 30 km (Heiskanen and Vening-Meinesz, 1958). The mantle structure for the remaining part of the profile was then varied so that the observed and theoretical gravity agreed. The shape of the model crust-mantle boundary is relatively insensitive to changes in the assumed depth to mantle; although, a change in this depth does result in a change in the amount of crustal downwarp (e.g. decreasing mantle depth to 28 km at the southeast end reduces the amount of downwarp under the Maracaibo basin from 8 km to 7.3 km.). Changes in the crust-mantle density contrast will affect the amount of relief in the boundary.

The depth to the mantle is 29 km at the northeastern end of the profile. The depth increases to approximately 38 km at the basin axis, and then decreases to 31 km under the Andes. The mantle dips to a depth of 33 km beneath the Barinas basin, and then rises to 30 km near the El Baul swell. The slope in the model of the crust-mantle boundary under the west side of the Andes was varied without significantly affecting the fit of the theoretical and observed gravity. It was necessary, however, to bring the crust-mantle boundary up to a depth of

31 km in all the models examined.

The crustal mass/cm^2 (to a depth of 40 km) relative to the value over the El Baul swell of 11220 kg/cm^2, is -90 kg/cm^2 at the northwest side of the Maracaibo basin and decreases to -420 kg/cm^2 over the axis of the basin. The value rises sharply over the Venezuelan Andes to a high of +850 kg/cm^2 that is coincident with the topographic high. Over the Barinas basin there is a mass deficiency of -140 kg/cm^2.

The region for which the model showed the poorest fit was the west flank of the Andes. The sharper rise in the theoretical gravity at this point is due to the density contrast between the light sediments of the Maracaibo basin and the heavier basement rock of the Andes. Two reasons may explain why the sharp rise is not seen in the observed gravity. First, the model assumes that the sediment-basement boundary is two dimensional, while on the geologic map (Fig. 3) the boundary is seen to be irregular. This has the effect of decreasing the maximum rate of change of the gravity anomaly. The second possibility is that the data points are too spread out to define the region of sharp increase. The root mean square (RMS) difference between theoretical and observed

gravity is 4.7 mgal.

There are two major features found in the structural model for this profile: 1) the amount of depression of the crust-mantle boundary under the Maracaibo basin is approximately equal to the amount of depression of the pre-Eocene basement under the basin, 2) there is no light root under the Venezuelan Andes.

Profile B

This profile runs approximately parallel to Profile A about 100 km to the northeast. For this profile the complete Bouguer anomalies over the Andes were calculated using an estimated terrain correction. The Bouguer anomaly is -75 mgal at the northwest edge of the Maracaibo basin. It decreases to -125 mgal over the axis of the basin and increases sharply to -60 mgal over the west flank of the Andes. It then increases more gradually to -30 mgal over the center of the Andes, decreases to -60 mgal in the center of the Barinas basin, and increases to +20 mgal over the El Baul swell. The free-air anomalies are similar to the Bouguer anomalies except over the Andes where the free-air anomaly increases to +160 mgal.

The formation densities used for the model are the same as used for Profile A. The depth to the mantle near the El

Figure 14: Profile B, (see Figure 13 for an explanation).

1. Post-Eocene Sediments, 2.3 gm/cm^3
2. Post-Eocene Sediments, 2.37 gm/cm^3
3. Eocene Sediments, 2.47 gm/cm^3
4. Eocene Sediments, 2.52 gm/cm^3
5. Eocene Sediments, 2.62 gm/cm^3
6. Basement, 2.67 gm/cm^3
7. Sediments, 2.5 gm/cm^3
8. Mantle, 3.3 gm/cm^3

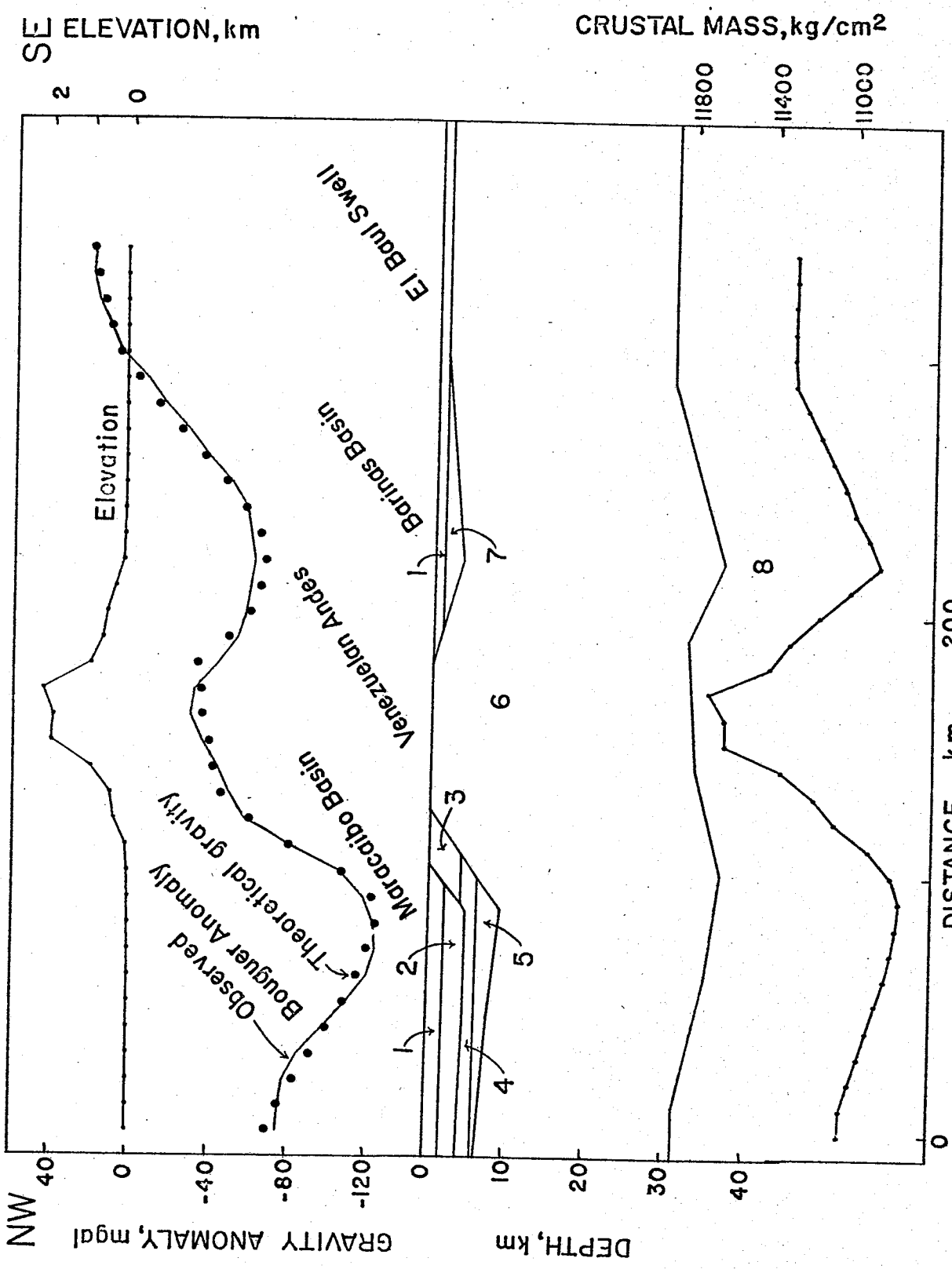
SW ELEVATION, km
CRUSTAL MASS, kg/cm²
2
0
11800
11400
11000
El Baul Swell
Barinas Basin
Venezuelan Andes
Maracaibo Basin
Elevation
Observed
Bouguer Anomaly
Theoretical gravity
1
2
3
4
5
6
7
8
NW
40
0
-40
-80
-120
GRAVITY ANOMALY, mgal
0
10
20
30
40
DEPTH, km
0
200
DISTANCE, km

Baul swell was assumed to be 30 km. The structure of the Eocene and post-Eocene sediments is taken from Miller, et al (1958).

The crust-mantle boundary of the structural model starts at a depth of 31 km at the northwestern side of the basin, dips to a depth of 37 km under the axis of the basin, rises to 33 km under the Andes, and then dips again to 34 km under the Barinas basin. It then rises to 30 km under the El Baul swell. All models examined showed crustal depression under the Maracaibo basin and uplift under the Andes. The amount of depression in the Maracaibo basin is less than that found in Profile A; whereas, in the Barinas basin there is more depression than is found in Profile A. The RMS difference between theoretical and observed gravity for the model shown is 4.0 mgal.

The crustal weight calculation shows that there is a relative mass per unit area excess beneath the Andes of 430 kg/cm^2. This mass per unit area excess is compensated by a mass per unit area deficiency in the Maracaibo basin of 540 kg/cm^2 and in the Barinas basin of -370 kg/cm^2.

Profile C

This long profile extends from the Venezuelan basin in the Caribbean, across the Curacao ridge, across the Falcon

Figure 15: Profile C, (see Figure 13 for an explanation).

1. Water, 1.03 gm/cm^3
2. Sediments, 2.2 gm/cm^3
3. Sediments on land and probably mixed basalts and sediments beneath ocean, 2.4 gm/cm^3
4. Oceanic Basement, 2.8 gm/cm^3
5. Continental Basement, 2.7 gm/cm^3
6. Cretaceous Sediments, 2.5 gm/cm^3
7. Sediments, 2.3 gm/cm^3
8. Cretaceous Sediments, 2.6 gm/cm^3
9. Sediments, 2.4 gm/cm^3
10. Mantle, 3.3 gm/cm^3

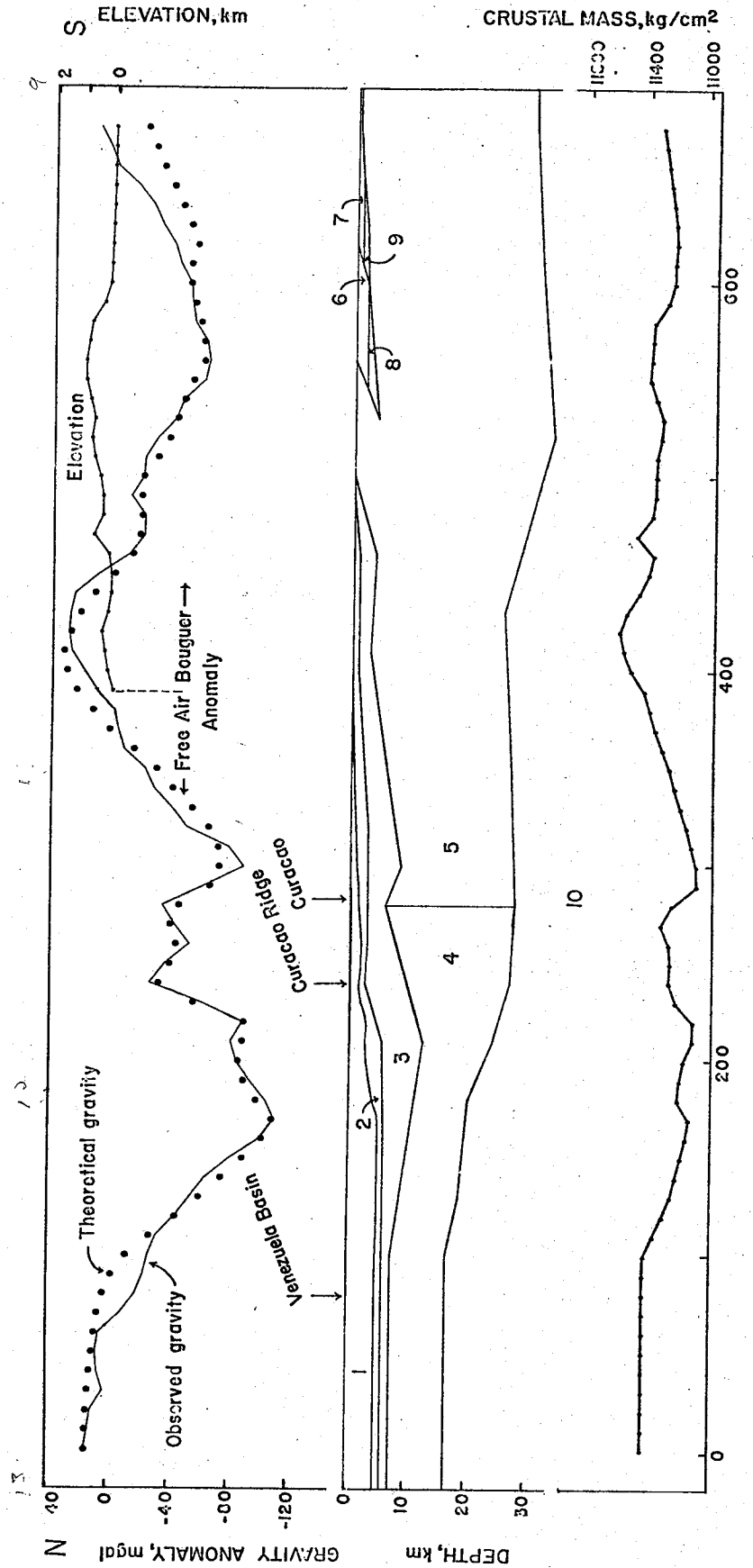
S
ELEVATION, km
2
0
CRUSTAL MASS, kg/cm²
11600
11400
11000
Elevation
Free Air
Bouguer
Anomaly
Theoretical gravity
Observed gravity
Curacao Ridge
Curacao
Venezuela Basin
1
2
3
4
5
6
7
8
9
10
0
200
400
600
40
0
-40
-80
-120
0
10
20
30
N
GRAVITY ANOMALY, mgal
DEPTH, km

basin, through the gap between the Venezuelan Andes and the Caribbean mountains, and across the Barinas basin to the El Baul swell. From an examination of the free-air anomaly map, it can be seen that the structure in this region is farther from two dimensionality than the structures of the other profiles.

The free-air anomaly over the center of the Venezuelan basin is about +15 mgal and decreases to a minimum of -110 mgal at the edge of the basin. It increases to -26 mgal over the Curacao ridge, decreases to -90 mgal between the island of Curacao and Venezuela, and increases to +10 mgal at the coastline. The gravity values over the land are Bouguer anomalies. The Bouguer anomaly increases to +40 mgal over the state of Falcon and decreases to a minimum of -60 mgal in the gap between the Venezuelan Andes and Caribbean mountains. The Bouguer anomaly increases across the Barinas basin until it reaches a value of +12 mgal at the El Baul swell.

Refraction data (Edgar, 1968) were used to provide structural information in the region of the Venezuelan basin and the Curacao ridge. The density used for the various rock units was calculated from the seismic velocities with the use of the Nafe-Drake tables (Talwani, et al ., 1959). Information about the geologic structure of Falcon was obtained from

Wheeler (1963).

The structural model shows that the gravity minimum over the southern edge of the Venezuelan basin is only partly due to an "edge effect". (Even if a topographic feature on the sea floor were in perfect isostatic equilibrium, the free-air gravity over the feature would not be constant, because the compensating surface is farther away from the measuring point than is the water-rock surface. The resulting variation in the free-air gravity anomalies is termed "edge effect".) Under the center of the basin the relative crustal mass per unit area is +70 kg/cm^2, while at the edge of the basin this has decreased to -170 kg/cm^2 indicating that a part of the negative free-air value is due to a deficiency of the mass per unit area at the edge of the basin. Under the Curacao ridge the depth to the mantle has increased to 27 km. The free-air low of -88 mgal south of the Curacao ridge appears to be the results of a trough filled with low density sediments. Although there is no increase in water depth over the trough, it may be a buried northwestern extension of the Bonaire trench. The trough may have been filled by sediments shed from Curacao and from the Paraguana peninsula.

The depth to the mantle decreases to 25.4 km at the Caribbean coastline. This decrease combined with a decrease

in water depth results in a gravity high over the northern edge of Falcon. The relative mass per unit area excess is +250 kg/cm^2. In the gap between the Andes and the Caribbean mountains, the depth to the mantle increases to 33km. The small relative mass per unit area excess of +50 kg/cm^2 indicates that in this region the Caribbean mountains, and possibly the Venezuelan Andes are supported by a light root of crustal material. The depth to the mantle decreases from the value of 34 km under the mountains to a value of 30 km at the El Baul swell. There is a mass deficiency of -100 kg/cm^2 under the northern end of the Barinas basin.

The most important features of Profile C are: the model indicates a buried extension of the Bonaire trench lying south of Curacao, the northern coast of Falcon is out of isostatic equilibrium, and the Caribbean mountains and the Andes appear to be in isostatic equilibrium in this region.

Profile D

This short profile runs north-south across the island of Trinidad. The purpose of this profile was to define the crust-mantle structure under the Coast range. It would have been preferable to locate the profile farther to the west on the Paria peninsula where the mountains are better developed,

Figure 16: Profile D, (see Figure 13 for an explanation).

1. Water, 1.03 gm/cm^3
2. Sediment, 2.55 gm/cm^3
3. Metamorphic, 2.67 gm/cm^3
4. Basement, 2.85 gm/cm^3
5. Mantle, 3.25 gm/cm^3
6. Sediment, 2.35 gm/cm^3
7. Sediments and Volcanics, 2.25 gm/cm^3

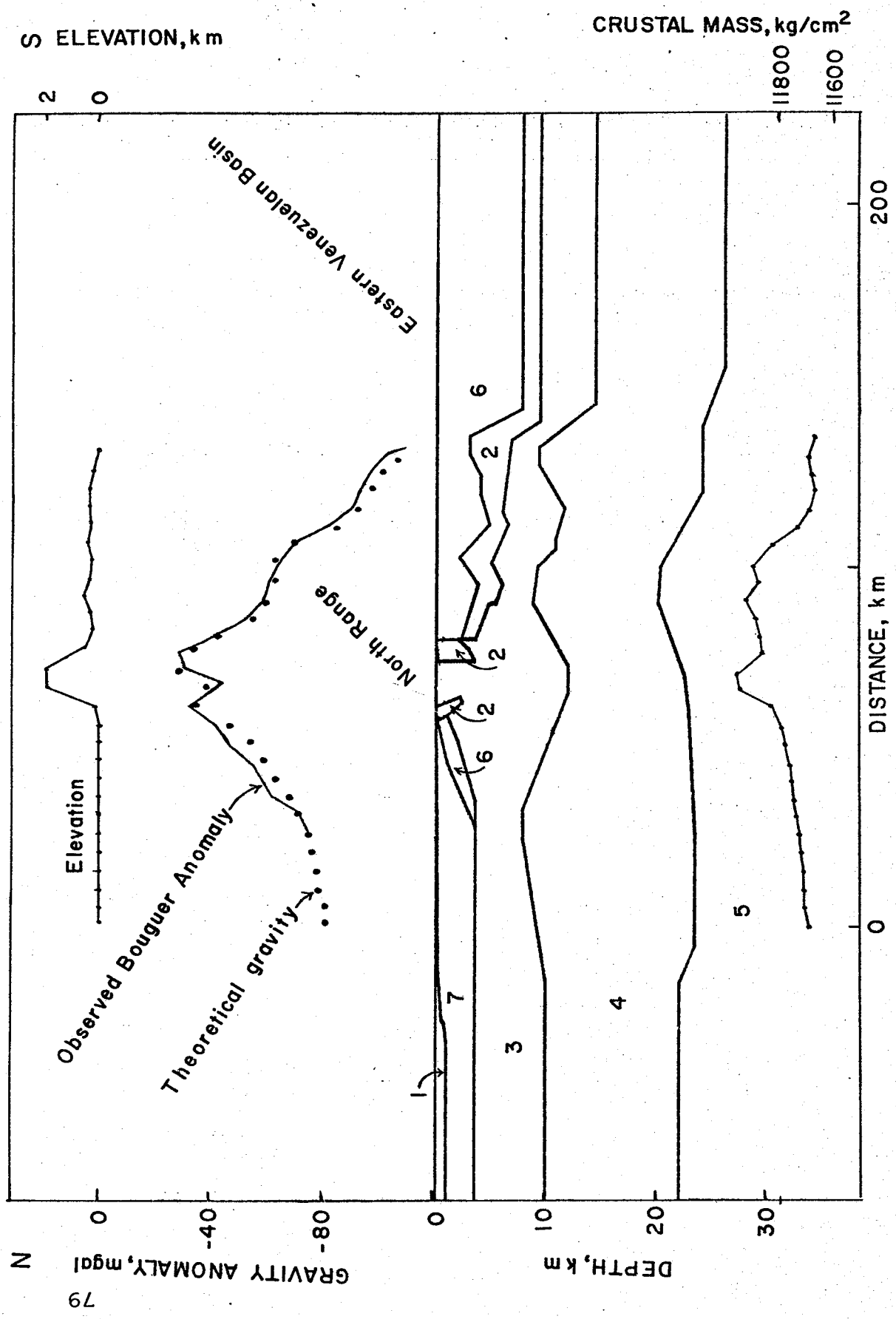
S ELEVATION, km
2
0
CRUSTAL MASS, kg/cm²
11800
11600
Eastern Venezuelan Basin
North Range
Elevation
Observed Bouguer Anomaly
Theoretical gravity
6
2
4
2
2
6
7
1
3
4
5
200
0
DISTANCE, km
0
-40
-80
GRAVITY ANOMALY, mgal
N
0
10
20
30
DEPTH, km

and the structure is closer to being two dimensional, but this was precluded by a lack of data in that region. The profile was not extended south of Trinidad also because of a lack of data in that region.

The Bouguer anomaly is slightly positive (+5 mgal) north of Trinidad and decreases to -45 mgal over the North range. Ir increases to -35 mgal on the south edge of the North range and then decreases continuously to less than -100 mgal at the southern end of the island.

The two dimensional models for this profile were constructed in the following way. The rock densities were obtained from three well logs run in central and southern Trinidad (Higgins, 1959). Figure 12 shows a summary of this well log information. The density of the metamorphic rocks of the North range was estimated as 2.67 gm/cm^3, based on the conversion of a refractive velocity (Higgins, 1959) to a density using the Nafe-Drake curves.

The following sources were used in the formulation of the model. The Geologic map of Trinidad (Kugler, 1959) was used for the surface structure. Ewing, et al (1957) published the results of several refraction profiles on the continental shelf surrounding the island. Edgar (1968) showed an isopach map of layers with velocity less than 4.5 km/sec. The velocity information obtained from the refraction profiles was con-

verted to density by means of the Nafe-Drake curves.

Using the crustal structure as determined by the above data, the crust-mantle boundary was then modified so that the observed and calculated gravity agreed. The final model and the results are shown in Figure 16. The fit between the observed and calculated gravity was good with a RMS difference of 4 mgal.

The crust-mantle boundary is at a depth of 28 km north of Trinidad, dips slightly to 29 km under the North range, and then rises sharply to 25 km along the southern edge of the mountains. It then dips to the south with approximately the same slope as the overlying sediments. At the southern end of the profile the depth is 32 km.

The relative mass per unit area is 0 kg/cm^2 at the north end of the profile. It rises gradually to 300 kg/cm^2 at the southern edge of the North range. There is a high of 400 kg/cm^2 under the center of the North range. The mass per unit area then decreases to -300 kg/cm^2 over the north flank of the Eastern Venezuela basin.

From this profile we see that the coastal mountains, at least in the vicinity of the North range, are supported in part by a low density root. There appears to be a rather broad (100 km) low amplitude (200 kg/cm^2) high associated with the North range.

Profile E

This profile runs almost north-south along the line 63°W. The profile starts at Los Testigos islands. It extends south across the mountains of the Paria-Araya peninsula. It then runs across the Eastern Venezuela basin to the Orinoco river which marks the boundary between the Eastern Venezuela basin and the Guiana shield. The profile extends a short distance onto the Guiana shield.

The Bouguer anomaly over Los Testigos is about 80 mgal. It decreases to 8 mgal 20 km north of the coastline, and then increases to 20 mgal at the coastline. In the center of the Eastern Venezuela basin there is a low of -145 mgal. A gradual rise occurs from -145 mgal over the basin to -10 mgal at the Guiana shield.

The following sources were consulted to provide quantitative information about the crustal structure of the Eastern Venezuela basin. The Geologic-Tectonic Map of Venezuela (Smith, et al, 1962) provides form lines that show the shape of the basement surface, but they provide no absolute depth information. Jacobsen (1961) based on seismic reflection surveys and well control, shows a depth to basement map for a part of the basin. Dallmus(1965) has compiled a contour map of the depth to the basement for the southern part of the

Figure 17: Profile E, (see Figure 13 for an explanation).

1. Water, 1.03 gm/cm^3
2. Sediments, 2.1 gm/cm^3
3. Sediments and Volcanics, 2.4 gm/cm^3
4. Metamorphics and Volcanics, 2.65 gm/cm^3
5. Basement, 2.7 gm/cm^3
6. Sediments, 2.2 gm/cm^3
7. Sediments, 2.5 gm/cm^3
8. Sediments, 2.6 gm/cm^3
9. Mantle, 3.3 gm/cm^3

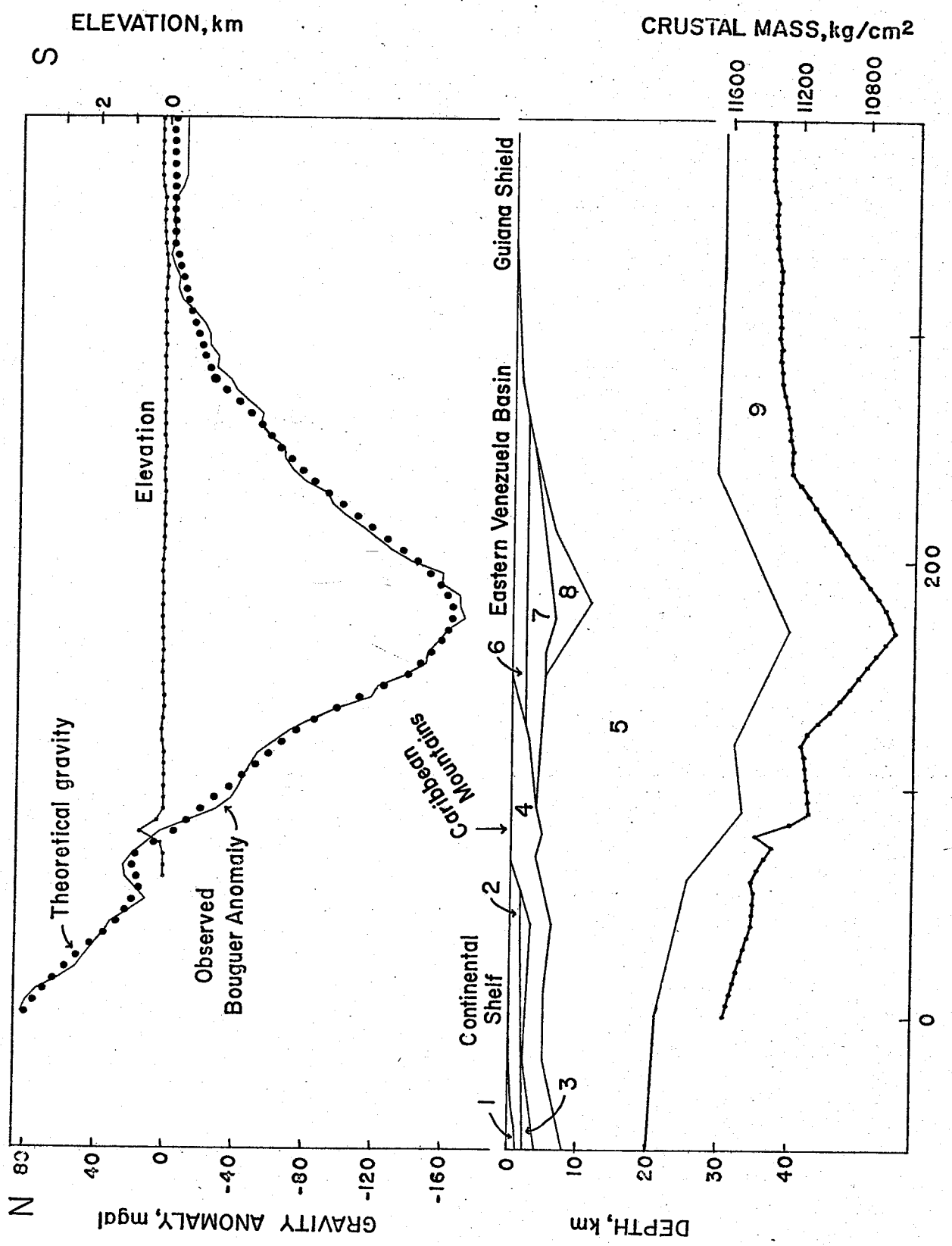
ELEVATION, km
S
2
0
Elevation
Theoretical gravity
Observed
Bouguer Anomaly
Caribbean
Mountains
Continental
Shelf
Eastern Venezuela Basin
Guiana Shield
1
2
3
4
5
6
7
8
9
CRUSTAL MASS, kg/cm²
11600
11200
10800
0
200
N
80
40
0
-40
-80
-120
-160
GRAVITY ANOMALY, mgal
0
10
20
30
40
DEPTH, km

of the basin, and also shows isopach maps for the thickness between several formations. The Tectonic Map of North America (King, 1969) shows a generalized depth to the basement for this area. Using data from these sources it was possible to make good quantitative estimates of the shallow structure in this area. There is a lack of information regarding the depth to the basement in the center of the basin, but because the density contrast between the deeply buried sediments and the basement is small, errors in estimating this depth will have relatively little effect on the model. Conversely, the gravity model provides little information about the depth to the basement in the center of the basin. Information about the shallow structure of the shelf and slope was obtained from Edgar (1968). The rock densities used for this profile were the same as those determined for Profile D in Trinidad.

The final model and the results are shown in Fig. 17. The observed and calculated gravity agree with a RMS difference of 5.5 mgal. The crust-mantle boundary 70 km north of the coastline is at a depth of 20 km. The depth increases to 26 km at the coastline. The minimum of the Bouguer anomaly north of the coastline is due entirely to a trough of low density sediments; there is no depression of the underlying crust mantle boundary. The Coast range appears to be

supported by a low density root, but due to the lack of gravity stations across the Coast range this conclusion is only tentative. The crust-mantle boundary is downwarped to a depth of 40 km under the center of the basin. The deepest part of the boundary is shifted 15 km north of the deepest part of the basin (defined as greatest thickness to basement). The crustal thickness decreases to 30 km at the basin-shield boundary, and appears to increase in thickness to 33 km under the shield; however, only a limited amount of gravity data supports this conclusion.

The relative mass per unit area over the continental shelf at the northern end of the profile is +290 kg/cm^2. The value decreases to +115 kg/cm^2 over the Paria-Araya peninsula. In the center of the Eastern Venezuela basin the relative mass per unit area is -680 kg/cm^2. Over the Guiana shield the value increases to +50 kg/cm^2.

The most significant feature of this profile is the increase in the depth to the mantle in the Eastern Venezuela basin and a large mass per unit area deficiency in that basin.

Crustal Deformation

Possible causes of the crustal downwarping in the Maracaibo basin were investigated. The causes considered

were: 1) elastic instability of the crust or the lithosphere, 2) plastic instability, 3) horst-graben formation, 4) flexing of the lithosphere due to crustal loading.

Elastic instability refers to the eventual bending of a thin plate while it is subject to increasing compressive stress in the plane of the plate. At low levels of stress the plate remains flat, but as the stress is increased the plate may assume a distorted shape. The flat shape is still an equilibrium state, but it is an unstable equilibrium, whereas the distorted shape is stable. This phenomenon does not involve non-elastic deformation, for if the stress is reduced the plate will return to its flat state. The analysis of the deformation given in Jeffreys (1959) shows that the maximum thickness of a layer with the elastic properties and strength of the Earth's lithosphere that can undergo elastic instability is less than 1 km. This rules out elastic instability as a cause of crustal downwarping, unless the lithosphere is made up of many separate layers all decoupled from each other. Since this is not observed, the lithosphere will react by failure (faulting) before the stress can build up to a level high enough to cause elastic instability.

Vening Meinesz first proposed elastic instability to explain the gravity anomalies observed in Indonesia. When

Figure 18: Diagrammatic sections showing different types of lithosphere deformation that would result in crustal downwarp and/or uplift. Section a) shows tensional forces in the lithosphere causing fracture and the center piece floating upward. Section b) shows crustal loading causing downwarping at the center and a small amount of uplifting at the sides. Section c) shows that the compressive stress in the lithosphere acting perpendicular to a dipping zone of weakness will cause downwarping of the lithosphere on the left and uplift of the lithosphere on the right. This is the shear fracture model proposed by Gunn (1947).

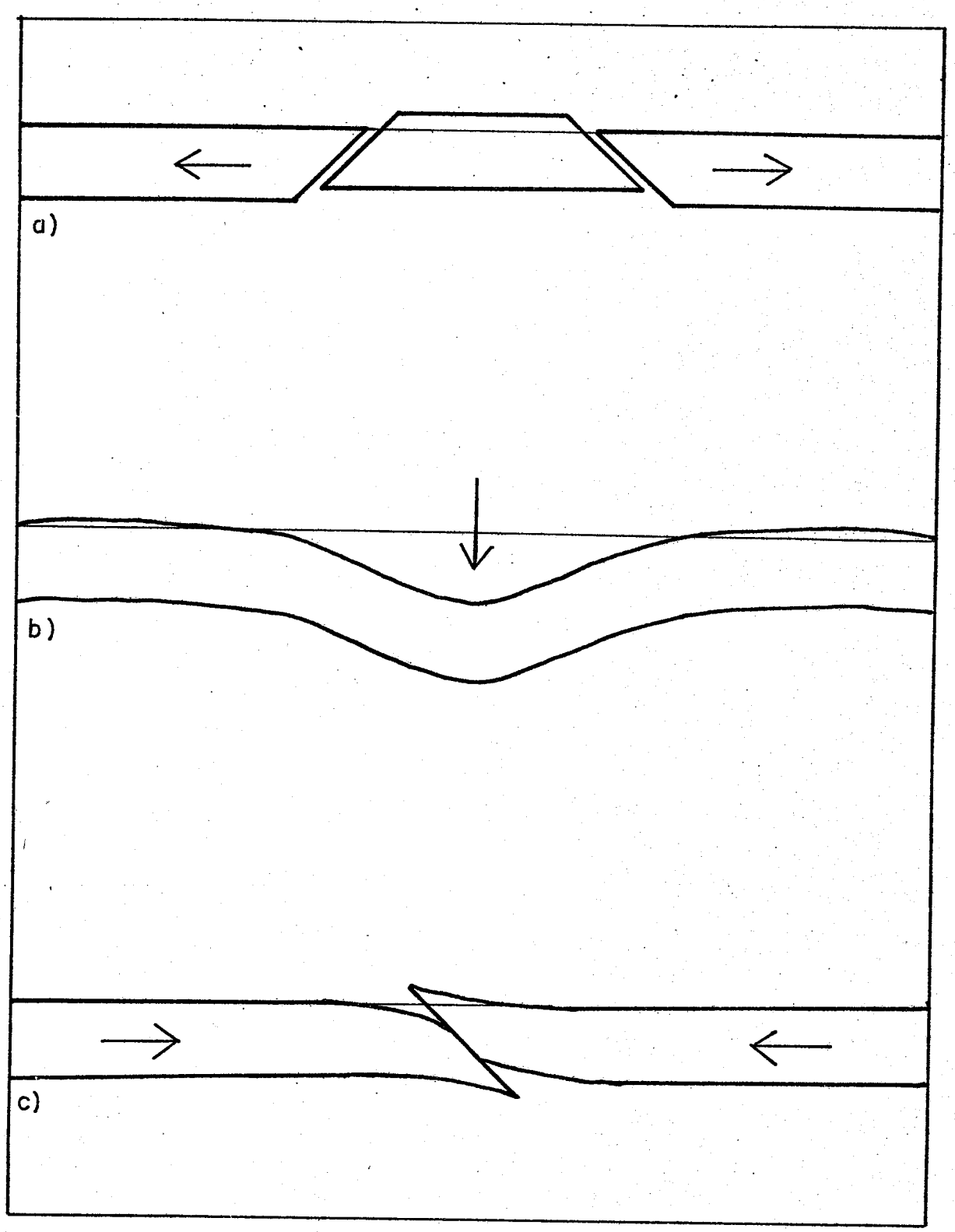
a)
b)
c)

analysis showed that this was not a possible cause, he proposed that the downbuckling of the crust was a result of plastic buckling (a concept that originated with Bijlaard; see Bijlaard, 1951, for a review).

The lithosphere is assumed to be floating on the underlying athenosphere, and is subject to a uniaxial compression which exceeds the elastic limit of the lithosphere. In the zone where the elastic limit is exceeded, the lithosphere begins to deform plastically and to thicken. Because the density of the crust is less than that of the mantle, the isostatic adjustment of the crust in this zone will cause the bottom layer of the crust to subside more than the top layer is uplifted. This increase in length causes an increase in the compressive stress at the top of the crust as compared to the bottom, which results in further downbuckling of the crust. This model has been analysed in detail by Heiskanen and Vening Meinesz (1958). Although this model may be able to explain the formation of some geosynclines, it does not appear to fit the case of the Maracaibo basin-Venezuelan Andes for the following reason. Plastic downbuckling leads to the formation of a symmetrical structure, whereas the basin-mountain structure in this region is clearly asymmetrical, with a mass deficiency under the basin and a mass excess

under the southeastern part of the Andes. Plastic downbuckling may be occurring under the Eastern Venezuela basin and this possibility will be discussed later.

In order for the Maracaibo downwarp-Andes uplift to be due to the formation of a horst and graben, it is necessary that the lithosphere in this region be under tensional stress. An analysis of the horst-graben model (Appendix III) shows that it is physically possible to account for the mass excess under the Andes with this model. However, the steeply dipping deformed beds observed on the northwest flank of the Venezuelan Andes and the thrust faults with the rocks on the northwest overriding those on the southwest observed on the southeast flank, indicate that the stress regime in this region has been compressional and not tensional.

Another possibility is that the crustal downwarping is due to the loading of the lithosphere by a mass excess. The model is again that of a solid lithosphere over a liquid athenosphere. McConnell (1968) in a study of the post glacial upwarping of Fennoscandia, concluded that the crust and upper mantle are rigid down to a depth of 120 km, and that they can withstand stress differences of 3×10^8 dynes/cm^2 over periods of 10^5 years or more, which implies that the viscosity of the lithosphere is greater than or equal to 10^{24} poises. The

underlying material (120-300 km) deforms by creep with a viscosity of 10^{21} poises. Below a depth of 300 km the viscosity appears to increase until it reaches a high of 10^{25} poises below 800 km. These results indicate that the lithosphere can be considered to be an elastic or perhaps viscoelastic plate floating on a liquid for disturbances with a period greater than 10^4 years.

The equation relating the equilibrium vertical displacement of a horizontal plate to the load (Jeffreys, 1959) is:

1) $$D \cdot \nabla_1^4 w = P \qquad \nabla_1^4 = \frac{\partial^4}{\partial x^4} + \frac{\partial^4}{\partial y^4} + \frac{2\partial^4}{\partial x^2 \partial y^2}$$

w = vertical displacement of plate, function of x,y
T = thickness
E = Young's modulous
σ = Poisson's ratio = .25
P = crustal loading

where D is a parameter known as the flexural rigidity of the plate and is defined as:

2) $$D = \frac{ET^3}{12(1-\sigma^2)}$$

If the deformed plate is overlain by a material of density ρ and the density of the underlying liquid is ρ_m then an additional set of terms is introduced into the equations due to the buoyant force of the displaced liquid, and the equation

becomes: $D \nabla^4 w + (\rho_m - \rho) \cdot w \cdot g = P$

3)

g = gravitational acceleration

Walcott (1970) gives an integral solution in polar coordinates for the general case. If we restrict ourselves to variation only in the x direction then the equation becomes:

4) $$D \frac{d^4 w}{dx^4} + (\rho_m - \rho) \cdot w \cdot g = P$$

Solutions to this equation are of the form:

5) $$w = e^{\alpha x}(A \cos^{\alpha x} + B \sin^{\alpha x})$$

where A and B are parameters that depend on the boundary conditions and:

6) $$\alpha^{-4} = \frac{4 \cdot D}{(\rho_m - \rho)g}$$

It is easy to show that for a line load of σ_L located at x=0 on an infinite plate, displacement at a point x is given by:

7) $$w = \frac{\alpha \sigma}{2(\rho_m - \rho)} \begin{cases} -e^{+\alpha x}(\sin^{\alpha x} - \cos^{\alpha x}) & x < 0 \\ e^{-\alpha x}(\sin^{\alpha x} + \cos^{\alpha x}) & x > 0 \end{cases}$$

Then using this equation we can integrate over any irregular load to obtain the total deflection at any point.

Walcott (1970) examined the crustal depression caused by various features and found that the flexural rigidity varied from 5×10^{22}N-m in the basin and range province to 10^{25}N-m

for the beaches of Pleistocene Lake Agassiz and Algonquin. Except for the Basin and Range province (which is anomalous due to the thin lithosphere caused by higher temperature gradients) observed flexural rigidity decreased as the age of the feature increased (see Fig. 19). This indicates that the lithosphere is responding non-elastically, with a viscous as well as elastic deformation. By assuming that the lithosphere was viscoelastic (a Maxwell body) with an elastic parameter defining short term behavior, and a viscous parameter defining long term behavior, Walcott obtained a curve that reproduced the rigidity versus age data.

If the equations are reformulated so that the upper layer is considered to be a viscoelastic body, then the two dimensional equation becomes (Nadai, 1963):

8) $$\frac{d}{dt}\left[\frac{d^4}{dx^4} + 4\alpha_o^4\right] w + 4\alpha_o \frac{w}{\tau} = \left(\frac{1}{\tau} + \frac{d}{dt}\right)\frac{P}{D}$$

where: τ = Maxwell time constant = $\frac{\eta_s}{E}$
η = Maxwell's viscosity

Nadai gives the solution to this equation for a line load.

Walcott (1970) shows that the deformation of a visco-elastic slab of rigidity D_{actual} is similar to that of a purely elastic slab of lower rigidity $D_{apparent}$, where the ratio $D_{apparent}/D_{actual}$ decreases monotonically as the elapsed

time since the introduction of the load increases.

Using equation 7 it is now possible to compute the theoretical crustal deformation under the Andes and the Maracaibo basin, assuming that the Andes are a load on the lithosphere. In Figure 19 it can be seen that this curve does not accurately predict the shape of the Maracaibo basin. In addition the theoretical downwarping of the crust under the Venezuelan Andes is as great as under the Maracaibo basin, which is not the case as was shown in Profiles A and B.

The following discussion provides an explanation for the observed asymmetry of the basin-mountain structure, as well as providing a realistic mechanism for the formation of the feature. A shear fracture model was first proposed by Gunn (1947) as a possible explanation of mountain building (see Fig. 18c). The upper layer is assumed to be under uniaxial compression which results in failure of this layer along a fault of dip ϕ. In the absence of internal friction or pre-existing planes of weakness $\phi = 45°$; internal friction will make ϕ less than 45°. Because of the lateral compression there will be vertical forces on the fractured ends of the plate of $S \sin \phi \cos \phi$, where S is the compressive force on the end of the slab. This results in a downwarping of the plate on the left, and an uplift of the plate on the right.

Gunn (1947) showed that the shape of the plates is given by:

9) $$w = \frac{2F\alpha e^{-\alpha x}\cos^{\alpha x}}{(\rho_m - \rho)g}$$

$$F = \text{vertical force} = S \sin \phi \cos \phi$$

The shape of the deformed plates is seen in Figure 18c. It can be seen that this model predicts a crustal deformation similar to that observed under the Venezuelan Andes-Maracaibo basin. The basin is deepest immediately next to the mountains. The sediment thickness decreases gradually on the left. The basin terminates abruptly on the right against the uplifted block that forms the mountains. The uplifted area is not supported by a root directly beneath it. The support for the mountains is provided by the compressive force acting on the slab.

In order to confirm that this model provides an explanation of the observed deformation, an attempt was made to fit the curve given by equation 9 to the observed downwarp of the Maracaibo basin along Profile A. From Figure 18c we see that the region of greatest mass deficiency is located near the origin. Using this criterion the origin of the fitted curve was taken to lie a distance of 130 km on the structure section. Then the curves defined by equation 9 were fitted to the observed data for values of α^{-1} = 60, 70, 80 km. The observed and predicted crustal structure are shown in Figure 19. From this

Figure 19: The observed downwarp of the Maracaibo basin and the theoretical downwarp of the basin as predicted by Equation 8, are plotted. Three different values of the flexural parameter, α^{-1}, are used to obtain the three theoretical curves. The dotted line shows the theoretical downwarp of the Maracaibo basin, assuming the Venezuelan Andes are passively resting on a floating lithosphere. The origin of the distance scale for these comparisons was assumed to be at a distance of 210 km along Profile A which is the approximate location of the relative mass/unit area equilibrium point.

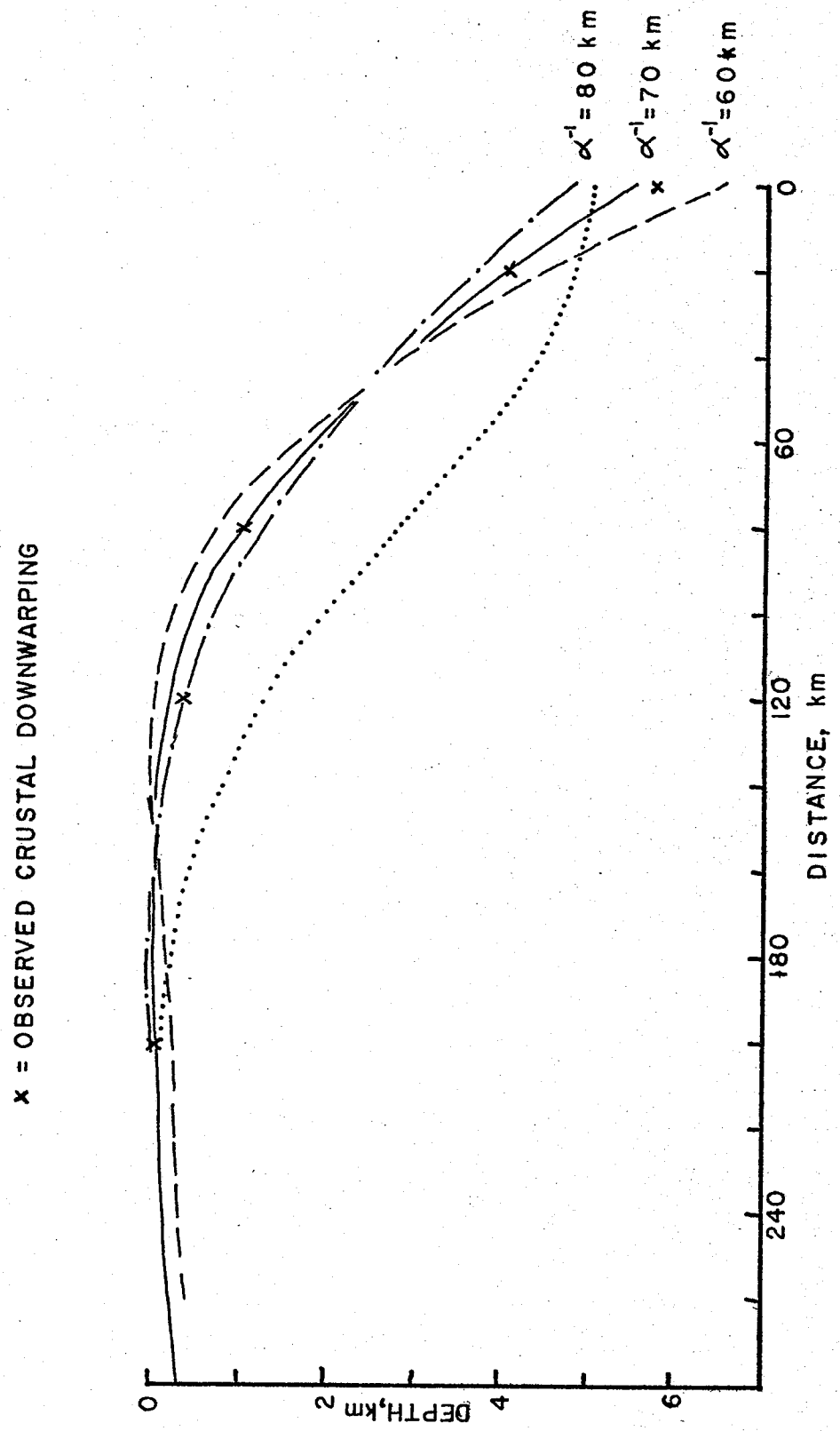
x = OBSERVED CRUSTAL DOWNWARPING
α^{-1} = 80 km
α^{-1} = 70 km
α^{-1} = 60 km
DEPTH, km
DISTANCE, km
0
2
4
6
60
120
180
240

we see that the best values of α^{-1} are 70 and 80 km. The curve for α^{-1} = 70 km gives a better fit for the area near the break, while α^{-1} = 80 km provides a better fit for distances further than 80 km from the break. In the following calculations an average value of α^{-1} = 75 km was used. From this value α^{-1}, the apparent flexural rigidity under the Maracaibo basin can be determined. As can be seen from equation 6, in order to calculate the apparent flexural rigidity, it is necessary to know the average density of the sediments (ρ) and water in the basin since the time of formation of the basin. Geologic studies (Mencher, 1953) indicate that most of the post-Eocene sediments are of shallow water origin, indicating that the rate of sedimentation has been high enough to keep the basin full of sediments. Since ρ is a time average as well as a space average over the sediments in the basin, ρ must be less than the present average sediment density. The value of ρ is also reduced because there is (and has been) a layer of water over the sediments. The present sediment density of post-Eocene rock (based on the same densities as used in the gravity model) is 2.4 gm/cm^3. This was reduced by 0.1 gm/cm^3, in order to obtain an estimate of ρ = 2.3 gm/cm^3. A mantle density of 3.3 gm/cm^3 was assumed. From equation 6 we see that:

10) $$D = \alpha^{-4} \frac{(\rho_m - \rho)g}{4}$$

$\alpha^{-1} = 7.5 \pm .5 \times 10^{10}$ meter

$(\rho_m - \rho) = 1 \pm .1 \times 10^3 kg/m^3$

$g = 9.8$ meter/sec^2

Substituting these values into equation 10 yields:

$D = .6 \pm 2 \times 10^{23}$ N-m = apparent flexural rigidity

In order to compare these results with those of Walcott (1970), it is necessary to determine an average age for the Andes. Since the previous evidence indicates that uplift started at the end of the Eocene, and has continued at least through the Miocene, and possibly into the Holocene, an average age for the feature is approximately $2 \pm .5 \times 10^7$ years. In Figure 20 we see that a lithosphere rigidity of $0.6 \pm .2 \times 10^{23}$ N-m, and an age of the feature of 2×10^7 years agrees with the data obtained by Walcott for other features.

The compressive force necessary to cause the uplift may also be calculated from equation 2. The vertical force is given by:

$$F = \frac{(\rho_m - \rho)g}{2\alpha}$$

while the horizontal compressive stress is given by:

$$S = \frac{F}{T \sin \phi \cos \phi}$$

Figure 20: Apparent rigidity vs age (modified from Walcott, 1970). The dotted lines show the expected relationship for various values of α^{-1} which is the relaxation coefficient of the lithosphere defined as (Maxwell viscosity)/(Young's modulus).

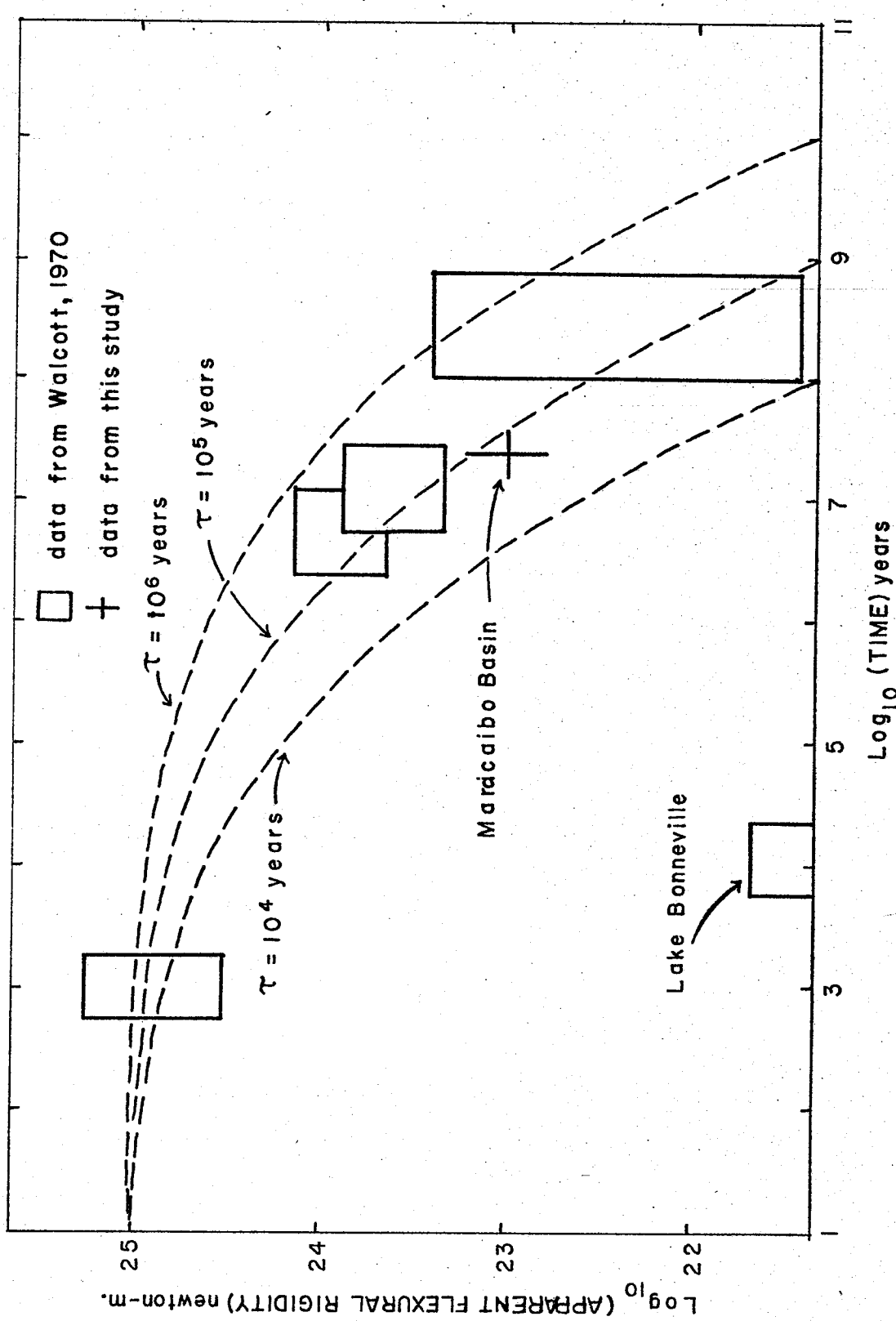
data from Walcott, 1970
data from this study
τ = 10⁶ years
τ = 10⁵ years
τ = 10⁴ years
Maracaibo Basin
Lake Bonneville
Log10 (APPARENT FLEXURAL RIGIDITY) newton-m.
Log10 (TIME) years
25
24
23
22
11
9
7
5
3

(The value of S is almost independent of the angle ϕ for $\phi = 45°$, $\sin \phi \cos \phi = .50$, $\phi = 35°$, $\sin \phi \cos \phi = .47$). Assuming a lithosphere thickness of 100 km (McKenzie, 1967) we have:

$$S = 3 \times 10^7 \text{ N m}^2$$

This value is approximately 1/2 that of the breaking strength of the mantle and lithosphere, and therefore appears reasonable.

The shape of the crust under the Andes is less well known than the shape under the basin. The structure sections indicate that the crust-mantle boundary under the Andes, is located at a depth of 31 km, but the gravity data cannot resolve the exact shape.

The maximum elevation observed in the Venezuelan Andes is about 4000 m or 4 km which means that the total crustal thickness in the Venezuelan Andes is 35 km, and would be more if erosion had not occurred. In the Maracaibo and Barinas basins the thickness from the top of the basement to the crust-mantle boundary is 30 km. This implies that prior to the deformation that uplifted the Venezuelan Andes the crust of the Andes was thicker than the crust on either side of the Andes, or that some mode of deformation has taken place that resulted in thickening of the crust. The deformation observed

in the Venezuelan Andes is primarily uplift and subsidence along vertical faults (Kovisars, 1971, and Stainforth, 1970). Because of these difficulties it does not appear that the shear fracture model will predict quantitatively the deformation under the Andes, but in a qualitative manner it does predict the deformation. If the shear fracture model is correct, the depth to the mantle should be less under the Venezuelan Andes than under the Maracaibo basin, which is what is observed. Under the Maracaibo basin the amount of observed downwarping agrees with that of the model.

Tectonic History of the Caribbean-South American Region

At the beginning of the Mesozoic, North and South America and Africa were joined together to form the continent of Pangea. The reconstruction of Freeland and Dietz (1971) shows an overlap of portions of Central and South America, and the Bahama platform and Africa. The basement rocks of Yucatan, Honduras-Nicaragua, and Oaxaca are pre-Mesozoic (McGillvary, 1970) indicating that these continental blocks were not in their present locations relative to North America at the beginning of the Triassic. The Isthmus of Panama contains no rocks older than lower Cretaceous, and was apparently formed after the rifting of North America from Pangea occurred.

Freeland and Dietz (1971) feel that the Yucatan and Honduras cratons were located in the Gulf of Mexico. This results in a Caribbean that is completely closed. Some authors (Weyl, 1966; and Dalmus, 1965) thought that the Caribbean was an area that was originally composed of continental crust, and had foundered at the end of the Cretaceous. Edgar,et al. (1971b) eliminated this as a hypothesis by showing that there had been uniform sedimentation since the Cretaceous. Edgar, et al. (1971b) felt that the Caribbean is a relic of Mesozoic Pacific crust that was emplaced between North and South America during their separation from Europe and Africa. Data from Leg 15 of the Deep Sea Drilling Project indicate that the major portion of the Caribbean did not exist until the late Cretaceous (Edgar, et al., 1971a). Site 149 in the center of the Venezuelan basin cored Coniacian (Upper Cretaceous) sediments overlying dolerite. Site 153 at the southern end of the Beata ridge also cored Coniacian sediments overlying basalt. In both holes the basalt was at a level corresponding to seismic reflector B", which is almost continuous over the Caribbean.

The initial rifting of North America and Africa occurred during the late Triassic (Freeland and Dietz, 1971). North America started to move to the northwest away from Africa and South America.

According to Freeland and Dietz this rifting was accompanied by left lateral shear along the Northern boundary of South America as the Yucatan and Honduras blocks started to move out of the Gulf of Mexico.

Although no determination of the sense of motion is possible from the geologic data in Venezuela, the initial rifting of North America away from South America appears to have been accompanied by the formation of a deep narrow trough in northwestern Venezuela in the Mesozoic and its infill by the redbeds of the La Quinta formation. These redbeds appear to be thickest along the axis of the Andes and the Perija range, (Stainforth, 1970). To the north of the Yucatan and Honduras blocks similar events occurred; the Triassic redbeds of the East Texas basin were deposited (Freeland and Dietz, 1971). This is in agreement with the concepts of Dewey and Bird (1970), who proposed that the initial rifting is accompanied by crustal downwarping at the edges of the continental blocks and the deposition of redbeds derived from uplifted areas in the center of the rift.

The continued deposition of sediments in the middle to late Jurassic from Trinidad to Margarita, and the lack of comparable sediments to the south indicates that rifting continued without interruption during this time.

At the beginning of the Cretaceous, South America began to move away from Africa (Freeland and Dietz, 1971). South and North America apparently began to move closer together, resulting in compression along the northern boundary. This compression caused the downbuckling of the crust of Venezuela and a shallow sea began to invade Venezuela from the north at this time.

In late Cretaceous through Paleocene time it appears that the rate of closure of North and South America increased. The change in the type of deposition occurring along the northern boundary of South America from miogeosynclinal deposits to eugeosynclinal deposits is interpreted to be caused by the initiation of underthrusting and subduction of the Caribbean plate under the South American plate. The concomitant uplift along the northern boundary was the cause of southward submarine gravity sliding of blocks such as the Villa del Cura formation. The metamorphism of the Jurassic sediments of the Caribbean mountains probably occurred at this time.

The geologic data indicate that by Eocene time the North and South American plates were probably moving parallel

to one another. The metamorphism and volcanism along the northern boundary had ceased. The northern branch of the Caribbean mountains (the Coast range) was uplifted. The uplift is interpreted as being due to the incorporation of a portion of the underthrusting oceanic crust into the continental crust at the time the underthrusting ceased. The mountains were then uplifted towards a position of isostatic equilibrium. The gravity data show that the Caribbean mountains are partially isostatically compensated by a light root; the underthrusting material was the source of this root. The uplift on the north provided a source for the flysch deposits that filled the Eocene basin to the south.

During the mid-Eocene orogeny the Eocene trough lying south of the Caribbean mountains was uplifted. This apparently was a result of new compression from the north. There is no evidence of a return to the eugeosynclinal conditions that existed during the late Cretaceous; the uplift was due to thrust faulting of crustal blocks from the North over the rocks on the south. The thrust faulting and compression caused the axis of deposition of the Eastern Venezuela basin to move farther to the south.

In post-Eocene time there was a continued southward movement of the deposition axis of the basin, as well as a southward movement along the thrust faults of the Caribbean mountains. The continued downwarp of the Eastern Venezuelan basin may be due to the mechanism of plastic downbuckling proposed by Bijaard (1951). The north-south compression along the coastline of Venezuela has apparently existed almost continuously from the Oligocene through the Pliocene, since there is an almost uninterrupted sequence of sediments from this time period deposited in the Eastern Venezuela basin. If the compression had ceased, the relative mass per unit area deficiency of -600 kg/cm^2 would have caused the Eastern Venezuela basin to be uplifted.

The uplift of the Venezuelan Andes began in the Oligocene. The large quantities of shallow water post-Eocene sediments deposited in the Maracaibo basin indicate that the downwarping of the basin occurred contemporaneously with the uplift. This pattern of deformation appears to be best explained by the shear fracture model of Gunn (1947). The uplift is due to compressional forces with a component of stress perpendicular to the axis of the Andes mountains. The compression resulted

in failure in the lithosphere along a plane dipping between 30° to 40° to the southwest. The failure may have occurred along a pre-existing sediment filled rift as was suggested by Stainforth (1969) which would account for the greater increase in the thickness of the basement (defined as rocks below the bottom of Eocene and above the mantle) under the Andes as compared to the basins on either side.

The shear fracture model would result in a linear topographic uplift along both flanks of the Venezuelan Andes. From Figure 2 it can be seen that the 200 m contour line is very straight along these flanks between the Perija range and the Falcon-Lara mountains. From the free-air anomaly map (Fig. 7) it can be seen that the free-air minimum over the Maracaibo basin also terminates at the Perija range and the Falcon-Lara mountains. Profile A and B both lie between the Perija range and the Falcon-Lara mountains and both structure models supported the shear fracture hypothesis. Profile C running between the Andes and the Caribbean mountains indicated that in this region both of these mountain ranges were supported by light crustal roots. These facts suggest that the shear

fracture model is only applicable at the present time to the region of the Andes between the Perija range and the Falcon-Lara mountains.

The reason the structure of the Venezuelan Andes is different than the Caribbean mountains is because in the case of the Caribbean mountains the compression took place across a continental-ocean boundary and underthrusting could occur. In the case of the Andes the compression occurred across a boundary with continental crust on both sides. Because the buoyancy of the continental crust prevents it from being underthrust, the compressive stress causes failure of the lithosphere along a pre-existing rift and the initiation of the uplift of the Andes and the downwarping of the basin.

Present Crustal Dynamics

Molnar and Sykes (1969), in their study of the tectonics of the Caribbean, considered North and South America to be one plate, and the Caribbean to be another. This meant that the rate of underthrusting of the American plate beneath the Lesser Antilles would be approximately equal to the rate of

right lateral strike-slip movement along the Caribbean-South American boundary. However, studies of spreading rates and poles of rotation in the Atlantic (Ball and Harrison, 1969; Phillips and Luyendyk, 1970) indicated that the North and South Atlantic had different spreading rates and poles of rotation. Ball and Harrison (1969) proposed a zone of separation between the two plates slightly north of the equator. Thus the underthrusting of the Atlantic sea floor beneath the Lesser Antilles is due to a faster rate of westward motion of the North American plate as compared with the South American plate. There is no need to account for this underthrusting by moving the Caribbean plate eastward towards South America. The earthquake focal mechanism determined for an event occurring on the Bocono fault showed right lateral strike-slip motion along the fault. Molnar and Sykes (1969) calculated the focal mechanism of an earthquake located near Caracas and found right lateral strike-slip motion. Schubert (1970) found that there had been 66 meters of post glacial right lateral strike-slip movement along the Bocono fault, an average rate of movement of .6 cm/yr.

From an examination of the proposed plate boundaries in the Caribbean (Fig. 21, modified from Molnar and Sykes, 1969), it can be seen that if the Caribbean plate is moving eastward with respect to South America, this will result in compression in the region of the Venezuelan Andes and right lateral strike-

Figure 21: Proposed plate boundaries in the Caribbean, (modified from Molnar and Sykes, 1969). The dashed line extending across the north coast of Venezuela marks the location of the boundary between the Caribbean plate and the South American plate. The dashed line to the east of Trinidad shows a possible boundary between the North and South American plate.

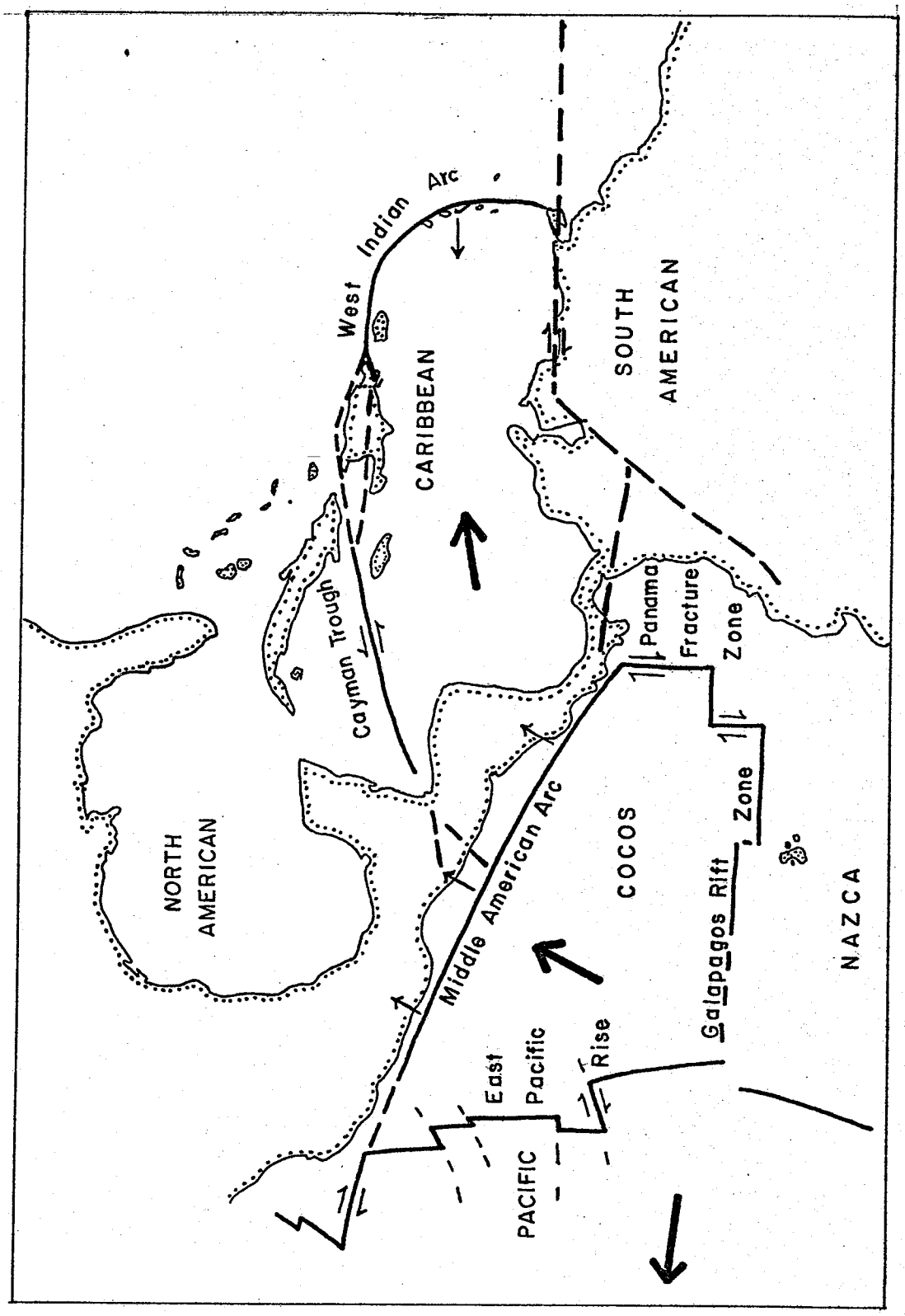
West Indian Arc
CARIBBEAN
SOUTH AMERICAN
Cayman Trough
Panama Fracture Zone
NORTH AMERICAN
Middle American Arc
COCOS
Galapagos Rift Zone
NAZCA
East Pacific Rise
PACIFIC

slip motion along the Caribbean mountains. It appears that from the beginning of the Oligocene through the Pliocene, the Caribbean plate shifted east with respect to the South American plate a distance of about 10 km. A displacement of this magnitude would account for the observed deformation of the Andes-Maracaibo basin. This amount of motion is not ruled out by the geologic data. Metz (1968) estimates that there is a maximum of 5-10 km of right lateral movement along the El Pilar fault. The focal mechanisms along the northern boundary of Venezuela and the Bocono fault were determined for only two events. The type of movement indicated for these two events may not be representative of the actual motion along the boundary.

At the present time it appears that the Caribbean mountains are relatively unaffected by the north-south compressive stress across the Caribbean-South American plate boundary while the Venezuelan Andes are held up above isostatic equilibrium by the compressive stress across the plate boundary lying along the Venezuelan Andes. This suggests that the relative movement of the Caribbean plate with respect to the South American plate is probably eastward.

CONCLUSIONS AND SUMMARY

The gravity model studies showed that the crustal downwarp under the Maracaibo basin is about 9 km; the crust was thickest on the northwest flank of the Venezuelan Andes, and it thinned rapidly towards the center of the Andes. This results in a large mass excess under the center of the Andes, and a large mass deficiency under the Maracaibo basin.

This structure is best explained by the shear fracture model of Gunn(1947). A southeast dipping fault exists along the northwest edge of the Andes. As a result of lateral compressive stress across the fault, the lithosphere under the Andes has been uplifted above isostatic equilibrium, and that under the Maracaibo basin has been depressed. The apparent flexural rigidity of the lithosphere of 0.6×10^{23} N-m, calculated from the shape of the Maracaibo basin, is in agreement with values calculated from the flexural deformation of normal lithosphere in other regions.

The compressive stress appears to be a result of an interaction between the Caribbean and the South American plates with the Caribbean plate having moved about 10 km eastward with respect to the South American plate beginning in the late Oligocene or the early Miocene time. This compression has led to the formation of the Andes, and probably

also to the formation of the Perjia range which appears to have formed contemporaneously with the Andes. The initial failure of the lithosphere in this region developed along a pre-existing zone of weakness marked by a rift into which large quantities of sediment had been deposited during the Jurassic.

The northern boundary is considerably different than the boundary in the Andes region despite the apparent topographic continuity between the Andes and the Coast ranges. The Coast ranges are much older than the Andes, with a date of formation in late Cretaceous time. In response to compression from the north, an east-west trending geosyncline was formed. During periodic episodes the northern boundary of the geosyncline was subject to uplift and folding, and moved by thrust faulting and gravity sliding towards the south. The increased crustal thickness under the Coast range is interpreted as being due to the underthrusting of oceanic crustal material beneath the continental crust of South America, and its incorporation into the continental crustal material when the underthrusting ceased at the end of the Cretaceous. The uplift of the southern part of the Caribbean mountains appears to be a result of crustal thickening caused by the thrust faulting of rocks from the north over the rocks on the south. The subsidence of the Eastern Venezuela basin is perhaps caused by plastic downbuckling of the lithosphere in response to compression from

the north.

There must be compression from the north at the present time, since there is no evidence of uplift in the basin, despite the large mass deficiency in the region. There must also be continuing compressive stress in the region of the Maracaibo basin - Venezuelan Andes; for the Andes are supported as a result of the horizontal compressive stress and would subside without this stress; whereas the Maracaibo basin would be uplifted.

At the present time there appears to be a limited right lateral strike-slip movement occurring on the Caribbean-South American boundary. Since there is right lateral strike-slip movement along both the Bocono fault and the north coast of Venezuela, it appears that the plates in this region must be deforming in a non-rigid fashion or there must be several smaller plates in the region, or the focal mechanism for these two events may not be representative of the total motion along these boundaries.

APPENDIX I

Gravity Base Station Descriptions

The gravity values typed at the bottom of each station description are the gravity values at that station referenced to a value of g=978065.87 mgal for station St. Innes #1

A complete listing of the principal facts for the gravity data used in this paper is on file at the Woods Hole Oceanographic Institution. These data may be obtained from Dr. C. O. Bowin.

COUNTRY	NEAREST CITY	GRAVITY STATION DESCRIPTION
Venezuela	Caracas	
STATE / PROVINCE		STATION NAME
PTO Federal		Maiquetia

LATITUDE	LONGITUDE	ELEVATION	W.H.O.I. STATION NO.	GRAVITY VALUE (g)
10°34.4'N	66°58.7'W	160'	556	

DESCRIPTION

This is Woollard Station - WA6131. In front of a Cartographia Plaque on the wall. The plaque is almost obscured by the candy stand in front of it. The plaque is right outside the street entrance to the main waiting room. The station is about 6' in front of the plaque (I doubt this is really WA 6131, but it is probably close). This is a wall plaque not a B.M. (W.H.O.I. 766 is probably closer)

DESCRIBED BY A. Folinsbee — DATE 5 Mar. '70

POSITION CONTROL DESCRIPTION
From Woollard & Rose (1963), Internation Gravity Measurements, p115

ELEVATION CONTROL DESCRIPTION
Ibid

DIAGRAM

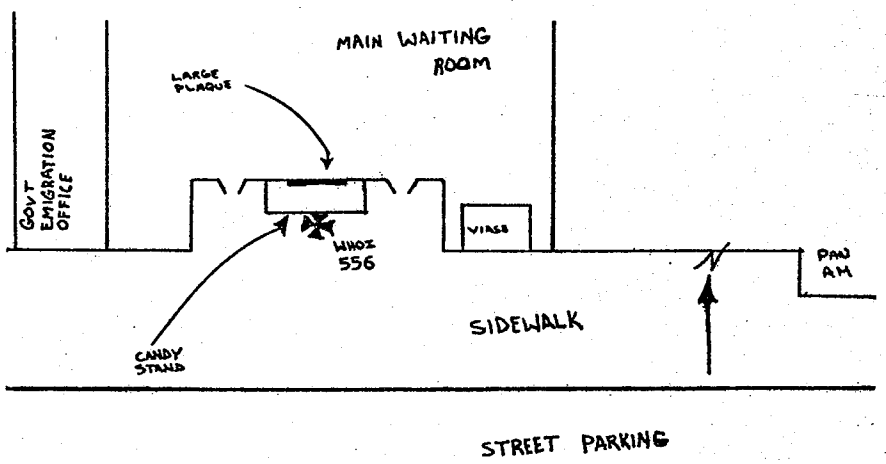

DIAGRAM BY A. Folinsbee — DATE 5 Mar. '70

Observed Gravity = 978245.80 (referenced to St. Innes #1 = 978065.87)

COUNTRY	NEAREST CITY	GRAVITY STATION DESCRIPTION		
Venezuela	Acarigua			
STATE / PROVINCE		STATION NAME		
Portugesa		Acarigua-Plaza Bolivar		
LATITUDE	LONGITUDE	ELEVATION	W.H.O.I. STATION NO.	GRAVITY VALUE (g)
9°33.5'N	69°11.9'W	198.08	644	

DESCRIPTION

The station is in the town of Acarigua in front of a church that is opposite the Plaza Bolivar (town square). It is above a bronze plaque on the sidewalk to the left of the church door.
Plaque BM # T.1
1959

DESCRIBED BY A+C. Folinsbee DATE 2-16-'70

POSITION CONTROL DESCRIPTION
M. O. P. - Carografia

ELEVATION CONTROL DESCRIPTION
Same as above.

DIAGRAM

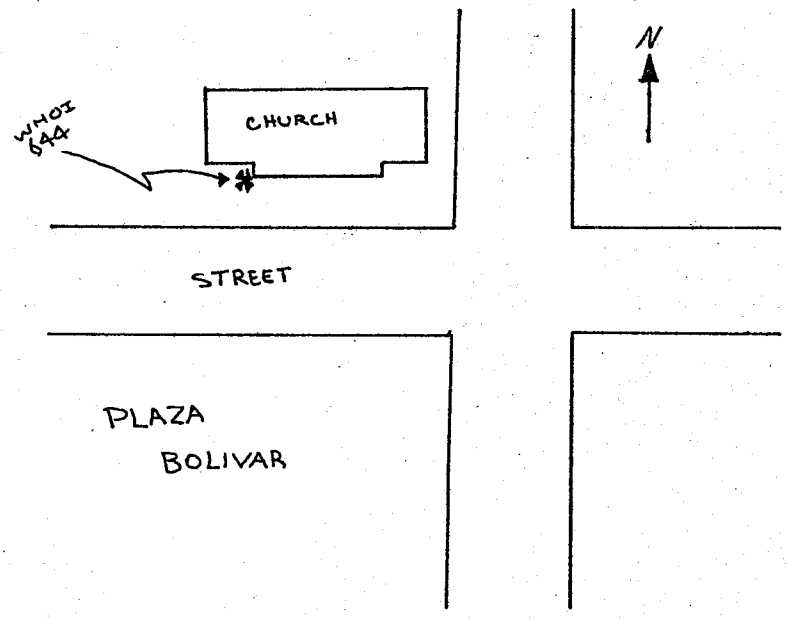

DIAGRAM BY A+C. Folinsbee DATE 2-16-70

Observed Gravity = 978097.06 (referenced to St. Innes #1 = 978065.87)

COUNTRY	NEAREST CITY	GRAVITY STATION DESCRIPTION
Venezuela	Guanare	
STATE/PROVINCE		STATION NAME
Portuguesa		Guanare Hotel Llanero

LATITUDE	LONGITUDE	ELEVATION	W.H.O.I. STATION NO.	GRAVITY VALUE (g)
69°02.4'N	69°45.1'W	--	655	

DESCRIPTION

Station is at Hotel Llanero in Guanare at main entrance on porch 8" above sidewalk.

DESCRIBED BY A. Folinsbee DATE 2-17-70

POSITION CONTROL DESCRIPTION

Approximate position - taken from M. O. P. Map

ELEVATION CONTROL DESCRIPTION

None

DIAGRAM

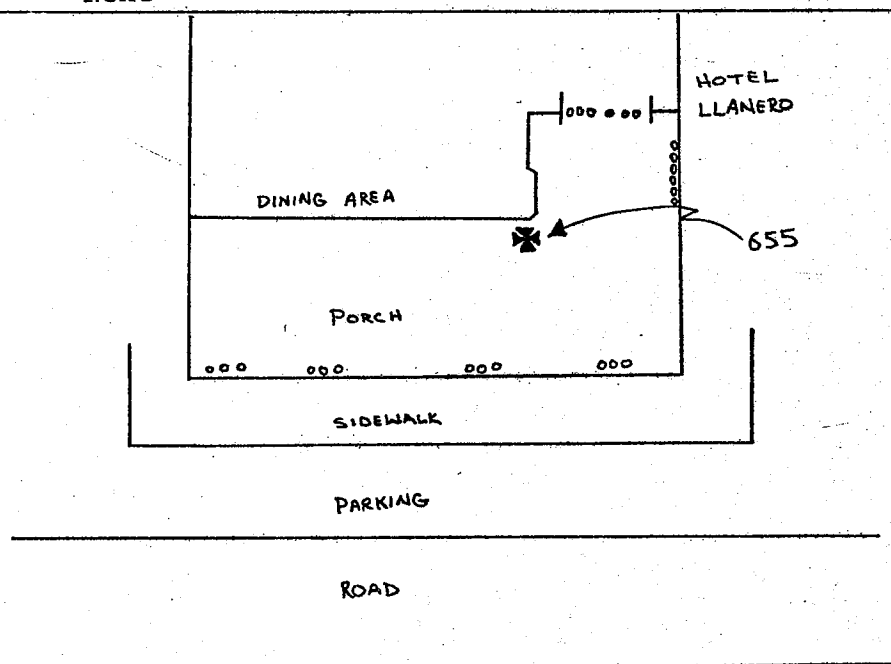

DIAGRAM BY A. Folinsbee DATE 2-17-70

Observed Gravity = 977750.57 (referenced to St. Innes #1 = 978065.87)

COUNTRY	NEAREST CITY	GRAVITY STATION DESCRIPTION		
Venezuela	Barinas			
STATE / PROVINCE		STATION NAME		
Barinas		Mene Grande Base 3		
LATITUDE	LONGITUDE	ELEVATION	W.H.Q.L. STATION NO.	GRAVITY VALUE (g)
8° 27.12' N	70° 3.90' W	139 m	669	

DESCRIPTION

The station is on trail from Campo Silvestre. The trail goes over a cattle guard + the 9 meters west of road +2.5 meters south of the third fence post from the road. It is this station that corresponds to Mene Grande Gravity Base 3 in Barinas.

DESCRIBED BY A. Folinsbee DATE 2-18-1970

POSITION CONTROL DESCRIPTION
From 1:100000 Barinas Topo sheet

ELEVATION CONTROL DESCRIPTION
same

DIAGRAM

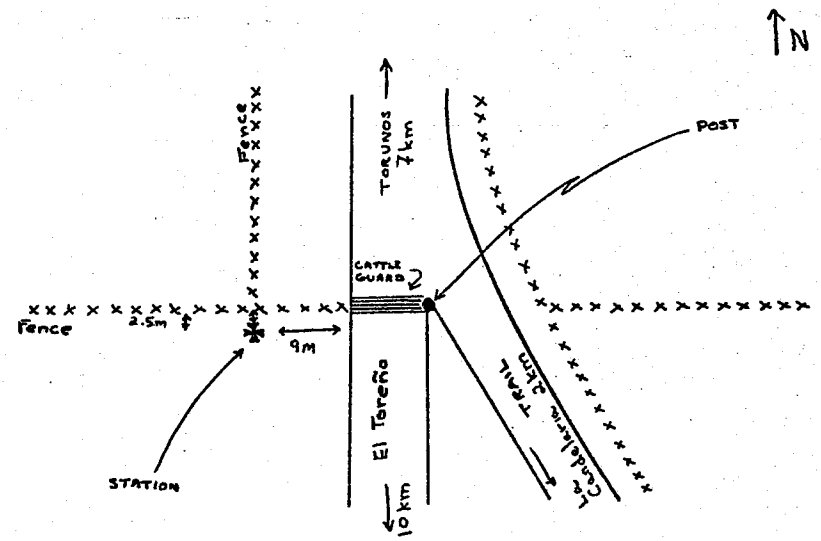

DIAGRAM BY A. Folinsbee DATE 2-18-1970

Observed gravity = 978085.98 (referenced to St. Innes #1 = 978065.87)

COUNTRY	NEAREST CITY	GRAVITY STATION DESCRIPTION		
Venezuela	Merida			
STATE / PROVINCE		STATION NAME		
Merida		Merida Airport		
LATITUDE	LONGITUDE	ELEVATION	W.H.O.I. STATION NO.	GRAVITY VALUE (g)
08°35.0'N	71°10.0'W	5000 ft.	694	

DESCRIPTION

This is Woollard station WA6187. The station is at Merida Airport in the main building, to the right of the door (as you stand in lobby) of the Airport Manager.

DESCRIBED BY A. Folinsbee — 20 Feb. '70

POSITION CONTROL DESCRIPTION

Woollard - P a 115

ELEVATION CONTROL DESCRIPTION

Same as above.

DIAGRAM

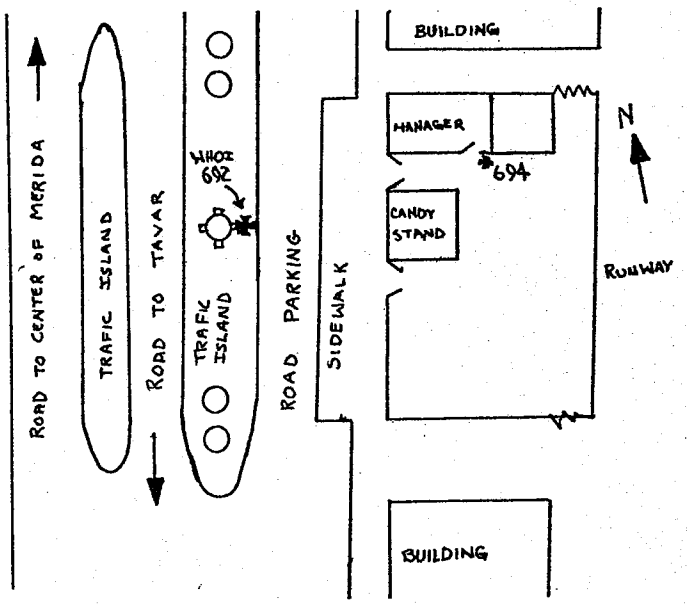

DIAGRAM BY A Folinsbee — DATE Feb 70

Observed Gravity = 978079.75 (referenced to St. Innes #1 = 978065.87)

COUNTRY	NEAREST CITY	GRAVITY STATION DESCRIPTION		
Venezuela	Maracaibo			
STATE/PROVINCE: Zulia		STATION NAME: Maracaibo-Grande Oro Airport		
LATITUDE: 10°40.5'N	LONGITUDE: 71°38.3'W	ELEVATION: -	W.H.O.I. STATION NO.: 715	GRAVITY VALUE (g)

DESCRIPTION

This station is at the old (abandoned) airport of Grande De Oro in Maricaibo. It is directly above a bronze plaque in the SW end of the traffic island to the left of the main building. The plaque is inscribed Gravidad MPA-1 1952.

DESCRIBED BY: A. Folinsbee — DATE: 2-21-'70

POSITION CONTROL DESCRIPTION

Woollard & Rose (1963) International Gravity Measurements, p. 115

ELEVATION CONTROL DESCRIPTION

DIAGRAM

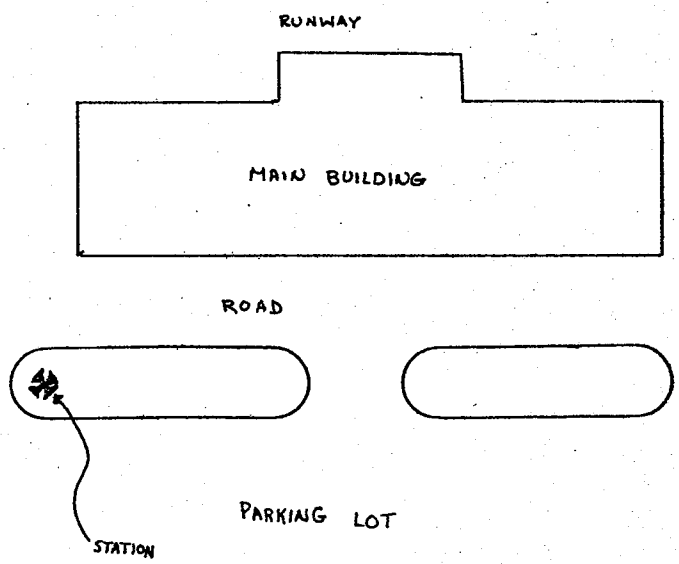

DIAGRAM BY: A. Folinsbee — DATE: 1-21-'70

Observed Gravity = 978199.54 (referenced to St. Innes #1 = 978065.87)

COUNTRY	NEAREST CITY	GRAVITY STATION DESCRIPTION		
Venezuela	Maracaibo			
STATE / PROVINCE		STATION NAME		
Zulaia	Dto. Paez	Sinamaica Church		
LATITUDE	LONGITUDE	ELEVATION	W.H.O.I. STATION NO.	GRAVITY VALUE (g)
11° 5.1' N	71° 50.2' W	?	717	

DESCRIPTION

Station is on road next to sidewalk (6" below sidewalk) in front of the south end of church in Sinamaica. (Shell Station 1738). Station is across street from Plaza Bolivar.

DESCRIBED BY A. Folinsbee DATE 2-21-1970

POSITION CONTROL DESCRIPTION

Shell Map 1:100000 No. GR132

ELEVATION CONTROL DESCRIPTION

None

DIAGRAM

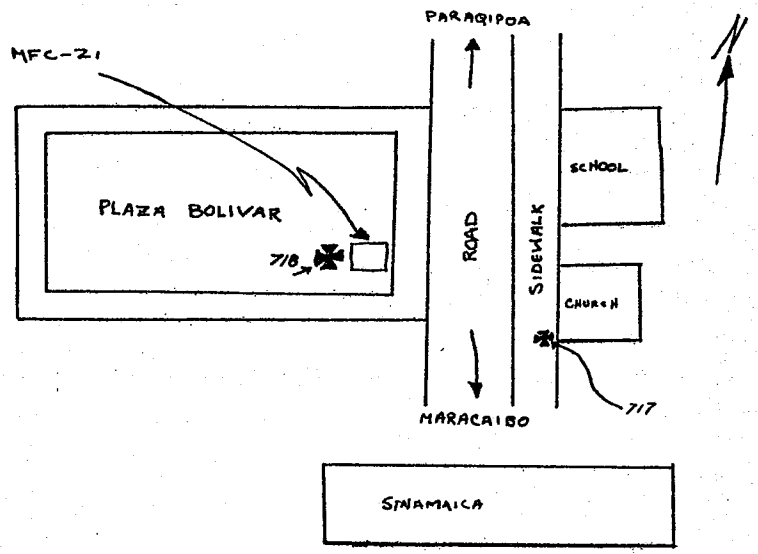

DIAGRAM BY A. Folinsbee DATE 2-21-1970

Observed Gravity = 978210.90 (referenced to St. Innes #1 = 978065.87)

APPENDIX II- Computer Programs

COORD

Subroutine COORD can be used to convert coordinates in any transverse Mercator system to latitude and longitude. The variables necessary to initialize the program are:

CMD, CMM } the central meridian of coordinate systems in degrees and minutes

PZD, PZM } the value of the latitude in degrees and minutes at the origin of the coordinate system

XZ, YZ } the value of the x and y coordinates of the origin of the coordinte system

ISR - is the ratio of the coordinate system, used if the coordinate system contains a scale reduction factor

After initialization, the program is entered with the argument string X,Y,RLONG,RLAT,ITST.

X= the value of the x coordinate in meters

Y= the value of the y coordinate in meters

ITST $\leq$ 0 to read in a new set of coordinate system parameters

ITST $\geq$ 1 to convert the point with coordinates X,Y, to latitude and longitude

RLAT - the calculated latitude of the point in radians

RLONG - the calculated longitude of the point in radians

```
      SUBROUTINE C0ORD(X,Y,RL0NG,RLAT,ITST)
      IIN=105
      II0UT=108
       IF(ITST) 1,1,102
    1  C0NTINUE
       ITST=1
       E2=.676865799E-2
       DTR=3.141592653/180.
       RTD=1./DTR
       ARCRD=3600.*RTD*30.713114
       AA=6378206.4
       AD=111132.089
       A=AD/DTR
       B=16216.944
       C=17.20937
       D=0.02273
       E=0.000033
       Q1=1./25.523932E-10
       AS=.484813681E-5
  101  C0NTINUE
      READ(IIN,601) CMD,CMM,PZD,PZM,ISR,XZ,YZ
  601 F0RMAT(F4.0,F6.3,F4.0,F6.3,I10,2F10.0)
      WRITE(II0UT,607) CMD,CMM,PZD,PZM,ISR,XZ,YZ
  607  F0RMAT(' CM=',F4.0,' DEG',F6.3,' MIN.,  PZ=',F4.0,' DEG',F6.3,' M
     1, ISR=',I6,'  XZ=',F6.0,'  YZ=',F6.0)
       PZ=PZD+PZM/60.
       CM=CMD+CMM/60.
        RCM=CM*DTR
        RPZ=PZ*DTR
        IF(ISR) 5,6,5
    5   R=FL0AT(ISR-1)/FL0AT(ISR)
        G0 T0 7
    6   R=1.
    7   C0NTINUE
        EL0=A*RPZ-B*SIN(2.*RPZ)+C*SIN(4.*RPZ)-D*SIN(6.*RPZ)
      1 +E*SIN(8.*RPZ)
        EL0=EL0*R
        RM=AD-566.05*C0S(2.*RPZ)+1.2*C0S(4.*RPZ)
        RM=RM*R*RTD
       RETURN
  102  C0NTINUE
       IFLG=2
       XP=X-XZ
       YP=Y-YZ
       P1=RPZ+YP/RM
   10  C0NTINUE
       ELN=(A*P1-B*SIN(2.*P1)+C*SIN(4.*P1)-D*SIN(6.*P1)
      1 +E*SIN(8.*P1))*R
       DY=ARCRD*R/SQRT((1.-E2*(SIN(P1))**2)**3)
       YN=ELN-EL0
       DPN=(YP-YN)/DY
       P1=P1+DPN
```

```
      IFLG=IFLG-1
      IF(IFLG) 11,11,10
   11 CONTINUE
CC
C     P1 IS NPW THE TABULAR LATITUDE
CC
      T=(1.-E2*(SIN(P1))**2)
      C=TAN(P1)*T**2/Q1
C     WE ARE NOW CALCULATING G RHO Z FACTOR
      SG1=(XP-(XP**3)*(T/R)**2/242.436946E+12)/R
      DELP=((SG1)**2*C/3600.)*DTR
      P1=P1-DELP
C     P1 IS NOW THE TRUE LATTITUDE
      T=(1.-E2*(SIN(P1))**2)
      RN=AA/SQRT(T)
      DELL1=SIN(SG1/RN)/COS(P1)
     DELLR=ARSIN(DELL1)
      RLONG=-DELLR+RCM
     RLONG=-RLONG
      RLAT=P1
      RETURN
      END
```

APPENDIX II- Computer Programs, continued

TALPLOT15

This program calculates the gravity anomalies due to a two dimensional set of polygons by the method of Talwani and Ewing (1960), and can automatically change the shape of one of the polygons so as to make the root mean square (RMS) difference between the observed and calculated gravity a minimum. It starts by reading in the values of observed gravity, elevation, and location for the field points at which the theoretical gravity is to be calculated. It then reads in the complete set of polygons and proceeds to calculate the theoretical gravity at each field point. The depth of any specified points of the last polygon to be read in will then be varied so as to reduce the RMS difference between the observed and calculated gravity. For each polygon point that is to be varied the effect of a change in the depth of that point on the gravity observed at all the field points is calculated. This is done by calculating the gravity attraction of a small triangular prism of material generated by moving the point up or down a distance of δ. The value for δ used in this program was 0.3 km.

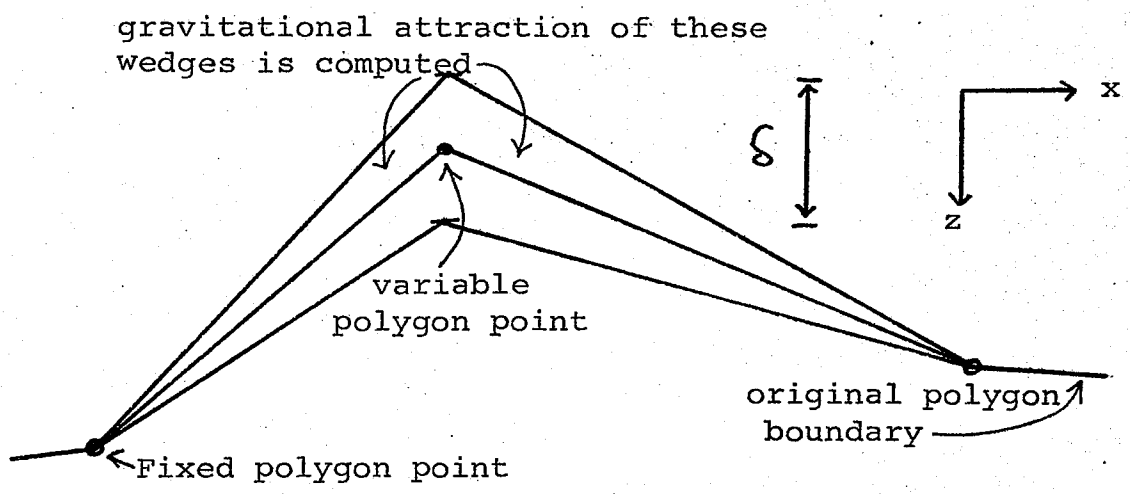

Let there be a total of M field points, and a total of N variable polygon points. For the i^{th} fieldpoint, let the observed gravity be g_i, the theoretical gravity t_i, and the residual $r_i = (g_i - t_i)$. If the two prisms of material about the j^{th} variable polygon point result in a gravity anomaly at the i^{th} field point of a_{ij} and if we require that the j^{th} variable polygon point be moved by an amount x_j such that the value of the residual r_i is reduced to zero for all i, this generates the following set of equations:

$$a_{11}x_1 + a_{12}x_2 + \ldots + a_{1N}x_N = r_1$$

$$a_{21}x_1 + a_{22}x_2 + \ldots + a_{2N}x_N = r_2$$

$$\vdots$$

$$a_{MN}x_1 + a_{M2}x_2 + \ldots + a_{MN}x_N = r_M$$

Since in general M is greater than N, this overdetermined set of equations must be reduced to a set of N normal equations. The k^{th} normal equation is obtained by multiplying each equation by the coeficient of x_k in that equation and summing the results. This set of N equations is then solved and the change of x_j is applied to the j^{th} variable polygon point. Because the change of gravity caused by a change in depth of the polygon is not a linear function of the depth, it is then necessary to calculate a new set values of theoretical gravity, and then to calculate a new set of changes to be applied to the variable polygon points. The number of iterations required depends on how far the initial polygon deviates from the final polygon. In practice it has been found that RMS of the residuals does not decrease significantly after 3 or 4 iterations.

The advantage of having the ability to automatically vary the shape of a polygon is that the effect of changes in the estimated depth to a layer, or the density of that layer can be quickly determined. Also by changing the location of the variable polygon points the range of polygons that will fit an observed gravity field can be determined.

```
C       PROGRAM TALPLOT 15
        OUTPUT 'TALPLOT: NOV15,1971'
C VERSION OF NOV15 TO CORRECT OUPUT ON JTAPE OF  NEW FIELD POINTS
C  SO THAT PLOTTING PROGRAM TERMINATES CORRECTLY
C  MOD OCT 14 TO CORRECT WEIGT BUG AND TO REMOVE PUNCHING OF
C    MODIFIED POINTS.  TIMER FEATURE ADDED
C      VERSION OF SEPT 28 CORRECTED WT CALCULATION FOR ELEVATION
C   AND IMPLEMENTED FILTERING OF RESIDUALS
C  MODIFIED SEPT 14,1971 BY FOLINSBEE
C     AND TO FILTER THE RESIDUAL BETWEEN OBSERVED AND THEORETICAL GRAVITY
C  MOD OF JUNE 9,1971  COMENST ON POLYGON CARDS,CORRECT WT CALC.
C   MODIFIED JUNE 2 71 TO USE ELEVATIONS IN CRUSTAL WT CALCULATION
C   VERSION OF 5 APRIL 1971, WRITES COMPLETE BOUGUER ON JTAPE
C LAST CHANGE FEB 3 71 TO READING OF ELEVATIONS
C     C LAST CHANGE JAN 19 71 TO REMOVE  OGGA BUG
C   LAST CHANGE(REMOVE OGA SET TO 0. BUG) ON JAN 14,71 AFOLINSBEE
C  TALPLOT 15 FROM TALPLOT 14 ON OCT 23,1970 BY AFOLINSBEE                T
C    THIS IS A PROGRAM TO SO BOTH LAND AND SEA DATA                       T
C   ELEVATION MUST FOLLOW OGA DAT , BEGINNING WITH A NEW CARD IN FORMAT   T
C      5F10.2                                                            T
C          FOR USE ON SIGMA 7,   7 TRACK MAGNETIC TAPE                   T
C            OUTPUT REPRODUCES INPUT AND ALSO RESULTS                    T
C                                                                        T
C    ASSIGN 9 TRACK MAG TAPE TO UNIT NUMBER 2                            T
C LAST BODY POINT IN EACH POLYGON MUST HAVE A 9 IN COL 21                T
C   WEIGH EXPECTS THE DIMENSION OF X,Z, TO BO BE 3 .GT. THE #OF POLY     T
C     POINTS                                                             T
C                                                                        T
C             LNO=1  SHOULD BE FOR WATER LAYER ONLY                      T
C             IF LNO=1, THEN  2-D BOUGUER ANOMALY IS CALULATED.          T
C             REFERENCE DENSITY AND WEIGHT INPUTS REQUIRED.              T
C      THE WEIGHT IS CACULATED FOR THE INPUT POLYGONS, Z AND NOT         T
C    FOR THE MODIFIED POLYGONS                                           T
C                                                                        T
C        ISW(1)=0    WRITE JTAPE                                         T
C              =1  NO WRITE JTAPE                                        T
C                                                                        T
C        ISW(2)=0  SETS ELEV     =0                                      T
C              = 1   READS IN ELEV   IN   KM                             T
C              =2    READS IN ELEV   IN   METERS                         T
C                                                                        T
C        ISW(3)=0      PRONTS INTERMEDIATE DATA FOR EACH PLOYGON          T
C              =1    NO PRITOUT OF INTERMED DATA                         T
C                                                                        T
C        ISW(4)=0    PLOT INTERMEDIATE DATA                              T
C              =1     NO PLOT                                           T
C                                                                        T
C        ISW(5)=0   NO PLOT OF ELEVATION                                 T
C              =1    PLOT ELEVATION                                      T
C      ISW(6) =1  TO ADJUST LAST CURVE TO FIT GRAVITY DATA               T
C    SSW(7) UP FOR OUTPUT DURING DEBUGING ONLY                           T
C                                                                        T
```

```
C       ISW(9)  =1 TO NOT WRITE INTERMEDIATE DATA FOR EACH POLYGON ONTO
C       JTAPE
C
C    SSW(11) UP TO NOT USES ELEVATION VALUES IN THE CALCULATION
C      OF THEORETICAL GRAVITY
C      IF SSW(11) IS UP THEN THE GRAVITY VALUES READ IN SHOULD
C      BE COMPLETE BOUGUER ANOMALIES
C    IALTE =1 MEANS THAT THIS POINT WI,L BE VARRIED TO COMPUTE A BEST FI
C      SSW(12) UP TO USE ELEVATION VALUES IN CRUSTAL WT CALCULATION
C     THIS SHOULD BE USED WHEN THE GRAVITY ANOMALIES ARE BOUGUER ANOMALI
C        AND THUS THE TOP OF THE MODEL IS AT SEA LEVEL,  A DENSITY OF  2
C      IS USED IN  AKING THE WT CORRECTION
C     SSW(13) =1 TO OUTPUT RESULTS OF INPUT POLYGONS BEFORE
C      ALTERING THE VARIABLE BOUNDARY POINTS
C       THE POLYGON THAT IS TO BE VARRIED MUST BE THE LAST POLYGON TO BE
C     THE POINT TO BE VARRIED MUST NOT BE THE FIRST OR LAST POINT IN TH
C       POLYGON
C      IMAX IS THE MAXIMUM NUMBER OF MODELS THAT WILL BE CZLCULATED
C    IMOD IS THE NUMBERR OF MODELS THAT HAVE BEEN CALCULATED
C
        LOGICAL BAR/.FALSE./
        COMMON FER(200),WFER(-10:10)
        DIMENSION LABEL(20)
        DIMENSION COME(5)
        DIMENSION FX(200),FZ(200)
        DIMENSION PDELZ(200),SSELZ(200),XO(1),X(200),ZO(1),Z(200),
     1  OGA(200),RESA(200),TEST(200),          DSU(200)
        DIMENSION ARRAY (200,5),SUM(200),DWGT(200),PCON(200),SUMW(200)
        DIMENSION RFDEL(20) ,XS(20)
        DIMENSION IALTE(150),AA(20,21),KK(5),D(5) ,DDELZ(20)
        DIMENSION OGGA(200)
        DIMENSION STSUM(200)
       EQUIVALENCE(ARRAY(1,1),FX(1)),(ARRAY(1,2),SSELZ(1)),
      1 (ARRAY(1,3),RESA(1)),(ARRAY(1,4),OGGA(1))
  100 FORMAT(5F5.1)
        CALL TIC
        DO 1 K=1,200
1       FER(K)=0.
        ILOOP=0
        SREFC=0
        IREST=0
        IFIRST=0
        RSQ=1.E70
        IMOD=0
        DEL=.15
        D(2)=-DEL
        D(4)=DEL
       KK(1)=-1
       KK(3)=1
       KK(5)=-1
        IIN=105
        IPUN=106
       IIOUT=108
```

```
      N4=4
      JTAPE=2
      KFXN=1
C   NOTE THAT THE LAST POLYGON MUST HAVE NUMBER 99
      L=99
 42   FORMAT(2F10.2)
 442  FORMAT(2F10.2,2I1)
   44 FORMAT(I5,4F10.2)
   45 FORMAT(//6H LNO =,I4,              10H     RHO =,F10.3,2X,5A4)
   47 FORMAT(/35H     K      FX(K)      FZ(K)    ANOMALY)
   51 FORMAT(/  '     K      FX(K)      FZ(K)    ANOMALY   CAL REF  RESIDUALT
   511  OBS ANOMALY          WEIGHT       WGT DIFF     WEIGHTEST',5X,'FILT')
C     RDENS =REFERENCE DENSITY FOR GRAVITY CALCULATIONS
C  RWGT = REFERENCE WEIGHT FOR MASS CALCULATIONS
C     RHOD=DIFFERENCE DENSITY FOR MODEL ADJUSTING =RHO LOWER)-RHO(UPPERT
      READ(IIN,446) (LABEL(KU),KU=1,20)
446   FORMAT(20A4)
      WRITE(IIOUT,447) (LABEL(KU),KU=1,20)
447   FORMAT(1X,20A4)
      I=ISW(-2)
      IF(ISW(1).EQ.0) WRITE(JTAPE,446) (LABEL(KU),KU=1,20)
      DO 56 K=1,80
56    IALTE(K)=ISW(K)
      IF(ISW(1).EQ.0) WRITE(JTAPE,419) (IALTE(K),K=1,80)
419   FORMAT(80I1)
      READ (IIN,427) RDENS,RWGT,RHOD,REFX,FXI,DELFX,M,NFER,IMAX
427   FORMAT(6E10.2, I10,2I5)
      OUTPUT RDENS,RWGT,RHOD,REFX,FXI,DELFX,M,NFER,IMAX
      IZERO=0
      IF(ISW(1).EQ.0) WRITE(JTAPE,427) RDENS,RWGT,RHOD,REFX,FXI,DELFX,MT
     *,IZERO,IMAX
      IF(NFER.LT.1) GO TO 5963
      OUTPUT 'WFER(K)    '
      DO 5960 K=0,NFER
      WFER(K)=(NFER-K+1.)/(NFER+1.)
      WFER(-K)=WFER(K)
      KL=-K
      WRITE(IIOUT,42) WFER(KL),WFER(K)
C     NOTE WE HAVE MADE A TRIANGULAR WEIGHTING FUNCTION
5960  CONTINUE
5963  CONTINUE
      DO 59 I=1,M
      SUM(I)=0.
      TEST(I)=0
      DSU(I)=0
  59  CONTINUE
      FX(KFXN)=FXI
      FZ(KFXN)=0.0
      ARRAY(KFXN,5)=0.
      K1=KFXN+1
      READ200,(OGA(I),I=1,M)
200   FORMAT(5F10.1)
      DO 620 I=1,M
```

```
      θGGA(I)=θGA(I)
      IF(θGA(I).GE.899.) θGGA(I)=0.
620   CθNTINUE
      IF(ISW(1).EQ.1) Gθ Tθ 7004
      WRITE (JTAPE,200) (θGA(I),I=1,M)
7004  CθNTINUE
      IF (ISW(2).EQ.0) Gθ Tθ 7021
      READ201,(FZ(I),I=1,M)
201   FθRMAT(5F10.1)
      IF(ISW(1).EQ.1) Gθ Tθ 7005
      WRITE(JTAPE,  201) (FZ(I),I=1,M)
7005  CθNTINUE
      CC= 1.
      IF(ISW(2).EQ.2) CC=1000.
      Dθ 7034 I=1,M
      FZ(I)=-FZ(I)/CC
      ARRAY(I,5)=FZ(I)*(-100.)
      IF(ISW(11).EQ.1) FZ(I)=0.
7034  CθNTINUE
7021  CθNTINUE
      Dθ 451 K=K1,M
      FX(K)=FX(K-1)+DELFX
4501  CθNTINUE
 451  CθNTINUE
      Dθ 96 K=KFXN,M
      SSELZ(K) = 0.0
  96  CθNTINUE
      Dθ 53J=KFXN,M
      IF(REFX-FX(J))53,21,53
  53  CθNTINUE
  21  J=J
      REFθGA = θGA(J)
      JREF=J
60    CθNTINUE
      READ(IIN,433) LNθ,RHθRK,CθME
433   FθRMAT(I5,F10.3,5A4)
      WRITE(IIθUT,45) LNθ,RHθRK,CθME
      IF(ISW(1).EQ.0) WRITE(JTAPE,433) LNθ,RHθRK
      RHθ=RHθRK-RDENS
799   CθNTINUE
      I=1
801   READ 442 ,XX,ZZ  ,ICθDE ,IAL
      X(I)=XX
      Z(I)=ZZ
      IALTE(I)=IAL
      PRINT 7032,X(I),Z(I),ICθDE ,IAL
7032  FθRMAT(2X,2F11.3,3X,2I1)
      IF(ISW(1).EQ.1) Gθ Tθ 7008
      IF(IREST.EQ.1) GθTθ 7008
      WRITE(JTAPE,442)X(I),Z(I),ICθDE,IAL
7008  CθNTINUE
      N=I
      I=I+1
```

137

```
      IF(ICODE-9)801,810,801                                            T
810    CONTINUE                                                         T
       IF(IREST .EQ.1) GO TO 811                                        T
      CALL WEIG2 (X,Z,N,FX,M,SUM,RHORK,TEST,DSU)                        T
811    CONTINUE                                                         T
       IF(ISW(3).EQ.0) PRINT 47                                         T
C                                                                       T
C      FIELD POINT DO LOOP                                              T
C                                                                       T
      DO 421 K=KFXN,M                                                   T
      SDELZ=0.                                                          T
C                                                                       T
C      POLYGON POINTS DO LOOP                                           T
C                                                                       T
      DO 3004I=1,N                                                      T
       IDUM=I                                                           T
  205 EXXX=X(I) - FX(K)                                                 T
      ZEEE=Z(I) - FZ(K)                                                 T
       CALL COMP                                                        T
 3004 CONTINUE                                                          T
       IF(ILOOP.EQ.1) PDELZ(K)=RHOD*(13.34*SDELZ-PCON(K)/RHO);GOTO3005  T
      PDELZ(K)=13.34*RHO*SDELZ                                          T
3005   CONTINUE                                                         T
      SSELZ(K)=SSELZ(K)+PDELZ(K)                                        T
       IF(LNO-1)4101,5001,4101                                          T
 5001  BGTD   =OGA(K)-PDELZ(K)                                          T
 5006  PRINT 5007,K,FX(K),FZ(K),PDELZ(K),BGTD                           T
 5007  FORMAT(I5,4F10.2)                                                T
C
C     TO WRITE COMPLETE BOUGUER ANOMALY ON JTAPE
C
       IF(ISW(1).EQ.1)  GO TO 7009
       WRITE(JTAPE,5007)K,FX(K),FZ(K),PDELZ(K),BGTD
        GO TO 7009
 4101 CONTINUE                                                          T
      IF(ISW(3).EQ.1) GO TO 7022                                        T
      PRINT44,K,FX(K),FZ(K),PDELZ(K) ,DSU(K)                            T
 7022 CONTINUE                                                          T
 5008  CONTINUE                                                         T
       IF(ISW(9).EQ.1) GO TO 7009                                       T
       IF(ILOOP.EQ.1) GO TO 7009                                        T
      IF(ISW(1).EQ.1) GO TO 7009                                        T
       IF(IREST.EQ.1) GOTO 7009
       WRITE(JTAPE,44)K,FX(K),FZ(K),PDELZ(K)                            T
 7009 CONTINUE                                                          T
  421 CONTINUE                                                          T
      IF(ISW(4).EQ.1) GO TO 423                                         T
      CALL PLOTER(PDELZ,M,BAR)                                          T
423   CONTINUE                                                         T
      IF(L-LNO) 60,430,60                                               T
  430  REFCOR = REFOGA-SSELZ(J)                                         T
      DO  422K=KFXN,M                                                   T
      SSELZ(K) = SSELZ(K) + REFCOR                                      T
```

```
 422     CONTINUE
         SREFC=SREFC+REFCOR
         IRES=0
         RSOLD=RSQ
         RSQ=0
         RESF=0
C
C      CALCULATING THE RMS ERROR
C
         DO 4422 K=KFXN,M
         IF(   OGA(K).GE.900) GOTO 4422
        RESA(K)=SSELZ(K)-OGA(K)
 4422    CONTINUE
         DO 4424 K=KFXN,M
         IF(OGA(K).GE.900) GO TO 4424
         IF(NFER.LT.1) FER(K)=RESA(K) ;GOT04029
         FER(K)=0
         WTFE=0
         KSTART=K-NFER
         KEND=K+NFER
         DO 4020 KH=KSTART,KEND
         IF(OGA(KH).GE.900. .OR.KH.LT.1 .OR. KH.GT.M) GO TO 4020
         FER(K)=FER(K)+RESA(KH)*WFER(K-KH)
         WTFE=WTFE+WFER(K-KH)
 4020     CONTINUE
         FER(K)=FER(K)/WTFE
 4029     CONTINUE
         IRES=IRES+1
         RESF=FER(K)**2+RESF
         RSQ=RESA(K)**2+ RSQ
  4424   CONTINUE
         RESF=SQRT(RESF/IRES)
         RSQ=SQRT(RSQ/IRES)
         WRITE(IIOUT,4425) IMOD,RSQ,IRES,RESF
 4425    FORMAT(2X,'IMOD=',I5,' RMS ERROR=',F10.5,' NUMBER OF POINTS=',I5,
     * ', FILTERED RMS ERROR= ' ,F10.5)
         IF(IMOD.GT.IMAX ) GO TO 438
         IF(ISW(13).EQ.1 .AND. IFIRST.EQ.0) GOTO 439
 4423    CONTINUE
         IFIRST=1
         IF(ISW(10).EQ.1.AND.IMOD.LE.1)  GO TO 4427
         IF(ISW(6).EQ.0 .OR.IMOD.GT.IMAX .OR.((RSOLD-.5).LT.RSQ  .AND.
     * (IMOD .GT. 1)))GOTO 438
C     BRANCHING OUT OF MODEL ALTERING PART OF M PROGRAM
 4427     CONTINUE
         DO 4426 LQ=1,MCH
         DO 4426 LQQ=1,MCH+1
 4426    AA(LQ,LQQ)=0
         XO(1)=X(N)
         ZO(1)=Z(N)
         K=JREF
         MCH=0
C
```

```
C    COMPUTATION OF D/DZ FOR THE REFERENCE POINT                        T
C                                                                       T
         DO 7650 I=1,N-1                                                T
         IF(IALTE(I).EQ.0) GO TO 7650                                   T
         SDELZ=0                                                        T
         DO 7640 IDUM=1,5                                               T
         II=IDUM                                                        T
         ARG=X(I+1)-X(I-1)                                              T
         EXXX=X(I+KK(II)) -FX(K)                                        T
         ZEEE=Z(I+KK(II))-FZ(K)+D(II)*SIGN(1.,ARG)                      T
         CALL COMP                                                      T
 7640    CONTINUE                                                       T
         MCH=MCH+1                                                      T
         RFDEL(MCH)=13.34*RHOD*SDELZ                                    T
7650     CONTINUE                                                       T
4701     FORMAT(1X,I2,10G10.3)                                          T
         KCODE=0                                                        T
         IF(ISW(7).EQ.1) WRITE(IIOUT,4701) KCODE,K, (RFDEL(KD),KD=1,MCH) T
C                                                                       T
C     STORING THE OLD VALUES OF PDELZ                                   T
C                                                                       T
         IF(ILOOP.EQ.1) GO TO 434                                       T
         DO 432 K=KFXN,M                                                T
432      PCON(K)=PDELZ(K)                                               T
         GO TO 436                                                      T
434      DO 435 K=KFXN,M                                                T
435      SSELZ(K)=SSELZ(K)-PDELZ(K)                                     T
C   SSELZ(K) IS NOW THE SUMMED VALUE OF ALL POLYGON CONTRIBUTIONS
C      EXCEPT THAT DUE TO THE CHANGED PART OF THE MODEL
         SREFC=SREFC-PDELZ(JREF)                                        T
436      CONTINUE                                                       T
         ILOOP=1                                                        T
         IMOD=IMOD+1                                                    T
CC                                                                      T
C      FIELD POINT DO LOOP                                              T
C                                                                       T
         DO 7850 K=KFXN,M                                               T
         IF(OGA(K).GE.900) GO TO 7850
         IF(K.EQ.JREF) GO TO 7850                                       T
         MCH=0                                                          T
C                                                                       T
C    COMPUTING D/DZ FOR EACH CHANGEABLE POLY POINT                      T
C                                                                       T
         DO 7830 I=1,N-1                                                T
         IF(IALTE(I).EQ.0) GO TO 7830                                   T
        SDELZ=0.                                                        T
         DO 7820 II=1,5                                                 T
         ARG=X(I+1)-X(I-1)                                              T
         EXXX=X(I+KK(II)) -FX(K)                                        T
         ZEEE=Z(I+KK(II))-FZ(K)+D(II)*SIGN(1.,ARG)                      T
         IDUM=II                                                        T
         CALL COMP                                                      T
7820     CONTINUE                                                       T
```

```
      MCH=MCH+1
      DDELZ(MCH)=13.34 *RH0D*SDELZ-RFDEL(MCH)
7830  C0NTINUE
      KC0DE=1
      IF(ISW(7).EQ.1) WRITE(II0UT,4701) KC0DE,K, (DDELZ(KD),KD=1,MCH
C   N0W ADD THE C0NTRIBUTI0N T0 THE N0RMAL EQUATI0N
C
      D0 7835 II=1,MCH
      D0 7834 IP=1,MCH
      AA(II,IP)=AA(II,IP)+DDELZ(IP)*DDELZ(II)
7834  C0NTINUE
      AA(II,MCH+1)=AA(II,MCH+1)+FER (K)*DDELZ(II)
7835  C0NTINUE
7850  C0NTINUE
C   WE HAVE N0W FINISHED SETTING UP THE N0RMAL EQUATI0NS
      EPS=1.E-20
      INDIC=+1
      NRC=20
C
C   N0TE THAT NRC IS THE NUMBER 0F C0LUMS IN THE MATRIX AA
C
      MP1=MCH+1
      IF(ISW(7).EQ.1) 0UTPUT 'N0RMAL EQUATI0NS';WRITE(II0UT,4540
     * ),(MP1,(AA(II,JJ),JJ=1,MP1),II=1,MCH)
4540  F0RMAT(NG10.3)
      CALL SIMUL(MCH,AA,XS,EPS,INDIC,NRC,DETER)
      IF(ISW(7).EQ.1) 0UTPUT DETER,(XS(Iw),IW=1,MCH)
C     CALCULATE THE NEW VALUES 0F THE P0YG0N P0INTS
      MCH=0
      D0 7860 K=1,N
      IF(IALTE(K).EQ.0) G0 T0 7860
      MCH=MCH+1
      Z(K)=Z(K)+XS(MCH)*2*DEL
      IF(Z(K).LT.0.2) Z(K)=.2
7860  C0NTINUE
      IF(ISW(7).EQ.1) 0UTPUT 'NEW P0LY P0INTS'; 0UTPUT,(Z(K),K=1,N)
      G0 T0 811
438   C0NTINUE
      IF(IL00P.EQ.0) G0 T0 439
C     MAKING THE WEIGT CALCULATI0N F0R THE M0DIFIED P0LYG0N
C   AA IS JUST A GARBAGE ARRAY
      CALL WEIG2(X,Z,N,FX,M,AA, 1.  ,AA,DWGT )
      D0 441 K=KFXN,M
      IF(IREST.EQ.1) SUM(K)=STSUM(K)
      STSUM(K)=SUM(K)
C     STORING THE VALUE 0F SUM T0 USE IN FUTURE CALCULATI0NW
441   SUM(K)=SUM(K)+(DWGT (K)-DSU(K)/RH0RK)        *RH0D
C   DWGT(K) IS BEING USED F0R TEMP0RARY ST0RAGE
      0UTPUT 'NEW P0LY P0INTS -FINAL VERSI0N'
      WRITE(II0UT,440)(X(K),Z(K),K=1,N)
440   F0RMAT(2X,2F10.2)
      IF(IREST.EQ.1) G0T0 4041
      IF(ISW(1).EQ.0) WRITE(JTAPE,42) (X(K),Z(K),K=1,N-1);
```

```
     * WRITE(JTAPE,442) X(N),Z(N),ICODE
4041   CONTINUE
439    PRINT 51                                                          T
       DO 7000 K=KFXN,M
       DWGT(K)=SUM(K)-RWGT                                               T
       SSSSS=SSELZ(K)-SREFC                                              T
       IF(ISW(12).EQ.1)
     *  DWGT(K) =DWGT(K) +ARRAY(K,5)*2.67
       PRINT52,K,FX(K),FZ(K),SSSSS,SSELZ(K),RESA(K),BGA(K)               T
     1,SUM(K),DWGT(K) ,TEST(K),FER(K)                                    T
  52   FORMAT(I5,6F10.2,F16.0,F16.0,F16.0,F6.1)
483    CONTINUE                                                          T
       IF(ISW(1).EQ.1) GO TO 7000                                        T
       IF(IREST.EQ.1) GOTO 7000
       WRITE(JTAPE,52)K,FX(K),FZ(K),SSSSS,SSELZ(K),RESA(K),BGA(K)        T
     1 ,SUM(K),DWGT(K)                                                   T
 7000 CONTINUE                                                          T
       CALL PLOTER(DWGT,M,BAR)                                          T
 4220     CONTINUE                                                      T
       IF(ISW(1).EQ.1) GO TO 7013                                       T
       END FILE JTAPE                                                   T
 7013 CONTINUE                                                          T
 610  CONTINUE                                                          T
       IF(ISW(5).EQ.1) N4=5
       ARRAY(200,1)=ARRAY(M,1)                                          T
       CALL PLOTA(LNO,ARRAY,200,N4,M,0.0,1.,FDUM,FDUM)                  T
       OUTPUT ' 1= THEORETICAL GRAVITY IN MILIGALS'                     T
       OUTPUT ' 2= DIFFERENCE BETWEEN THEORETICAL AND OBSERVED GRAVITY' T
       OUTPUT ' 3= OBSERVED GRAVITY'                                    T
       OUTPUT ' 4= ELEVATION IN 10 S OF METERS'                         T
       IF(ISW(13).EQ.1 .AND. IFIRST .EQ.0) GOTO 4423
 999  CONTINUE                                                          T
C   STORING THE VALUE OF X
       IF(ISW(6) .NE.1) GO TO 7011
       READ(IIN,433,END=7011) LNO,RHONEW
       IF(LNO.NE.99) GO TO 7011
       IREST=1
       IMOD=0
       RSQ=1.E70
       DO 630 K=KFXN,M
630    SSELZ(K)=SSELZ(K)-PDELZ(K)
C  SSELZ(K) IS NOW THE SUMMED VALUE OF ALL POLYGON CONTRIBUTIONS
C      EXCEPT THAT DUE OT THE CHANGED PART OF THE MODEL
       OUTPUT ' NOW RECALCULATING THE MODEL USING NEW VARIABLE POLYPOINT
     *S'
       GO TO 799
C     IREST IS SET EQUAL TO 1 TO INDICATE THAT
C    WE ARE READING AN ADDITION SET OF POINTS FOR THE LAST
C     POLYGON  TO SEE THE EFFECT OF USING DIFFERENT
C     VARIABLE POLYGON POINTS
7011   CONTINUE
       CALL TOC(TIME)
       OUTPUT TIME
```

```
      STOP
      SUBROUTINE COMP
     RR=EXXX**2+ZEEE**2
     IF(EXXX)210,240,280
 210 IF(ZEEE)220,230,230
 220 THETB=ATAN(ZEEE/EXXX)-3.1415927
     GO TO 301
 230 THETB=ATAN(ZEEE/EXXX)+3.1415927
     GO TO 301
 240 IF(ZEEE)250,260,270
 250 THETB=-1.5707963
     GO TO 301
 260 THETB=0.
     GO TO 301
 270 THETB=1.5707963
     GO TO 301
 280 THETB=ATAN(ZEEE/EXXX)
 301  IF(IDUM-1) 3001,3002,3001
3001 CHECK=EXX*ZEEE-ZEE*EXXX
     IF(CHECK)320,310,320
 310 DELZ=0.
     GO TO 401
 320 OMEGA=THETA-THETB
     IF(OMEGA)3201,3202,3202
3202 IF(OMEGA-3.1415927)330,330,340
3201 IF(OMEGA+3.1415927)340,330,330
 330 DTHET=OMEGA
     GO TO 370
 340 IF(OMEGA)351,360,360
 351 DTHET=OMEGA+6.2831853
     GO TO 370
 360 DTHET=OMEGA-6.2831853
 370 A=CHECK/((EXXX-EXX)**2+(ZEEE-ZEE)**2)
     B=(EXXX-EXX)*DTHET
      C=0.5*(ZEEE-ZEE)*ALOG(RR/R)
     DELZ=A*(B+C)
 401 SDELZ=SDELZ+DELZ
3002 EXX=EXXX
     ZEE=ZEEE
     R=RR
     THETA=THETB
      RETURN
      END
```

APPENDIX II- Computer Programs, continued

WEIG2

This subroutine calculates the total vertical thickness of a polygon beneath any point on the horizontal axis. It will calculate the thickness for any arbitrary shape of polygon subject to the restriction that the line segments defining the polygon may not cross each other. This subroutine is used by TALPLOT15 to calculate the mass per unit area for the model.

```
      SUBROUTINE WEIG2(XPOL,ZPOL,NVERT,X,NPTS,SUM,RHO,TEST,DSU)
C     THIS IS VERSIONS 2 WHICH ALSO DOES WEIGHTEST
C      THIS SUBROUTINE IS TO BE USED  WITH TALPLOT.  IT COMPUTES
C       THE DENSITY CONTRIBUTION OF A POLYGON OF    DENSITY RHO
C      AND ADDS THE CONTRUIBUTION TO THE SUM.
C       XPOL, ZPOL ARE THE COORDINATES OF THE VERTICES OF THE POLYGON
C       NVERT  IS THE # OF VERTICES IN A POLYGON
C      X   IS THE COORDINATEE AT WHICH WE WISH THE SM CALCULATED.
C    NPTS IS THE # OF POINTS AT WHICH WE WISH THE SUM CALCULATED
C    SUM IS THE ACCUMULATED DENSITY CONTRIBUTION
C      A RESTRICTION IS THAT THE FIRST THREE (3) POINTS OF A POLYNOMIA
C      MAY NOT HAVE THE SAME X COORDINATE.  ,  THE FIRST TWO(2) MAY
C      BE THE SAME, AND AFTER THE FIRST VERTICE ANY NUMBER MAY
C      THE DIMENSION OF XPOL,ZPOL, MUST BE  3 GREATER IN THE MAIN
C     PROGRAM THEN THE ACTUAL NO OF VERTICES (NVERT)
      DIMENSION XPOL(1),ZPOL(1),X(1),Z(1),WT(1),SUM(1),NFLAG(10),
     1DIS(10),SORT(10) ,KFLAG(10) ,TEST(1) ,DSU(1)
      ZPOL(NVERT+1)=ZPOL(2)
      ZPOL(NVERT+2)=ZPOL(3)
      ZPOL(NVERT+3)=ZPOL(4)
      XPOL(NVERT+1)=XPOL(2)
      XPOL(NVERT+2)=XPOL(3)
      XPOL(NVERT+3)=XPOL(4)
      DO 300 I=1,NPTS
      SU =0.
      INTER=1
      IIOUT=108
      NDUM=NVERT+2
      JJ=3
      XX=X(I)
      DO 9 IQ=1,10
      DIS(IQ)=0.
9     NFLAG(IQ)=-1
      IF(XX-XPOL(3)) 11,15,80
 15   JJ=2
      NDUM=NVERT+1
      IF(XX-XPOL(2)) 11,14,80
14    JJ=1
      NDUM=NVERT
      IF (XX-XPOL(1)) 11,17,80
17     CONTINUE
      WRITE(IIOUT,18)
18    FORMAT(' ********* FIRST 3 VERTICES HAVE .EQ. X COORD. ' )
 10   CONTINUE
11    CONTINUE
12    JJ=JJ+1
      IF(JJ.GT.NDUM ) GO TO 100
      IF (   XX-XPOL(JJ)) 11,20,21
20    JAC=JJ
22    IF (XX.NE.XPOL(JJ+1 )) GO TO 24
      JJ=JJ+1
      GO TO 22
```

```
21     DIS(INTER)=((XPOL(JJ)-XX)*ZPOL(JJ-1)+(XX-XPOL(JJ-1))*ZPOL(JJ))
      C/((XPOL(JJ)-XPOL(JJ-1)))
       INTER =INTER+1
       GO TO 80
C      THIS SECTION HANDLES INTERSECTION WITH A VERICAL
C      LINE OR INTERSECTION THRU ONE OF THE VERTICES OF THE POLYGON
24     IF(XPOL(JJ+1).GT.XX) GO TO 26
       IF (JJ.GE.NDUM  ) GO TO 100
       DIS(INTER)=(ZPOL(JJ)+ZPOL(JAC))/2.
       INTER=INTER+1
       GO TO 80
26     IF (JAC.EQ.JJ) GO TO 11
       DIS(INTER)=ZPOL(JAC)
       NFLAG(INTER)=INTER
       INTER=INTER+1
       DIS(INTER)      =ZPOL(JJ)
       NFLAG(INTER)=INTER-1
       INTER=INTER+1
       GO TO 11
80     CONTINUE
       JJ=JJ+1
       IF (JJ.GT.NDUM ) GO TO 100
       IF (XPOL(JJ)-XX) 80,90,91
90     JAC=JJ
92     IF (XX.NE.XPOL(JJ+1) ) GO TO 94
       JJ=JJ+1
       GO TO 92
91     DIS(INTER)=((XX-XPOL(JJ))*ZPOL(JJ-1)+(XPOL(JJ-1)-XX)*ZPOL(JJ))
      1/(XPOL(JJ-1)-XPOL(JJ))
       INTER =INTER+1
       GO TO 11
94     IF (  XPOL(JJ+1).LT.XX) GO TO 96
       DIS(INTER)=(ZPOL(JJ)+ZPOL(JAC))/2.
       INTER=INTER+1
       GO TO 11
96     IF(JAC.EQ.JJ) GO TO 80
       DIS(INTER)=ZPOL(JAC)
       NFLAG(INTER)=INTER
       INTER=INTER+1
       DIS(INTER)=ZPOL(JJ)
       NFLAG(INTER)=INTER-1
       INTER=INTER+1
       GO TO 80
100    CONTINUE
C      WRITE (108,517)
 517   FORMAT('DIS   (NFLAG')
C
C
C
C      WE HAVE NOW LOCZTED ALL THE INTERSECTIONS WHICH RUN DOWN THE
C      BODY OF A POLYGON AND NEVER CROSSES IN OR OUT
C      THE INTERSECTION WILL   NOW BE SORTED FROM SMALLEST TO LARGEST
       INTER=INTER-1
```

```
C       THIS CHANGES INTER  SO THAT IT NOW = THE # OF INTERSECTIONS
        IF(INTER.EQ.0) GO TO 300
C   IF THERE ARE NO INTERSECTINS WE BYPASS THE COPUTATION
C    OF THE SDISTANCE
C     SORT FROM SMALLEST TO LARGESR
        DO 112 IU=1,INTER
        JJU=1
        KFLAG(IU)=NFLAG(1)
        SORT(IU)=DIS(1)
        DO 110 JU=2,INTER
        IF(SORT(IU).LE.DIS(JU)) GO TO 110
        SORT(IU)=DIS(JU)
        KFLAG(IU)=NFLAG(JU)
        JJU=JU
 110    CONTINUE
        DIS(JJU)=1.E70
 112    CONTINUE
        SUBT=0.
        IF(SORT(1)) 2201,2202,2202
 2201   CONTINUE
        DSOR=0.
        IF(SORT(2).LT.0) DSOR=SORT(2)
        SUBT=(SORT(1)-DSOR)
 2202   CONTINUE
C       WRITE (108,52) INTER
C       WRITE (108,518),(SORT(IX),KFLAG(IX),IX=1,4)
  52    FORMAT (1X,I3)
 518    FORMAT(1X,F6.3,1X,I3)
C       THE NO ARE ALL SORTED NOW
C       WE ARE NOW GOING TO COMPUTE THE SI DISTANCE
C
        MDID=0
 201    IF(INTER-MDID) 999,999,202
 202    MDID=MDID+1
        IF(KFLAG(MDID)) 203,203,221
 203    SU     =SU     +SORT(MDID+1)-SORT(MDID)
        IF (     KFLAG(MDID+1))204,204,245
 204    MDID=MDID+1
        GO TO 201
C    THIS HAS NOW HANDLED THE NORMAN SECTION
 221    IF (  KFLAG(MDID).NE.KFLAG(MDID+1)) GO TO 224
        SU     =SU     +(SORT(MDID+1)-SORT(MDID))/2.
        MDID=MDID+1
        GO TO 201
  224   SU     =SU     +(SORT(MDID+3)+SORT(MDID+2)-SORT(MDID+1)-SORT(MDID))
      C/2.
        MDID=MDID+3
        GO TO 201
 245    IF(  KFLAG(MDID+1).NE.KFLAG(MDID+2)) GO TO 248
        SU     =SU     +(SORT(MDID+2)-SORT(MDID+1))     /2.
        MDID=MDID+2
        GO TO 203
  248   SU     =SU     +(SORT(MDID+2)-SORT(MDID+1)+SORT(MDID+4)-SORT(MDID+3)
```

```
     8)/2.
      MDID=MDID+4
      GO TO 203
 999  SUM(I)=SUM(I)+RHO*SU     *100.
      TEST(I)=TEST(I)+(SU+SUBT)*267.
      DSU(I)=SU*RHO*100.
 300  CONTINUE
      RETURN
      END
```

APPENDIX III- Mathematical Derivation

This section derives the equations describing the position of a horst block in isostatic equilibrium. The material of the uplifted block is assumed to be of constant density. An additional mass is assumed to be resting on top of the block. The shape of the block is assumed to be symmetrical about the middle.

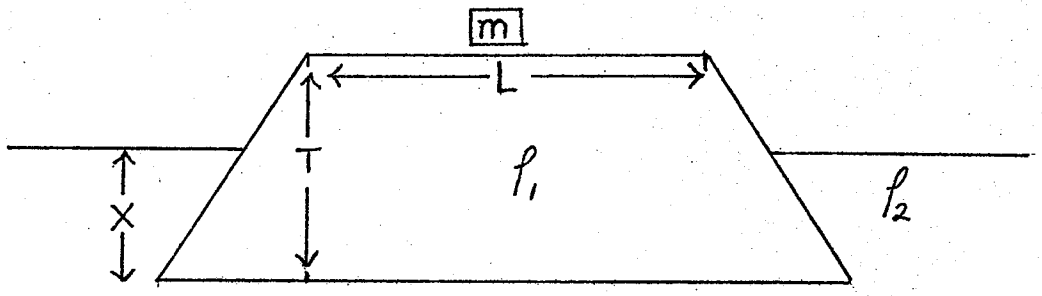

ρ_1 = density of block
ρ_2 = density of supporting material
L = length of block at surface
X = depth of bottom of block below surface of supporting liquid
m = mass resting on top of block
D = 1/2 (length of block on bottom - L)

Since the block is in isostatic equilibrium, the mass of the displaced material must equal the mass of the block + that of the load. The following equation is obtained:

III-1) $$(L+D)T\rho_1 + m = X\rho_2(L+2D) - \frac{X^2 D}{T}\rho_2$$

Solving for D we get:

III-2) $$D = \frac{L(T\rho_1 - X\rho_2) + m}{X\rho_2\left(2 - \frac{X}{T}\right) - T\rho_1}$$

For the Venezuelan Andes the distance from the 300 m contour on one flank to the 300 m contour on the other is 75 km. Thus a value of 75 km was used for L. The thickness of the crust in the Andes was taken to be 29 km. The total mass load represented by the Andes was obtained by determining the area under the elevation curve shown on profile A (Fig. 13) and assuming that the density of the material was 2.7 gm/cm^3. This gave a value for m of 5.6×10^{12} gm per cm of width. The density assumed for the crustal material (ρ_1) was 2.7 gm/cm^3 and for the mantle 3.3 gm/cm^3 (ρ_2).

For profile A at the El Baul swell the "normal" crustal thickness was 30 km. If the crust there is in isostatic equilibrium then the value of X at the El Baul Swell is X= x 30. = 24.5 km. In the Venezuelan Andes the crust-mantle boundary was at a depth of 29 km, so the value of X there is 24.5 -(30.-29.)= 23.5 km. Substitution of the following values into equation III-2 gives:

$L = 7.5 \times 10^6$ cm
$X = 2.35 \times 10^6$ cm
$\rho_1 = 2.7$ gm/cm^3
$\rho_2 = 3.3$ gm/cm^3
$m = 5.6 \times 10^{12}$ gm/cm

and the value of D is found to be:

D = 44 km

This means that if the mass excess of the Andes were to be supported by a block of the shape shown above, the angle of dip of the fault would be $\tan^{-1}(29./44.)$, or 33^{o}.

APPENDIX IV - Discussion of Error Bounds

The error bounds given for the data are not the result of any statistical treatment of the data, and are not standard deviations or root-mean-square errors. In making the new gravity measurements at undescribed stations the errors were estimated by first selecting stations for which there were available described positions (relative to some prominent feature such as a church or stream) and plotted positions on a 1:1,000,000 scale Shell GR series map. The known positions relative to the prominent features were compared with the positions of the stations as shown on the map. The difference between the positions was found to be less than 50 meters. It was then assumed that the error in the plotted position of the undescribed station was also 50 meters, however the actual error could be larger. The elevation error (the difference between the elevation of the old station and the elevation of the new station) was kept below 1 meter by only making measurements at stations where the elevation change within 50 meters of the presumed location of the station was less than 1 meter.

Since the maximum horizontal variation of the gravity field in this region was about 2 mgal/km, an error of 50 meters in

position causes a change in the measured value of gravity of 0.1 mgal. The elevation error of 1 meter causes a change of (1 m)(0.22 mgal/m) or 0.22 mgal in the gravity. (The factor 0.22 mgal/m is the sum of the free-air and Bouguer correction factors.) The total error causes by errors in position and elevation is 0.3 mgal.

Anderson, D. L., and R. O'Connell, 1967. Viscosity of the earth, Geophys. J. Roy. Astron. Soc., 14, 287-295.

Ball, M. M., and C. G. A. Harrison, 1970. Crustal plates in the central Atlantic, Science, 167, 1128-1129.

Barr, K. W., 1963. The geology of the Toco district, Trinidad, West Indies, part 1 and 2, Overseas Geol. and Miner. Resources, 8, 379-415, and 9, 1-29.

Barr, K. W., and J. B. Saunders, 1968. An outline of the geology of Trinidad, Trans. of the 4th Caribbean Geol Conf., 1-10.

Bassinger, B. G., R. N. Harbison, and L. A. Weeks, 1971. Marine geophysical study northeast of Trinidad-Tobago, Amer. Assoc. Petrol. Geol. Bull., 55, 1730-1740.

Bell, J. S., 1967. Geology of the Camatagua area Estado Aragua, Venezuela, unpubl. Ph.D. thesis, Princeton University.

Birch, F., 1952. Elasticity and constitution of the earth's interior, J. Geophys. Res., 57, 227-286.

Bowin, C. O., 1968. Geophysical study of the Cayman trough, J. Geophys. Res., 73, 5159-5173.

Bowin, C., C. G. Wing, T. C. Aldrich, 1969. Test of the MIT vibrating string gravimeter, 1967, J. Geophys. Res., 74, 3278-3280.

Bunce, E. T., J. D. Phillips, R. L. Chase, and C. O. Bowin, 1971. The Lesser Antilles arc and the eastern margin of the Caribbean sea, The Sea, 4, 359-385.

Crittenden, M. D., Jr., 1967. Viscosity and finite strength of the mantle as determined from water and ice loads, Geophys. J. Roy. Astron. Soc., 14, 261-279.

Dallmus, K. F., 1965. The geology and oil accumulations of the Eastern Venezuela basin. Boletin Informativo Asociacion Venezolana de Geologia, Mineria y Petroleo, 8, 5-26.

Dewey, J. F., and J. M. Bird, 1970. Plate tectonics and geosynclines, Tectonophysics, 10, 625-638.

Dobrin, M. B., 1960. Introduction to geophysical prospecting, McGraw-Hill Book Co., N. Y.

Edgar, N. T., 1968. Seismic refraction and reflection in the Caribbean Sea, Ph. D. thesis, Columbia University, (unpublished).

Edgar, N. T., J. B. Saunders, and scientific staff, 1971a. Deep-Sea Drilling Project, Leg 15, Geotimes, 8-16.

Edgar, N. T., J. I. Ewing, and J. Hennion, 1971b. Seismic refraction and reflection in Caribbean Sea, Amer. Assoc. Petrol. Geol. Bull. 55, 833-870.

Emery, K. O., E. Uchupi, J. D. Phillips, C. O. Bowin, E. T. Bunce, and S. T. Knott, 1970. Continental rise off Eastern North America. Amer. Assoc. Petrol. Geol. Bull. 54, 44-108.

Ewing, M., and J. L. Worzel, 1954. Gravity anomalies and structure of the West Indies, Part 1, Bull. Geol. Soc. Amer., 65, 165-174.

Freeland, G. L., and R. S. Dietz, 1971. Plate tectonic evolution of Caribbean-Gulf of Mexico region, Nature, 232, 20-23.

Gaposchkin, E. M., and K. Lambeck, 1969. 1969 Smithsonian standard Earth(II), Smithsonian Astophysical Observatory Special Report 315.

References continued:

Gunn, R., 1947. Quantitative aspects of juxtaposed ocean deeps, mountain chains and volcanic ranges, Geophysics, 12, 238-255.

Hedberg, H. D., 1950. Geology of the eastern Venezuela basin, Geol. Soc. Amer. Bull., 61, 1173-1216.

Handin, J., 1966. Strength and ductility, Handbook of Physical Constants, edit. S. P. Clark, Jr., Geol. Soc. Amer., N.Y.

Heiskanen, W. A., and F. A. Vening-Meinesz, 1958. The earth and its gravity field, McGraw-Hill Book Co., New York.

Higgins, G. E., 1959. Seismic velocity data from Trinidad, B.W.I., and comparison with the Caribbean area, Geophys. 24, 580-597.

Hospers, J., and J. C. Van Wijnen, 1959. The gravity field of the Venezuelan Andes and adjacent basins, Verh. Kon. Ned. Akad. Wetensch., Amsterdam, 23, 1-95.

Jacobsen, P., Jr., 1961. An evaluation of basement depth determinations from airborne magnetometer data, Geophysics, 26, 309-319.

Jeffreys, Sir H., 1959. The Earth: Its Origin, History and Physical Constitution, 4th ed., Cambridge University Press.

King, P. B., 1969. The tectonics of North America: a discussion to accompany the tectonic map of North America, Geol. Soc. Amer. Prof. Paper, 628, 77-83.

Kovisars, L., 1971. Geology of a portion of the North-Central Venezuelan Andes, Geol. Soc. Amer. Bull., 82, 3111-3138.

Kugler, H. G. 1959. Geological map of Trinidad, Petroleum Assoc. of Trinidad.

Lagaay, R. A., 1969. Geophysical investigations of the Netherlands Leeward Antilles, Verh, Kon. Ned. Akad. Wetensch., Amsterdam, 25, 1-86.

McConnell, R. K., 1968. Viscosity of the mantle from relaxation time spectra of isostatic adjustment, J. Geophys. Res., 73, 7089-7107.

MacDonald, W. D., and P. M. Hurley, 1969. Precambrian gneisses from northern Colombia, South America, Geol. Soc. Amer. Bull., 80, 1867-1872.

MacGillavry, H. J., 1970. Geological history of the Caribbean, I and II, Koninkl. Nederlandsch. Akad. Wetensch. Proc., Series B, 73, 64-96.

Mattson, P. H., and E. A. Pessagno, Jr., 1971. Caribbean Eocene volcanism and the extent of horizon A, Science, 174, 138-139.

Mencher, E., H. J. Fichter, H. H. Renz, W. E. Wallis, H. H. Renz, J. M. Patterson, and R. H. Robie, 1953. Geology of Venezuela and its oil fields, Bull. Amer. Assoc. Petrol. Geologists, 37, 690-777.

Menendez, A., 1962. Geology of the Tinaco area north central Cojedes Venezuela, unpubl. Ph.D. thesis, Princeton Univ.

Metz, H. L., 1968a. Geology of the El Pilar fault zone, State of Sucre, Venezuela, Transactions of the 4th Caribbean Geol. Conf., 293-298.

Metz, H. L., 1968b. Stratigraphic and geologic history of extreme northeastern Serrania del Interior, State of Sucre, Venezuela, Trans. 4th Caribbean Geol. Conf., 275-292.

Miller, J. B., K. L. Edwards, P. P. Wolcott, H. W. Anisgard, R. Martin, and H. Aderegg, 1958. Habitat of oil in the Maracaibo basin, Venezuela, in symposium volume Habitat of Oil, Amer. Assoc. Petrol. Geol., 601-640.

Molnar, P., and L. R. Sykes, 1969. Tectonics of the Caribbean and middle America regions from focal mechanisms and seismicity, Bull. Geol. Soc. Amer., 80, 1639-1684.

Nadai, A., 1963. Theory of flow and fracture of solids, Vol. 2, McGraw-Hill Book Co., Inc., New York, Toronto, and London.

Officer, C. B., J. I. Ewing, R. S. Edwards, and H. R. Johnson, 1957. Geophysical investigations in the eastern Caribbean: Venezuelan basin, Antilles island arc, and Puerto Rico trench, Bull. Geol. Soc. Amer., 68, 359-378.

Officer, C. B., J. I. Ewing, J. F. Hennion, D. G. Harkrider, and D. E. Miller, 1959. Geophysical investigations in the Eastern Caribbean: Summary of 1955 and 1956 cruises, Phys. and Chem. of the Earth, 3, 17-109.

Oxburgh, E. R., 1960. Geology of the eastern Carabobo area Venezuela, unpubl. Ph.D. thesis, Princeton University.

Peter, G., 1971. Geology and geophysics of the Venezuelan continental margin between Blanquilla and Orchilla islands, Ph.D. thesis, University of Miami, (unpublished).

Peirson, A. L., 1965. Geology of the Guarico mountain front, Boletin Informativo Asociacion Venezolana de Geologia, Mineria y Petroleo, 8, 181-214.

Phillips, J. D., B. P. Luyendyk, D. W. Forsyth, 1971. Central north Atlantic plate motions, Science, 174, 845-846.

Phillips, J. D. and B. P. Luyendyk, 1970. Central north Atlantic plate motions over the last 40 million years, Science, 170, 727-729.

Potter, H. C., 1968. A preliminary account of the stratigraphy and structure of the eastern part of the northern range, Trinidad, Trans. 4th Caribbean Geol. Conf., 15-20.

Press, F., 1968. Earth models obtained by Monte Carlo inversion, J. Geophys. Res., 73, 5223-5234.

Priem, H. N. A., N. A. I. M. Boelrijk, R. H. Verschure, E. H. Hebeda, and R. A. Lagaaij, 1966. Isotopic age of the quartz-diorite batholith on the island of Aruba Netherlands Antilles, Geol. en Mijnb., 45, 188-190.

Rod, E., 1956. Strike-slip faults of northern Venezuela, Bull. Am. Assoc. Petrol. Geol., 40, 457-476.

Rod, E., 1959. West end of Serrania del Interior eastern Venezuela, Amer. Assoc. Petrol. Geol., Bull., 43, 772-789.

Salvador, A., and R. M. Stainforth, 1968. Clues in Venezuela to the geology of Trinidad, and vice versa, Transactions of 4th Caribbean Geol. Conf., 31-40.

Schubert, C., and R. S. Sifontes, 1970. Bocono fault, Venezuelan Andes: evidence of postglacial movement, Science, 170, 66-69.

Smith, R. J., 1957. Gravity cross section of the coast range of Venezuela, Trans. Amer. Geophys. Union, 38, 372-378.

Stainforth, R. M., 1970. Geology of the Venezuelan region, Summarized notes prepared for Caribbean Seminar, W.H.O.I. October 1970. (unpublished)

Stainforth, R. M., 1966. Gravitational deposits in Venezuela, Boletin Informativo Asociacion Venezolana de Geologia, Mineria y Petroleo, 9, 275-290.

Stainforth, R. M., 1969. The concept of seafloor spreading applied to Venezuela, Boletin Informativo, Asociacion Venezolana de Geologia, Mineria y Petroleo, 12, 257-274.

Talwani, M., and M. Ewing, 1960. Rapid computation of gravitational attraction of three-dimensional bodies of arbitrary shape, Geophys. 25, 203-225.

Taylor, G. C., 1960. Geology of the island of Margarita, unpubl. Ph.D. thesis, Princeton University.

Venezuelan Oil Scouting Agency, 1957. Coordinate Systems of Venezuela, Venezuelan Oil Scouting Agency, Caracas.

Vine, F. J., 1966. Spreading of the ocean floor: new evidence, Science, 154, 1405-1415.

Walcott, R. I., 1970. Flexural rigidity,thickness, and viscosity of the Lithosphere, J. Geophys. Res., 75, 3941-3954.

Weeks, L. A., R. K. Lattimore, R. N. Harbison, B. G. Bassinger, and G. F. Merrill, 1971. Structural relations among Lesser Antilles, Venezuela, and Trinidad-Tobago, Bull. Amer. Assoc. Petrol. Geologists, 55, 1741-1752.

Weyl, R., 1966. The paleogeographic development of the Central American-West Indian region, Boletin Informativo Asociacion Venezolana de Geologia, Mineria y Petroleo, 9, 89-122.

Wheeler, C. B., 1963. Oligocene and lower Miocene stratigraphy of western and northeastern Falcon basin, Venezuela, Bull. Amer. Assoc. Petro. Geol., 47, 35-68.

Woollard, G. P. and J. C. Rose, 1963. International gravity measurements, Society of Exploration Geophysicists.

BIOGRAPHY

R. Allin Folinsbee attended the University of Alberta from 1961 to 1965, receiving his B.Sc. degree in 1964. He started graduate work at the Massachusetts Institute of Technology in 1965, and received his S.M. degree in 1969: his thesis was entitled "Heat Flow Over the Equatorial Mid-Atlantic Ridge." In 1969 he was accepted in the MIT-Woods Hole Oceanographic Institution "Joint Program in Oceanography". He has published a paper entitled "Heat Flow Measurements Between the Caribbean Sea and Mid-Atlantic Ridge" (Simmons et al., 1970).